NASA TECHNICAL MEMORANDUM

UB
NASA TM X-1225

UB
NASA TM X-1225

STATIC WIND-TUNNEL INVESTIGATION AND MOTION STUDIES OF THE M2-F2 VEHICLE LAUNCHED FROM A PRELIMINARY LOCATION ON THE B-52 AIRPLANE

by Linwood W. McKinney, Richmond P. Boyden, and Robert T. Taylor

Langley Research Center
Langley Station, Hampton, Va.

NATIONAL AERONAUTICS AND SPACE ADMINISTRATION • WASHINGTON, D. C. • APRIL 1966

[redacted]

NASA TM X-1225

STATIC WIND-TUNNEL INVESTIGATION AND MOTION STUDIES OF THE M2-F2 VEHICLE LAUNCHED FROM A PRELIMINARY LOCATION ON THE B-52 AIRPLANE

By Linwood W. McKinney, Richmond P. Boyden, and Robert T. Taylor

Langley Research Center
Langley Station, Hampton, Va.

NOFORN

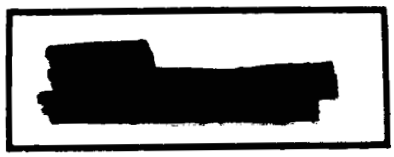

NATIONAL AERONAUTICS AND SPACE ADMINISTRATION

STATIC WIND-TUNNEL INVESTIGATION AND MOTION STUDIES OF THE M2-F2 VEHICLE LAUNCHED FROM A PRELIMINARY LOCATION ON THE B-52 AIRPLANE*

By Linwood W. McKinney, Richmond P. Boyden,
and Robert T. Taylor
Langley Research Center

SUMMARY

A high-speed wind-tunnel investigation and six-degree-of-freedom motion studies have been made to determine the aerodynamic interference effects on and the launch characteristics of the M2-F2 lifting body traversing the B-52 flow field. The wind-tunnel investigation was conducted at Mach numbers of 0.60, 0.80, 0.85, and 0.90, and the motion studies were made at Mach numbers of 0.60, 0.80, and 0.85. The primary purpose is to determine launch safety, that is, to ascertain whether the M2-F2 can be launched without contact between the M2-F2 fins and the attachment pylon. Although calculated motion transients are presented, no attempt has been made to assess the controllability problem. In the motion studies of the M2-F2/B-52 combination, the minimum altitude for launches without contact between the M2-F2 fins and the attachment pylon was about 40 000 feet (12 192 m) at a Mach number of 0.60 and 50 000 feet (15 240 m) at a Mach number of 0.80 for B-52 gross weights of 250 000 pounds (1 112 055 N) and 190 000 pounds (845 162 N). The maximum altitude for safe launches is determined by the B-52 airplane buffet boundary and was therefore different for the two weight conditions. No successful launches for the design incidence angle of -5° between the B-52 reference line and M2-F2 reference line were obtained at a Mach number of 0.85. At Mach numbers of 0.60 and 0.80, launch characteristics deteriorated as the incidence angle was increased from -5° to 4°. The stability augmentation system had only a minor effect on the path of the M2-F2 fin tips after launch over the time period that contact between the fins and pylon is possible. As a result of the present study the captive flight location for the final M2-F2/B-52 configuration has been altered to provide more clearance between the M2-F2 fins and the attachment pylon.

*Title, Unclassified.

INTRODUCTION

Experience with the X-15 research airplane, which is carried in a location off the plane of symmetry of the B-52 carrier airplane, has shown that the B-52 flow field has a marked influence on the X-15 motions immediately after launch. Reference 1 investigated the general problem with wind-tunnel tests and computer studies prior to the X-15 flights and pointed out that if certain control positions or control motions are avoided at launch, trouble-free launches should be expected. Reference 2, which presents records of the motions experienced by the X-15 during some early launches, and subsequent flight experience substantiated the conclusion of reference 1 that although the flow field of the carrier airplane affects the motions of the drop vehicle, safe launches are normally obtained. Also included in reference 2 are calculations obtained by using the time history of an early flight launch and the aerodynamic data obtained during the wind-tunnel investigation. These calculations show the general applicability of the analysis used in reference 1.

The Flight Research Center of the National Aeronautics and Space Administration is currently engaged in a flight research program to determine the subsonic handling qualities and landing characteristics of a number of proposed lifting-body reentry vehicles, one of which is the M2-F2. It is proposed that these vehicles be carried to altitudes of 40 000 feet (12 192 m) to 50 000 feet (15 240 m) at high subsonic speeds beneath the wing of the B-52 airplane and launched in the same manner as the X-15.

Since the size, the weight, and the inertial characteristics, as well as the aerodynamic configuration, of each of the proposed reentry vehicles is markedly different from the X-15 airplane, past experience with X-15 launches is not sufficient to determine whether these vehicles can be launched safely. Therefore, a wind-tunnel investigation has been made to determine the aerodynamic interference characteristics, and six-degree-of-freedom motion studies have been made to assess the effect of the flow-field interference on the motions of the M2-F2 vehicle immediately after launch. This study was made with the M2-F2 located beneath the B-52 wing in the originally proposed location with respect to the attachment pylon, as indicated in figure 1. It should be noted that, as a result of this study, the captive flight location for the final M2-F2/B-52 configuration has been altered to provide more clearance between the M2-F2 fins and the attachment pylon.

The purpose of this paper is to present the results of both the wind-tunnel interference tests and the drop motion studies of the M2-F2. Wind-tunnel data are presented for Mach numbers of 0.60, 0.80, 0.85, and 0.90 for a range of angles of attack and sideslip of the B-52/M2-F2 combination and for angles of attack and sideslip of the M2-F2 in the presence of the B-52 model at several separation distances. Calculated drop motions of

the M2-F2 are presented for B-52 flight altitudes varying from 25 000 feet (7 620 m) to 54 000 feet (16 459 m) at Mach 0.60, from 40 000 feet (12 192 m) to 61 500 feet (18 745 m) at Mach 0.80, and from 44 000 feet (13 411 m) to 59 000 feet (17 983 m) at Mach 0.85. The initial incidence angle between the M2-F2 reference line and the B-52 reference line was varied from -5° to 4°. The effects of increasing the weight of the M2-F2 and of stability augmentation are also presented. The calculated drop motions are discussed with respect to contact between the vertical fins of the M2-F2 and the attachment pylon. Calculated motion transients are also presented, but no attempt has been made to assess the controllability problem.

SYMBOLS

The longitudinal force and moment coefficients are referred to the stability axes and the lateral data are referred to the body axes, as shown in figure 2(a). The reference dimensions used in reducing the data are model projected area ($S = 0.0998\ ft^2 = 0.00927\ m^2$), model length ($l$ = 6.65 in. = 0.1689 m), and maximum body width (b = 2.89 in. = 0.0734 m). The angles and normal acceleration presented in the form of time histories are with reference to the principal-axis system, as indicated in figure 2(b).

Measurements for this study were taken in the U.S. Customary System of Units. Equivalent values are indicated herein parenthetically in the International System (SI) in the interest of promoting use of this system in future NASA reports. Details concerning the use of SI, together with physical constants and conversion factors, are given in reference 3.

a speed of sound, feet per second (m/sec)

b reference span, 2.89 inches (0.0734 m)

C_D drag coefficient, $\frac{\text{Drag}}{\bar{q}S}$

C_L lift coefficient, $\frac{\text{Lift}}{\bar{q}S}$

$C_{L_{\delta_u}}$ lift effectiveness parameter for upper-surface-flap control, $\partial C_L/\partial \delta_u$, per degree

$C_{L_{\delta_l}}$ lift effectiveness parameter for lower-surface-flap control, $\partial C_L/\partial \delta_l$, per degree

C_l rolling-moment coefficient, $\frac{\text{Rolling moment}}{\bar{q}Sb}$

C_{l_p} rolling-moment coefficient due to rolling velocity, $\frac{\partial C_l}{\partial\left(\frac{pb}{2V}\right)}$, per radian

C_{l_r} rolling-moment coefficient due to yawing velocity, $\frac{\partial C_l}{\partial\left(\frac{rb}{2V}\right)}$, per radian

C_{l_β} effective-dihedral parameter (measured between $\beta = 5^\circ$ and $\beta = -5^\circ$), per degree

$C_{l_{\delta_a}}$ rolling-moment coefficient per degree of aileron deflection, $\partial C_l / \partial \delta_a$

$C_{l_{\delta_r}}$ rolling-moment coefficient per degree of rudder deflection, $\partial C_l / \partial \delta_r$

C_m pitching-moment coefficient, $\frac{\text{Pitching moment}}{\bar{q}Sl}$

C_{m_q} pitching-moment coefficient due to pitching velocity, $\frac{\partial C_m}{\partial\left(\frac{ql}{2V}\right)}$, per radian

$C_{m_{\delta_u}}$ pitching-moment coefficient per degree of upper-surface-flap deflection, $\partial C_m / \partial \delta_u$

$C_{m_{\delta_l}}$ pitching-moment coefficient per degree of lower-surface-flap deflection, $\partial C_m / \partial \delta_l$

C_n yawing-moment coefficient, $\frac{\text{Yawing moment}}{\bar{q}Sb}$

C_{n_p} yawing-moment coefficient due to rolling velocity, $\frac{\partial C_n}{\partial\left(\frac{pb}{2V}\right)}$, per radian

C_{n_r} yawing-moment coefficient due to yawing velocity, $\frac{\partial C_n}{\partial\left(\frac{rb}{2V}\right)}$, per radian

C_{n_β} directional-stability parameter (measured between $\beta = 5^\circ$ and $\beta = -5^\circ$), per degree

$C_{n_{\delta_a}}$ yawing-moment coefficient per degree of aileron deflection, $\partial C_n / \partial \delta_a$

$C_{n_{\delta_r}}$ yawing-moment coefficient per degree of rudder deflection, $\partial C_n / \partial \delta_r$

C_Y side-force coefficient, $\frac{\text{Side force}}{\bar{q}S}$

C_{Y_β} side-force coefficient per degree of sideslip angle (measured between $\beta = 5^o$ and $\beta = -5^o$)

$C_{Y_{\delta_a}}$ side-force coefficient per degree of aileron deflection, $\partial C_Y / \partial \delta_a$

$C_{Y_{\delta_r}}$ side-force coefficient per degree of rudder deflection, $\partial C_Y / \partial \delta_r$

g acceleration due to gravity, 32.2 feet per second per second (9.81 m/sec^2)

h altitude, feet (m)

$I_{X_p}, I_{Y_p}, I_{Z_p}$ moments of inertia about X_p, Y_p, and Z_p, slug-ft^2 (m-N-sec^2)

K_I rudder interconnect gain, δ_r / δ_a

K_p roll damper gain, δ_a / p, seconds

K_q pitch damper gain, δ_l / q, seconds

K_r yaw damper gain, δ_r / r, seconds

l model length, 6.65 inches (0.1689 m)

M Mach number, V/a

n normal acceleration along principal axes of M2-F2, g units

p rolling velocity, radians per second or degrees per second

q pitching velocity, radians per second or degrees per second

$\bar{q}$ free-stream dynamic pressure, $\frac{1}{2}\rho V^2$, pounds per square foot (N/m^2)

r	yawing velocity, radians per second or degrees per second
S	reference area, 0.0998 square foot (0.00927 m^2)
t	time, seconds
V	free-stream velocity, feet per second (m/sec)
W_{B-52}	weight of B-52 airplane, pounds (N)
W_{M2-F2}	weight of M2-F2 vehicle, pounds (N)
X,Y,Z	Euler axes
X_p, Y_p, Z_p	M2-F2 principal axes
$X_{ref}, Y_{ref}, Z_{ref}$	M2-F2 reference axes
Z'	vertical axis normal to B-52 reference line
z	distance along Z-axis, feet (m)
z'	distance along Z'-axis, feet (m)
α	angle of attack of M2-F2 reference line, degrees
α_{B-52}	angle of attack of B-52 reference line, degrees
$\Delta\alpha$	incidence angle of M2-F2 reference line relative to B-52 reference line, degrees
β	angle of sideslip of M2-F2 reference line, degrees
β_{B-52}	angle of sideslip of M2-F2/B-52 combination, degrees
$\Delta\beta$	angle of sideslip of M2-F2 reference line relative to B-52 reference line, degrees
δ_a	differential deflection of upper-surface flaps when used as ailerons, $\delta_{u,R} - \delta_{u,L}$, degrees

δ_l lower-surface-flap deflection measured from local body surface, positive when trailing edge is down, degrees

δ_r rudder deflection, positive when trailing edge is deflected to left, degrees

δ_u upper-surface-flap deflection measured from local body surface, positive when trailing edge is down, degrees

ϵ inclination of M2-F2 principal axes from angle-of-attack reference axes, positive when principal axes are inclined nose down with respect to reference axes, degrees

θ Euler pitch angle, degrees

ρ mass density of air, slugs per cubic foot (kg/m^3)

ϕ Euler roll angle, degrees

ψ Euler yaw angle, degrees

Subscripts:

d effect of dampers

L left

R right

A dot over a symbol indicates the first derivative with respect to time.

MODELS AND APPARATUS

The models used were 0.025-scale representations of the B-52 airplane and the M2-F2 lifting-body configuration. The B-52 model was the same model used in the investigation in reference 4. A sketch showing pertinent dimensions of the M2-F2 model is presented in figure 3(a). The aft end of the M2-F2 body was modified to accommodate the strain-gage balance used to measure the forces and moments, as shown in figure 3(b). The M2-F2 model was sting supported from a tripod support system rigidly mounted

beneath the B-52 wing. All supports were streamlined to provide a minimum of aerodynamic interference on the flow field. Photographs of the M2-F2/B-52 combination showing the M2-F2 model at various vertical locations beneath the B-52 wing are presented in figure 4.

TESTS AND CORRECTIONS

The force tests were made in the Langley high-speed 7- by 10-foot tunnel at Mach numbers of 0.60, 0.80, 0.85, and 0.90, corresponding to Reynolds numbers based on M2-F2 length from approximately 1.8×10^6 to 2.3×10^6. The test parameters were angles of attack and sideslip of the M2-F2/B-52 combination and angles of attack and sideslip of the M2-F2 in the presence of the B-52 model at several separation distances. All tests were made with the M2-F2 control surfaces deflected $(\delta_l = 30^o; \delta_u = -10^o;$ and $\delta_{r,R} = -10^o;$ and $\delta_{r,L} = 10^o)$.

During the tests of the M2-F2 in the carry location, sufficient clearance between the attachment pylon fairing and the M2-F2 fins was allowed to insure that fouling was not encountered as a result of sting and balance deflections. Corrections to the angles of attack and sideslip due to bending of the main support system and the M2-F2 sting and balance system have been applied to the data. Blockage corrections, obtained by the method of reference 5, by considering the drag of both models, have been applied to the data. In addition, the jet-boundary corrections to the angles of attack were obtained by the method of reference 6 for the B-52 model and have been applied. The drag data are presented uncorrected for base pressure.

PRESENTATION OF RESULTS

The results of the study are presented in the following figures:

	Figure
Wind-tunnel data:	
M2-F2 alone	5 and 6
M2-F2 in B-52 flow field	7 to 14
Effects of B-52 angle of attack for $\Delta\alpha = -5^o$	15
B-52 buffet boundary	16
Motion-study calculations:	
M2-F2 reference section used in motion studies	17
Effects of B-52 angle of attack when W_{B-52} = 250 000 pounds (1 112 055 N)	18 to 20

Figure

Effects of B-52 angle of attack when W_{B-52} = 190 000 pounds (845 162 N) . . . . . 21 and 22
Effect of dampers . . . . . 23 to 25
Effect of $\Delta\alpha$ . . . . . 26 to 32
Effect of M2-F2 launch weight . . . . . 33 and 34
Launch envelope 35

DISCUSSION OF RESULTS

Wind-Tunnel Data and Motion Calculations

The results of the wind-tunnel force tests are presented in figures 5 to 14. Figure 5 presents the basic interference-free data obtained on the 0.025-scale model of the M2-F2 launch vehicle. A comparison of the data presented in figure 5 with data obtained at the Ames Research Center on a larger model is presented in figure 6 for Mach numbers of 0.60 and 0.80. The differences in the longitudinal data may be the result of modification to the aft end of the model used for the present tests. This modification was required to accommodate the strain-gage balance. The difference in the model lines (fig. 3(a)) was such that the model used for these tests had an effective upper flap setting δ_u greater than -10°. The comparison in figure 6(b) shows a reasonable agreement between lateral-directional data from the two models. Since the purpose of this investigation is to make a preliminary assessment of the gross effects of the interference flow field on the M2-F2 launch characteristics, the differences in longitudinal interference-free data are not considered to have a significant effect on the analysis. Figures 7 to 14 show the longitudinal and lateral-directional data obtained on the M2-F2 model in the B-52 interference flow field as functions of B-52 angle of attack for several values of M2-F2 incidence angle $\Delta\alpha$, separation distance z', and sideslip angle $\Delta\beta$ or β_{B-52} at Mach numbers of 0.60, 0.80, 0.85, and 0.90. Physical and aerodynamic damping and control characteristics intended to be representative of the launch vehicle were compiled by the Flight Research Center and are given in tables I to III.

In order to assess the launch safety of the M2-F2/B-52 combination, M2-F2 interference data as functions of incidence angle, separation distance, and sideslip angle are required at a constant B-52 angle of attack and Mach number. As an example of the gross effects of the interference flow field on the M2-F2 forces and moments, figure 15 is included. In this figure C_L, C_m, C_l, C_n, and C_Y at $\Delta\alpha = -5^o$ for several B-52 angles of attack are shown as functions of separation distance z', with free-stream values of the coefficients appearing on the plots at z' = 40 feet (12.2 m). Figure 15 also illustrates the linear interpolation used in the motion calculations. Interference data

together with the physical and aerodynamic damping and control characteristics given in tables I to III are used as input to the computer which solves the six-degree-of-freedom equations of motion for the path and resulting motion of the M2-F2 immediately after launch. There are a large number of possible points in the altitude – Mach number flight envelope from which launches may be made and several conditions (e.g., M2-F2 launch weight and attitude) which can be studied. In order to proceed in an orderly fashion with the assessment of the effects of altitude and Mach number, figure 16 has been prepared. Shown in this figure are the B-52 buffet boundary as a function of Mach number and the variation of altitude with Mach number for trimmed flight at various B-52 angles of attack for B-52 gross weights of 250 000 pounds (1 112 055 N) and 190 000 pounds (845 162 N), which were taken to be maximum and minimum weight conditions, respectively. It is possible to fly the B-52 at all points beneath the buffet boundary in the altitude – Mach number envelope. The area between the buffet boundary and the line for $\alpha_{B-52} = -2^{o}$ represents the region where launches have been studied. The variables in the launch studies were B-52 altitude and angle of attack, launch attitude of the M2-F2 vehicle with respect to the B-52, gross weight of the M2-F2, Mach number, and stability augmentation.

Since the study is designed to determine launch safety, that is, to ascertain that the launch vehicle does not make contact with the carrier airplane, the primary emphasis is placed upon a consideration of the vehicle parts which are most likely to contact the carrier airplane during the initial phase of the launch, with some attention directed to the motion as it develops during launch. The results are presented in the form of locus plots of the trailing edge of the M2-F2 fin tips and the center of gravity in the YZ reference plane at discrete values of time. In figure 17 a sketch of the vehicle shows the points for which loci were computed in figures 18 to 34. A cross section showing the initial relationship between the M2-F2 fins and the attachment pylon (as seen by looking through the M2-F2 center of gravity in the direction of flight) is included on each figure for reference purposes. Also the location of the rear attachment shackles is indicated by cross marks. Time histories of the quantities z, n, α, θ, ϕ, β, and ψ are presented on facing pages to the locus plots to aid in interpreting the loci and to indicate the trends of the motions that develop during the time required for the M2-F2 to fall clear of the B-52 interference flow field. Although in some of the locus plots contact is indicated between the M2-F2 fin tips and parts of the B-52, the subsequent effect of the contact is not included in the time-history calculations. Most of the calculated launches were made without stability augmentation; however, to assess the effects of artificial damping on the drop motions, a rate damper system about all axes was included in the equations of motion. Limits for damper-imposed control deflection rate and magnitude are given in table II.

Launch Characteristics

Effect of B-52 angle of attack.- Figure 18 shows the effect of B-52 angle of attack on the computed fin-tip paths and vehicle motion after launch at $M = 0.60$. As the angle of attack of the B-52 airplane increases, the flight altitude must also increase so that inherently this analysis reflects changes in the dynamic pressure as well as changes in the interference forces and moments due to angle of attack. At B-52 angles of attack of 2°, 4°, and 6°, the M2-F2 can be launched without contact between the tips of the M2-F2 vertical fins and the attachment pylon. An examination of the motion curves (fig. 18(b)) shows less rapid angular motion during the launch as B-52 angle of attack is increased. The distance z traveled by the center of gravity in the first four-tenths of a second after launch is nearly constant for all angles of attack of the B-52, and since the angular rotations are less rapid at the higher B-52 angles of attack, the path of the fin tips tends to become more nearly vertical. From $\alpha_{B-52} = 2^{\circ}$ to $\alpha_{B-52} = 6^{\circ}$ the center-of-gravity paths as well as the paths of the fin tips can be seen to drift to the right due to increased side force. In general, the same comments apply for the drop motion calculated at $M = 0.80$ and shown in figure 19. That is, increasing the B-52 angle of attack reduces the rapidity of the angular motions after launch. At $M = 0.85$ (fig. 20) the fin tips contact the pylon and support structure at all B-52 angles of attack. This contact at $M = 0.85$ is associated with large negative roll and yaw angles resulting from the increased interference rolling and yawing moments obtained on the M2-F2 in the carry location, as shown in figure 15.

Calculated launches with the B-52 weight reduced to 190 000 pounds (845 162 N) are shown in figures 21 and 22 at Mach numbers of 0.60 and 0.80, respectively. Figure 21 shows launches without contact at B-52 angles of attack of 0°, 2°, 4°, and 6° at $M = 0.60$. Figure 22 indicates that at $M = 0.80$ the M2-F2 can be launched without contact at B-52 angles of attack of 0° and 2°.

Effect of dampers.- The effect of the vehicle stability augmentation system on the launch characteristics at $M = 0.60$ is shown at B-52 angles of attack of -2°, 2°, and 6° in figures 23, 24, and 25, respectively. In general, the dampers with the rate and authority limits used have only a minor effect on the path of the M2-F2 fin tips after launch in the time period in which contact between the fin tips and the attachment pylon is possible. These figures show that, from contact considerations, the safe launch envelope is not significantly changed by stability augmentation. There is, however, a definite influence of the dampers on the motion after launch as it develops at times greater than about four tenths of a second. Since this paper is primarily concerned with the contact problems associated with the launches, the remaining analysis is made without the dampers operating.

Effect of incidence angle.- The effect of M2-F2 incidence angle $\Delta\alpha$ on the launch characteristics at $M = 0.60$ for B-52 angles of attack of -2°, 2°, and 6° is shown in figures 26, 27, and 28, respectively. As $\Delta\alpha$ is increased from -5° to 4°, the time histories indicate a less rapid angular buildup of the motion. It can be seen though that the reduction in vertical descent velocity of the center of gravity keeps the M2-F2 fins in the proximity of the pylon for a longer period of time and the angular rotations combined with large positive side force acting on the M2-F2 in the carry location always result in a deterioration in launch characteristics with increasing $\Delta\alpha$ in figures 26 to 28. The same general comments apply for the launches computed at $M = 0.80$, as shown in figures 29 and 30. However, the motions shown for a Mach number of 0.85 in figures 31 and 32 indicate a somewhat different trend. For a B-52 angle of attack of 0° (fig. 32), reductions in the magnitude of the roll and yaw angles with increasing $\Delta\alpha$ were sufficient to allow drops without fin-tip contact to be calculated at values of $\Delta\alpha$ of 0°, 2°, and 4°.

Effect of M2-F2 launch weight.- In order to indicate the effect of M2-F2 launch weight on the launch characteristics, drop motions were calculated for the heavy-weight M2-F2 $\left(W_{M2-F2} = 9030 \text{ lb } (40\,167 \text{ N})\right)$ at a B-52 angle of attack of 2° and a B-52 gross weight of 250 000 pounds (1 112 055 N) for $\Delta\alpha = -5^{\circ}$ and $\Delta\alpha = 4^{\circ}$ at $M = 0.60$ and at $M = 0.80$. The resulting motions are shown in figures 33 and 34. Also shown in these figures, for a comparison, are the motions for the light-weight M2-F2 $\left(W_{M2-F2} = 5576 \text{ lb } (24\,803 \text{ N})\right)$ at the same launch conditions. Increasing the M2-F2 launch weight and changing the inertial characteristics (see table I) retards rotational velocities and increases the vertical descent rate, with the result being improved launch characteristics.

Expected launch envelope.- The important factors shown herein to affect the launch contact problem are B-52 angle of attack, launch Mach number, and launch altitude. In order to combine these effects figure 35 has been prepared. Figure 35 shows the predicted allowable launch conditions as functions of altitude and Mach number for the dampers off at B-52 gross weights of 250 000 pounds (1 112 055 N) and 190 000 pounds (845 162 N) and a M2-F2 weight of 5576 pounds (24 803 N) at $\Delta\alpha = -5^{\circ}$. The area between the boundaries indicates a region where safe launches, that is, launches without contact between the M2-F2 lifting body and the B-52 airplane, were calculated. The maximum altitude for safe launches is determined by the B-52 airplane buffet boundary and was therefore different for the two weight conditions. At a B-52 weight of 250 000 pounds (1 112 055 N), launches without contact are indicated between altitudes of about 40 000 feet (12 192 m) and 48 000 feet (14 630 m) at $M = 0.60$ and between 51 000 feet (15 545 m) and 56 000 feet (17 069 m) at $M = 0.80$. For a B-52 weight of 190 000 pounds (845 162 N), launches without contact are indicated between altitudes of about 40 000 feet (12 192 m) and 54 000 feet (16 459 m) at $M = 0.60$ and between 51 000 feet (15 545 m) and 61 500 feet (18 745 m) at $M = 0.80$. At a Mach number of 0.85 no successful launches for the design

incidence angle of -5° were obtained. In figure 35 the launch envelope appears to be enlarged at the lower B-52 weight. The reason for this enlargement is that buffeting occurs at a higher altitude for the lower B-52 weight. The minimum altitude for launches without contact appears to be independent of B-52 weight although the angle of attack is reduced for the lighter weight B-52. This fact indicates that the increased dynamic pressure at the lower altitude has more influence on the motions of the M2-F2 at launch than the changes in interference forces and moments resulting from changes in B-52 angle of attack.

CONCLUDING REMARKS

A high-speed wind-tunnel investigation and six-degree-of-freedom motion studies have been made to determine the aerodynamic interference effects on and the launch characteristics of the M2-F2 lifting body traversing the B-52 flow field. The wind-tunnel investigation was conducted at Mach numbers of 0.60, 0.80, 0.85, and 0.90, and the motion studies were made at Mach numbers of 0.60, 0.80, and 0.85. The primary purpose is to determine launch safety, that is, to ascertain whether the M2-F2 can be launched without contact between the M2-F2 fins and the attachment pylon. Although calculated motion transients are presented, no attempt has been made to assess the controllability problem.

In the motion studies of the M2-F2/B-52 combination, the minimum altitude for launches without contact between the M2-F2 fins and the attachment pylon was about 40 000 feet (12 192 m) at a Mach number of 0.60 and 50 000 feet (15 240 m) at a Mach number of 0.80 for B-52 gross weights of 250 000 pounds (1 112 055 N) and 190 000 pounds (845 162 N). The maximum altitude for safe launches is determined by the B-52 airplane buffet boundary and was therefore different for the two weight conditions. No successful launches for the design incidence angle of -5° between the B-52 reference line and M2-F2 reference line were obtained at a Mach number of 0.85. At Mach numbers of 0.60 and 0.80, launch characteristics deteriorated as the incidence angle was increased from -5° to 4°. The stability augmentation system had only a minor effect on the path of the M2-F2 fin tips after launch over the time period that contact between the fins and pylon is possible. As a result of this study the captive flight location for the final M2-F2/B-52 configuration has been altered to provide more clearance between the M2-F2 fins and the attachment pylon.

Langley Research Center,
National Aeronautics and Space Administration,
Langley Station, Hampton, Va., December 21, 1965.

REFERENCES

1. Alford, William J., Jr.; and Taylor, Robert T.: Aerodynamic Characteristics of the X-15/B-52 Combination. NASA MEMO 6-8-59L, 1959.

2. Matranga, Gene J.: Launch Characteristics of the X-15 Research Airplane as Determined in Flight. NASA TN D-723, 1961.

3. Mechtly, E. A.: The International System of Units – Physical Constants and Conversion Factors. NASA SP-7012, 1964.

4. Taylor, Robert T.; and Alford, William J., Jr.: A Wind-Tunnel Investigation of the Carry Loads and Mutual Interference Effects of 1/40-Scale Models of the X-15 and B-52 Airplanes in Combination. NASA TM X-184, 1959.

5. Herriot, John G.; Blockage Corrections for Three-Dimensional-Flow Closed-Throat Wind Tunnels, With Consideration of the Effect of Compressibility. NACA Rept. 995, 1950. (Supersedes NACA RM A7B28.)

6. Gillis, Clarence L.; Polhamus, Edward C.; and Gray, Joseph L., Jr.: Charts for Determining Jet-Boundary Corrections for Complete Models in 7- by 10-Foot Closed Rectangular Wind Tunnels. NACA WR L-123, 1945. (Formerly NACA ARR L5G31.)

TABLE I.- PHYSICAL AND DAMPER CHARACTERISTICS OF THE M2-F2

Measurement	Values for –	
	Light-weight M2-F2	Heavy-weight M2-F2
Weight of M2-F2, W_{M2-F2}, lb (N) . . .	5576 (24 803)	9030 (40 167)
Moment of inertia about X principal axis, I_{X_p}, slug-ft^2 (m-N-sec^2) . . .	931.84 (1263.02)	1041.2 (1411.24)
Moment of inertia about Y principal axis, I_{Y_p}, slug-ft^2 (m-N-sec^2) . . .	6049.0 (8198.81)	6607.0 (8955.13)
Moment of inertia about Z principal axis, I_{Z_p}, slug-ft^2 (m-N-sec^2) . . .	6281.3 (8513.67)	6915.8 (9373.68)
Inclination, ϵ, deg	-4.9	-4.6
Pitch damper gain, K_q, sec	0.5	----------
Roll damper gain, K_p, sec	-0.25	----------
Yaw damper gain, K_r, sec	0.25	----------
Rudder interconnect gain, K_I	-0.30	----------

TABLE II.- DAMPER LIMITS FOR THE M2-F2

Damper authority limits:

$\delta_{a,d}$, deg . . . . . ±20

$\delta_{l,d}$, deg . . . . . ±5

$\delta_{r,d}$, deg . . . . . ±5

Damper rate limits:

$\dot{\delta}_{a,d}$, deg/sec . . . . . ±30

$\dot{\delta}_{l,d}$, deg/sec . . . . . ±25

$\dot{\delta}_{r,d}$, deg/sec . . . . . ±30

TABLE III.- AERODYNAMIC CONTROL CHARACTERISTICS AND DAMPING DERIVATIVES OF THE M2-F2

Measurement	Values at –		
	M = 0.60	M = 0.80	M = 0.85
$C_{m_{\delta_l}}$, per deg	-0.0027	-0.00191	-0.00191
$C_{m_{\delta_u}}$, per deg	-0.0023	-0.00225	-0.00225
$C_{L_{\delta_l}}$, per deg	0.00423	0.0055	0.0055
$C_{L_{\delta_u}}$, per deg	0.0078	0.00849	0.00849
$C_{l_{\delta_r}}$, per deg	0.000374	0.00038	0.00038
$C_{l_{\delta_a}}$, per deg	0.000625	0.000658	0.000658
$C_{n_{\delta_r}}$, per deg	-0.00178	-0.00192	-0.00192
$C_{n_{\delta_a}}$, per deg	-0.00058	-0.000615	-0.000615
$C_{Y_{\delta_r}}$, per deg	0.0016	0.0016	0.0016
$C_{Y_{\delta_a}}$, per deg	0.00055	0.00055	0.00055
C_{m_q}, per rad	-0.145	-0.490	-0.490
C_{l_p}, per rad	-0.205	-0.235	-0.235
C_{n_p}, per rad	0.122	0.1715	0.1715
C_{l_r}, per rad	0.348	0.4320	0.4320
C_{n_r}, per rad	-1.395	-1.630	-1.630

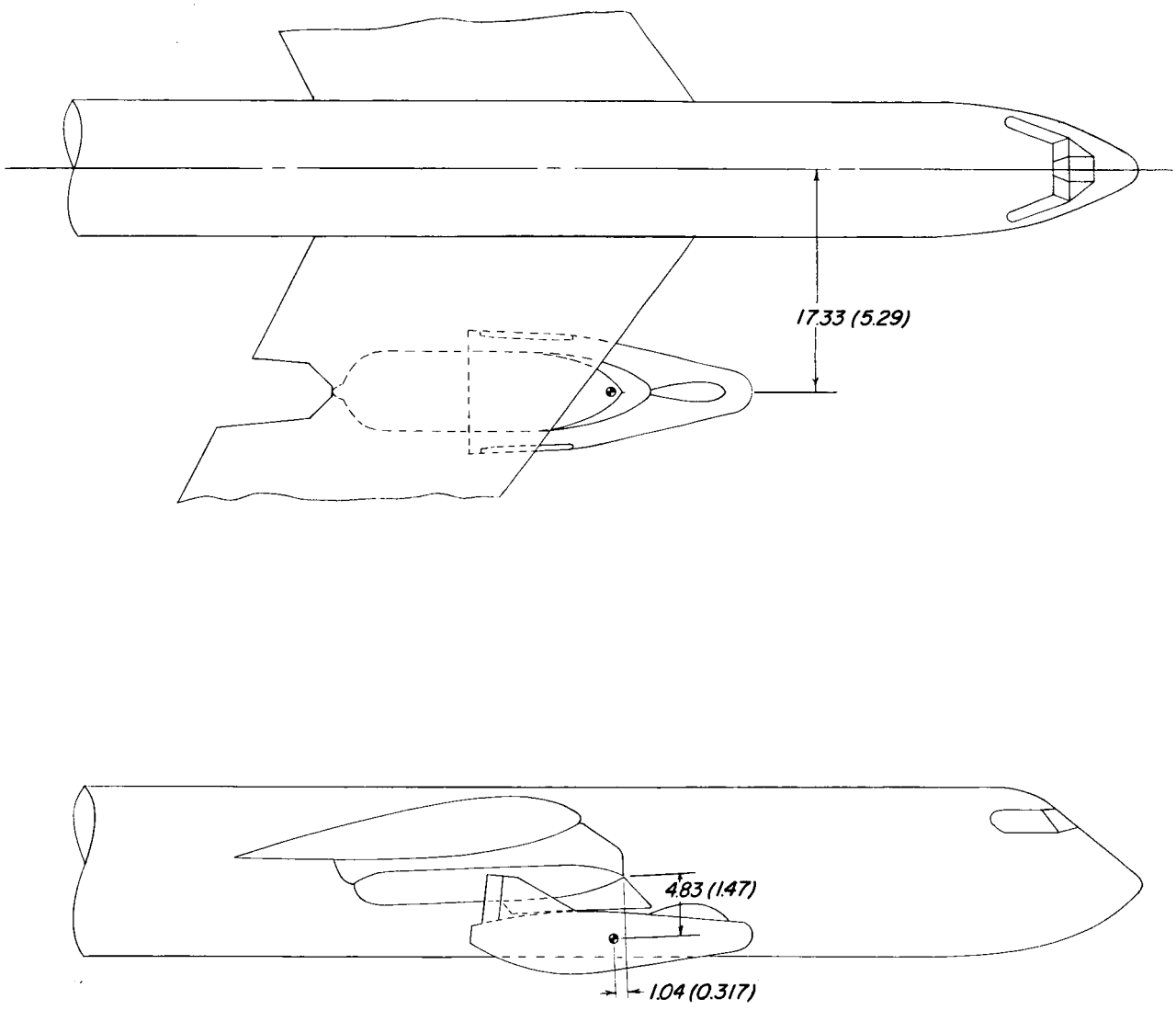

Figure 1.- Preliminary location of the M2-F2 lifting body on the B-52 airplane. Full-scale dimensions are given first in feet and parenthetically in meters.

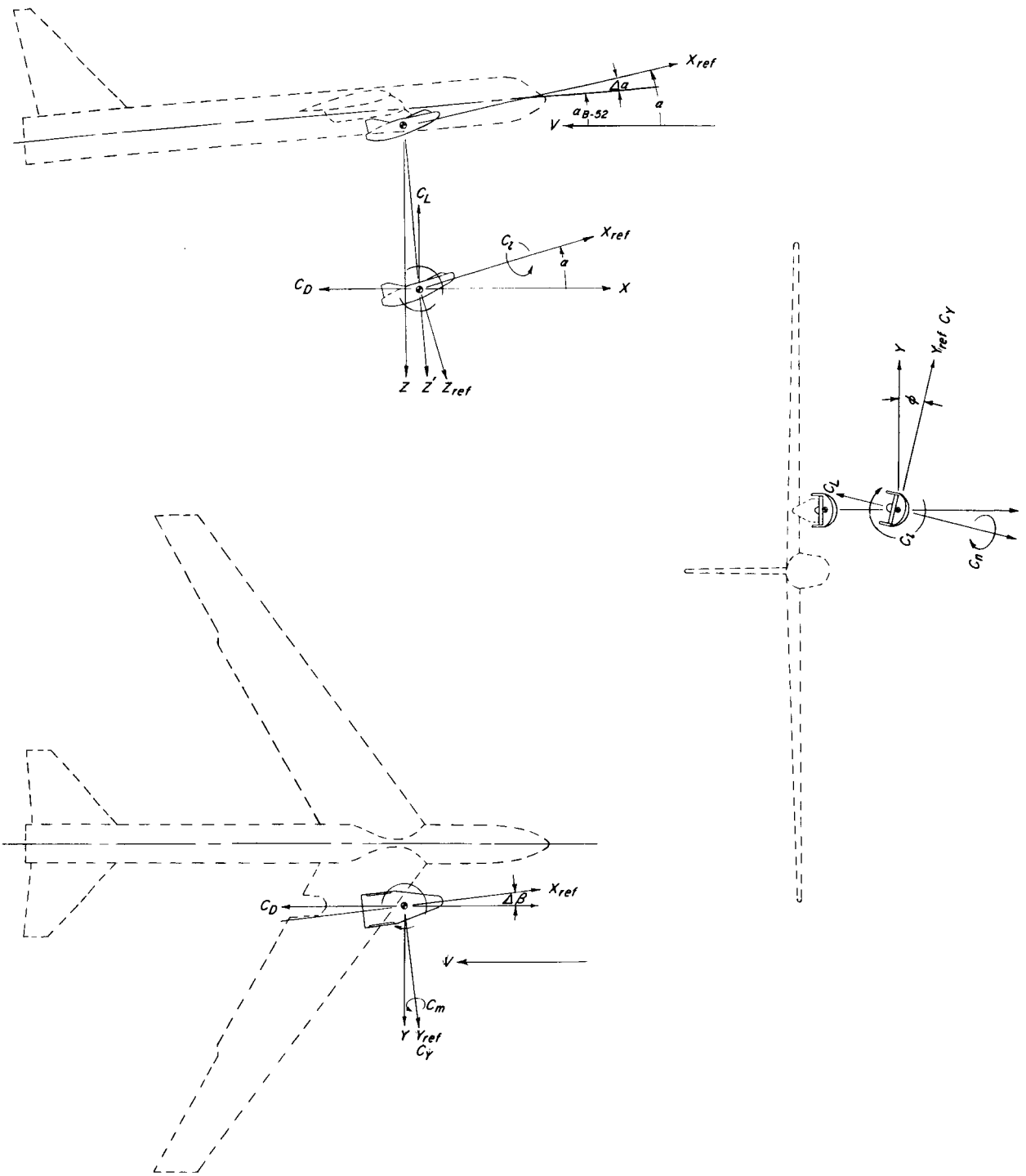

(a) Axis system used in wind-tunnel investigation.

Figure 2.- Systems of axes used in the study.

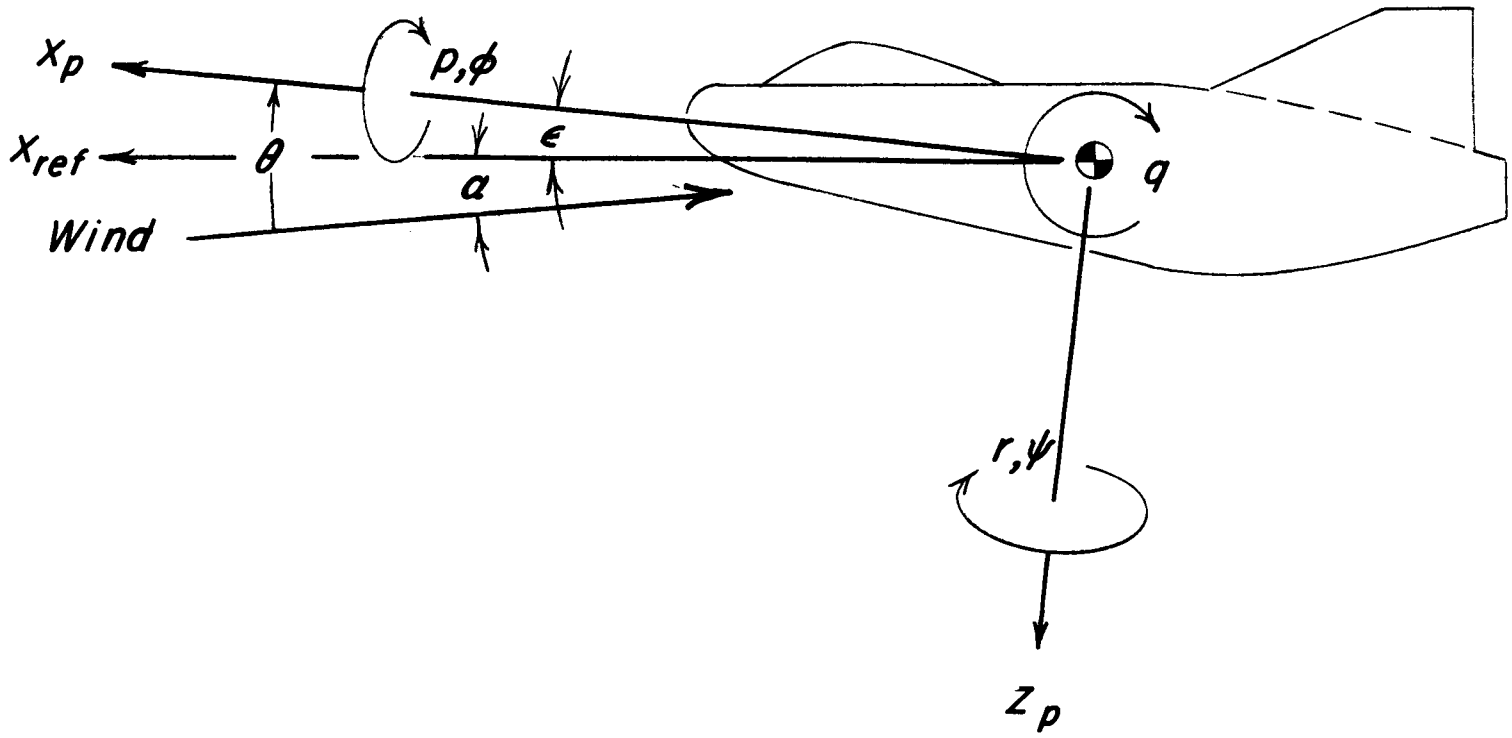

(b) Axis system used in motion calculations.

Figure 2.- Concluded.

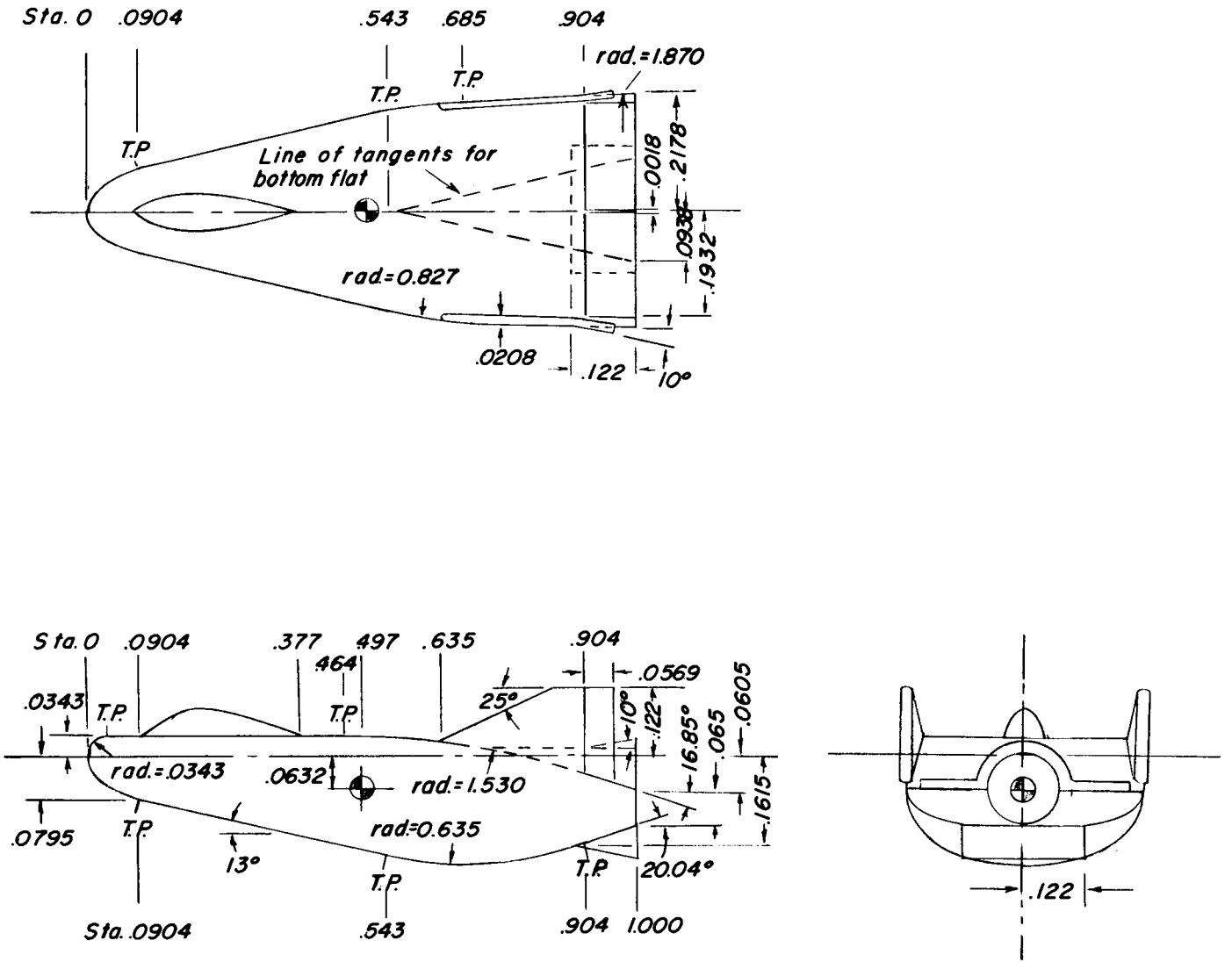

(a) Geometric characteristics, with dimensions given in percent body length l, where l = 0.554 foot (0.169 m). (T. P. denotes tangent point.)

Figure 3.- Details of M2-F2 model.

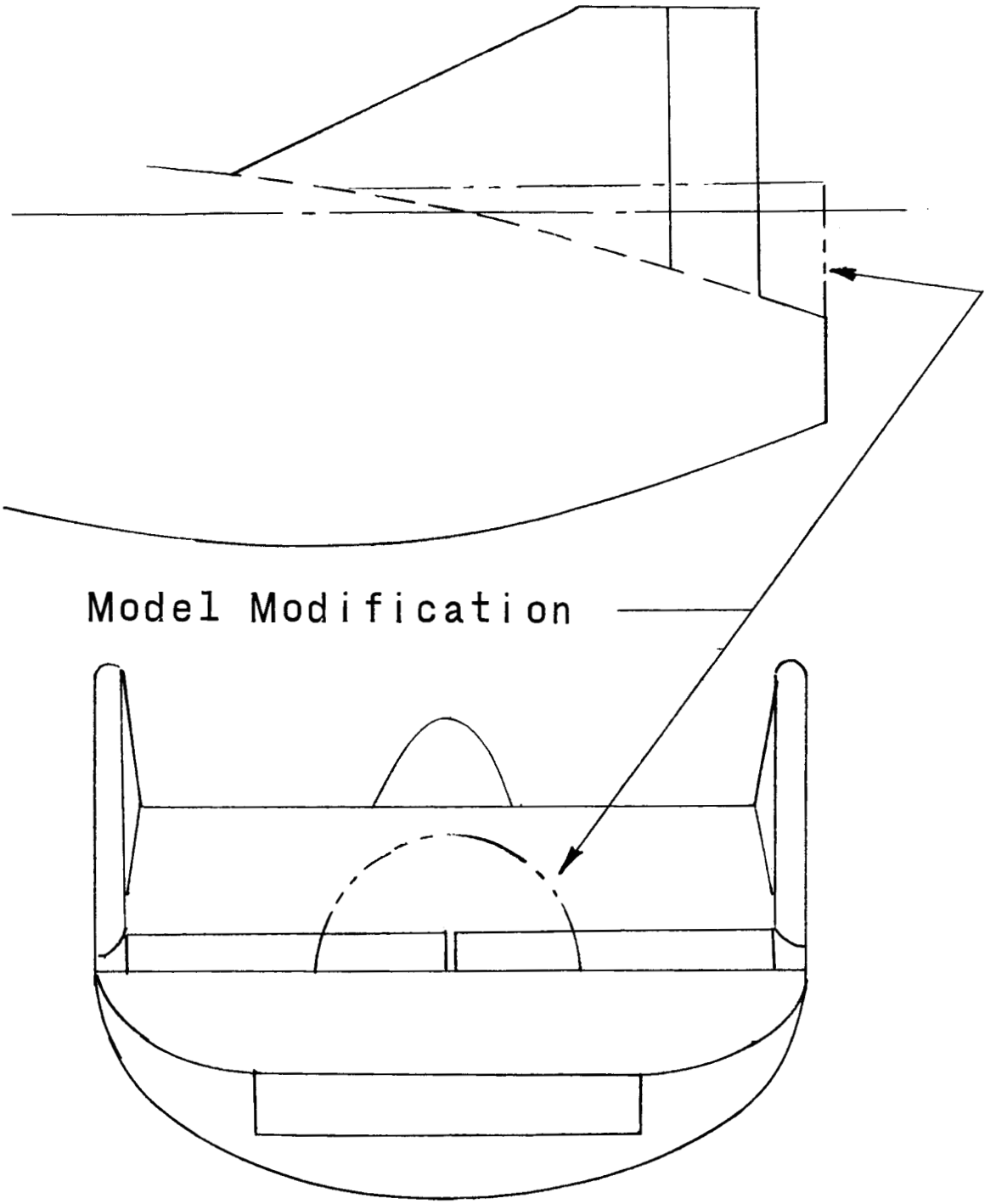

(b) Sketch showing modification to aft section of M2-F2 model required for balance adapter.

Figure 3.- Concluded.

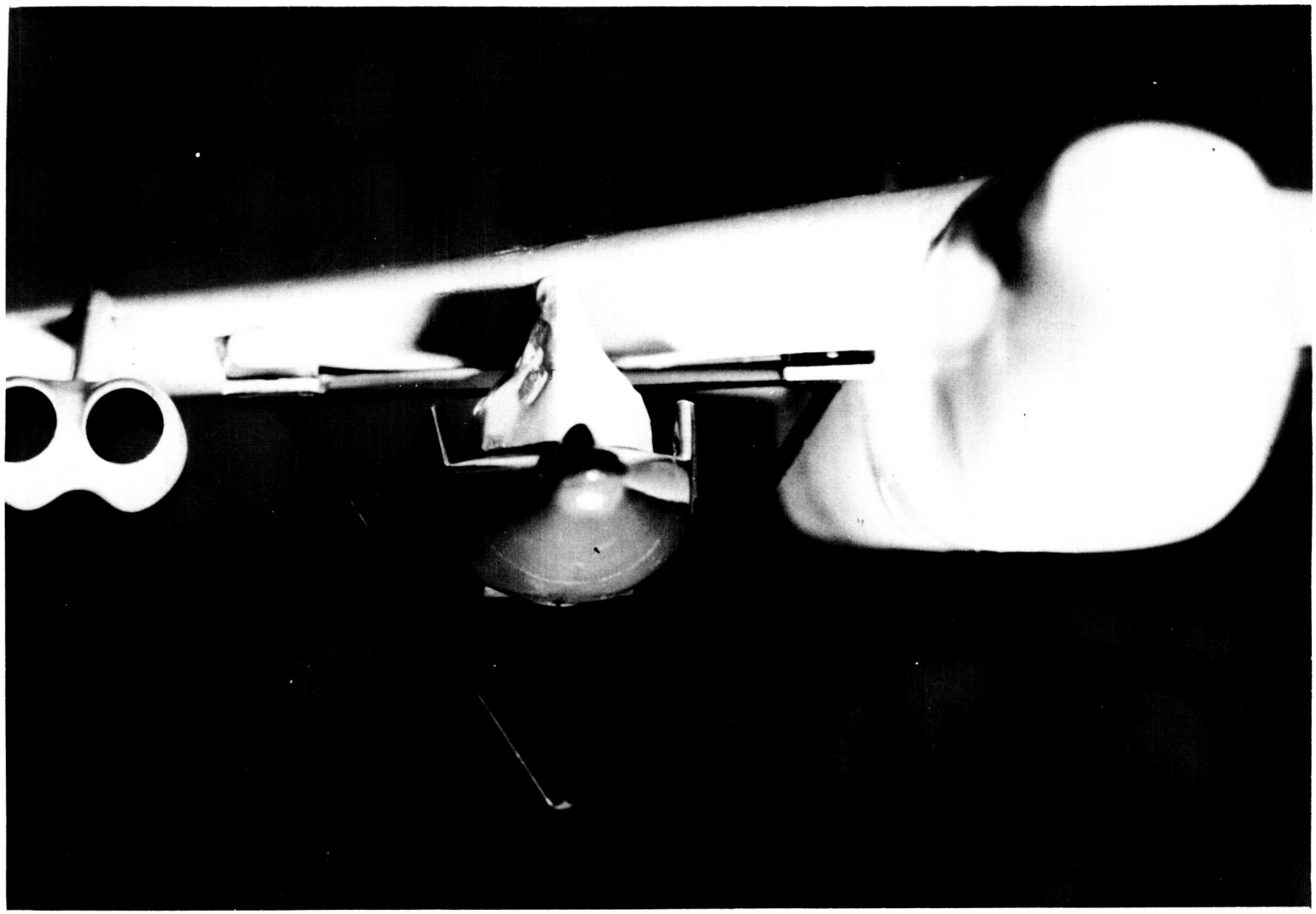

(a) z' = 0 feet (0 meters). L-64-8039

Figure 4.- Photographs of 0.025-scale M2-F2 and B-52 wind-tunnel models.

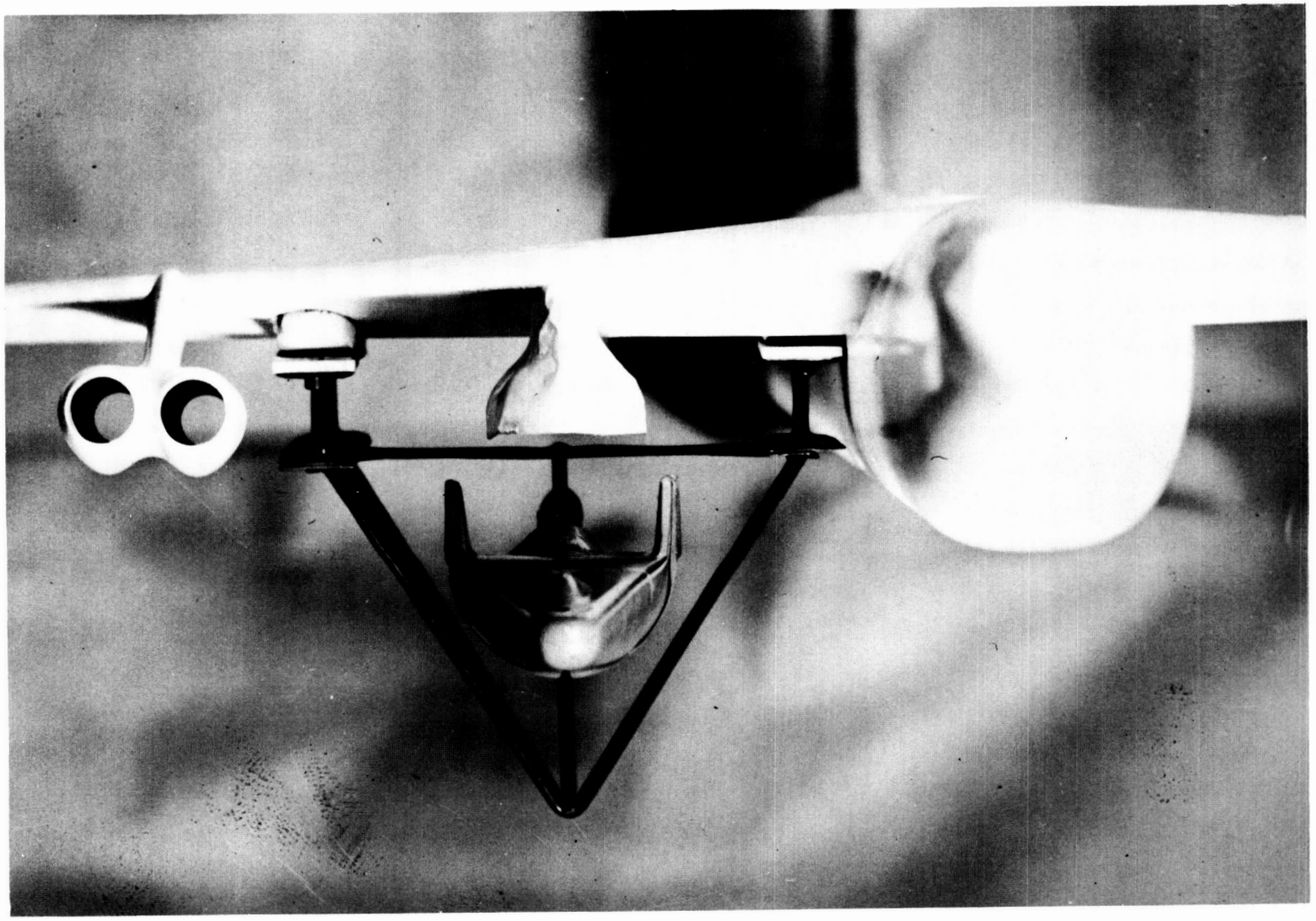

(b) z' = 4.0 feet (1.22 m) full scale. L-64-8042

Figure 4.- Continued.

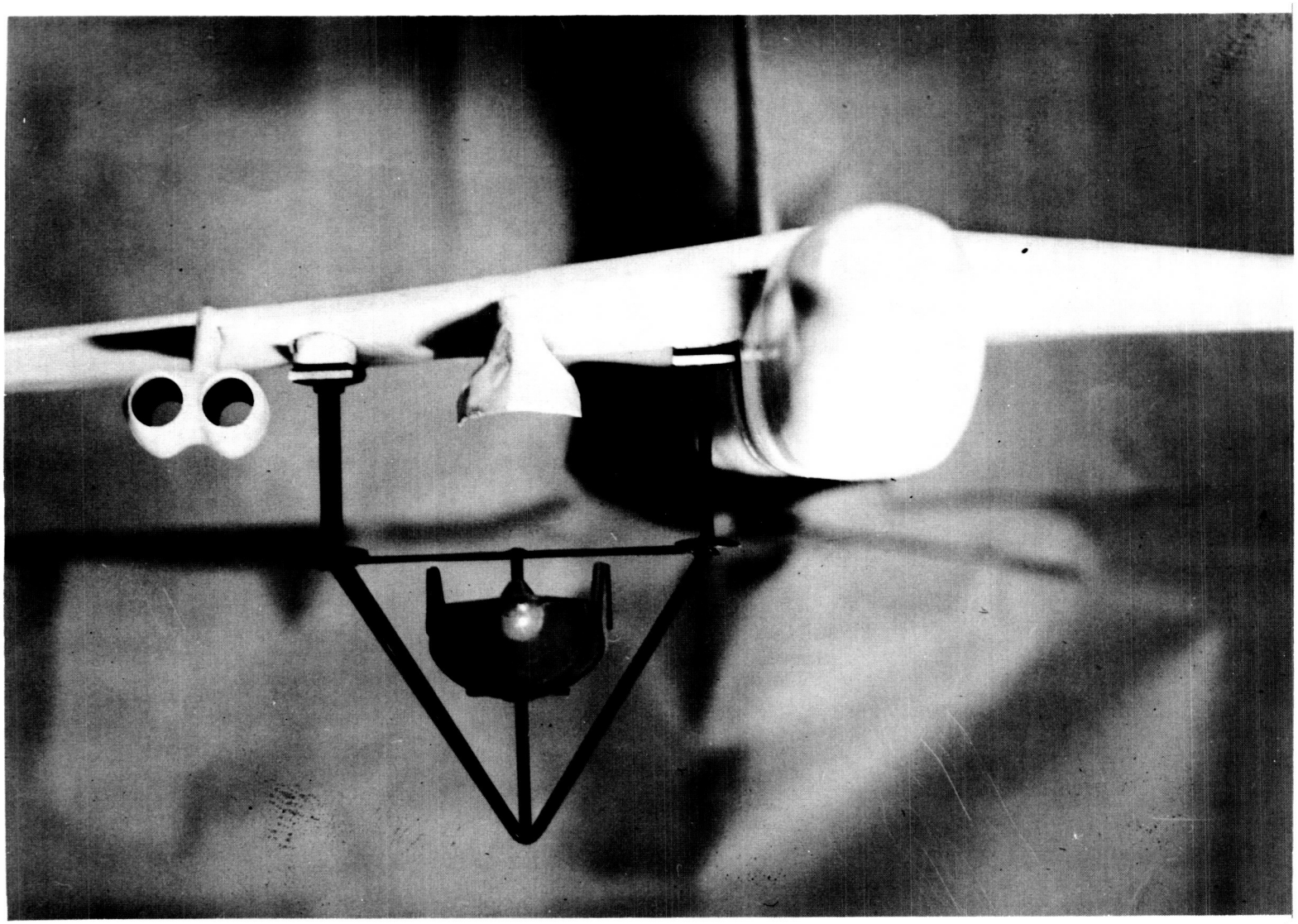

(c) z' = 10.0 feet (3.05 m) full scale. L-64-8046

Figure 4.- Concluded.

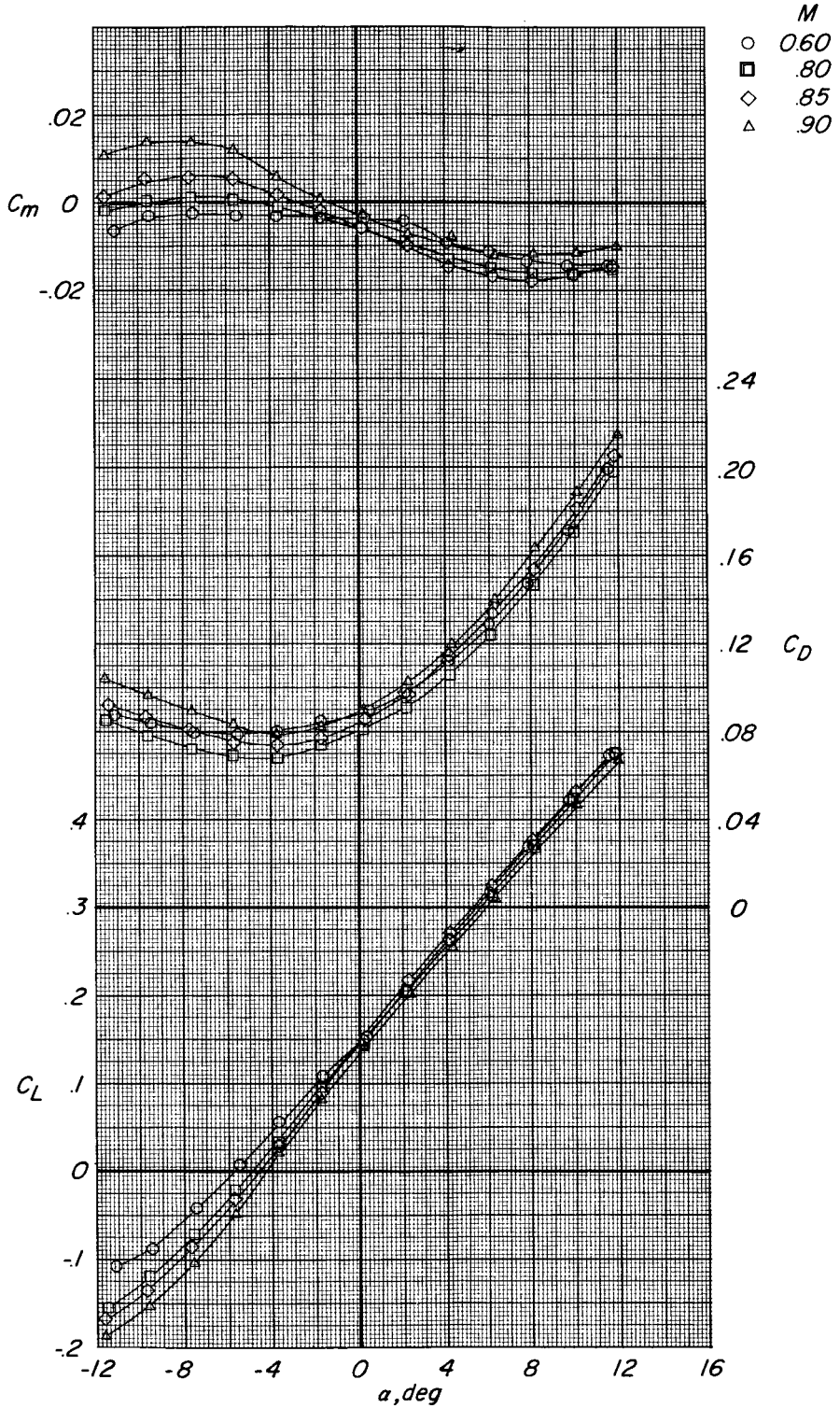

Figure 5.- Aerodynamic characteristics of M2-F2 model. $\delta_l = 30^0$; $\delta_u = -10^0$; 10^0 rudder flare.

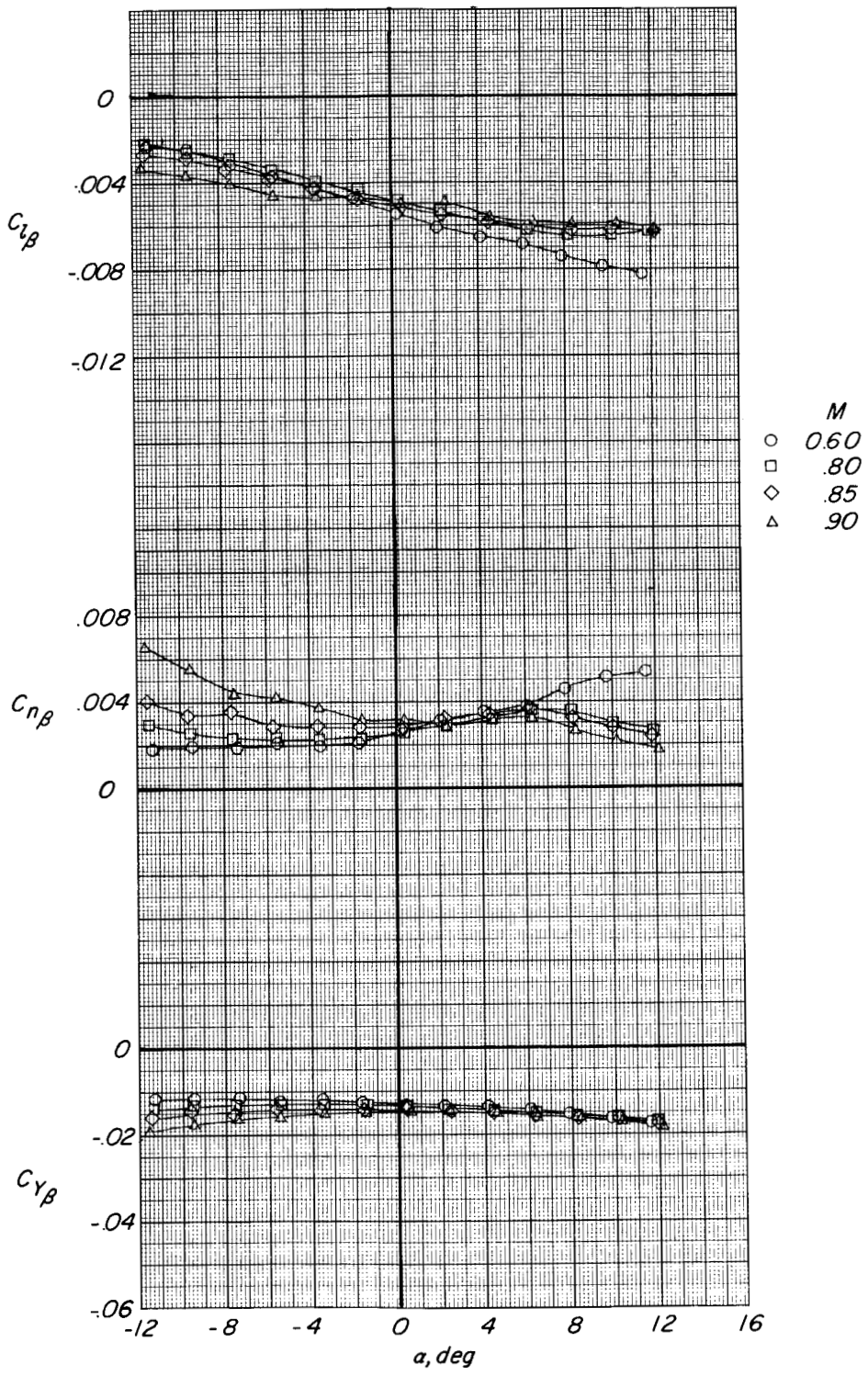

Figure 5.- Concluded.

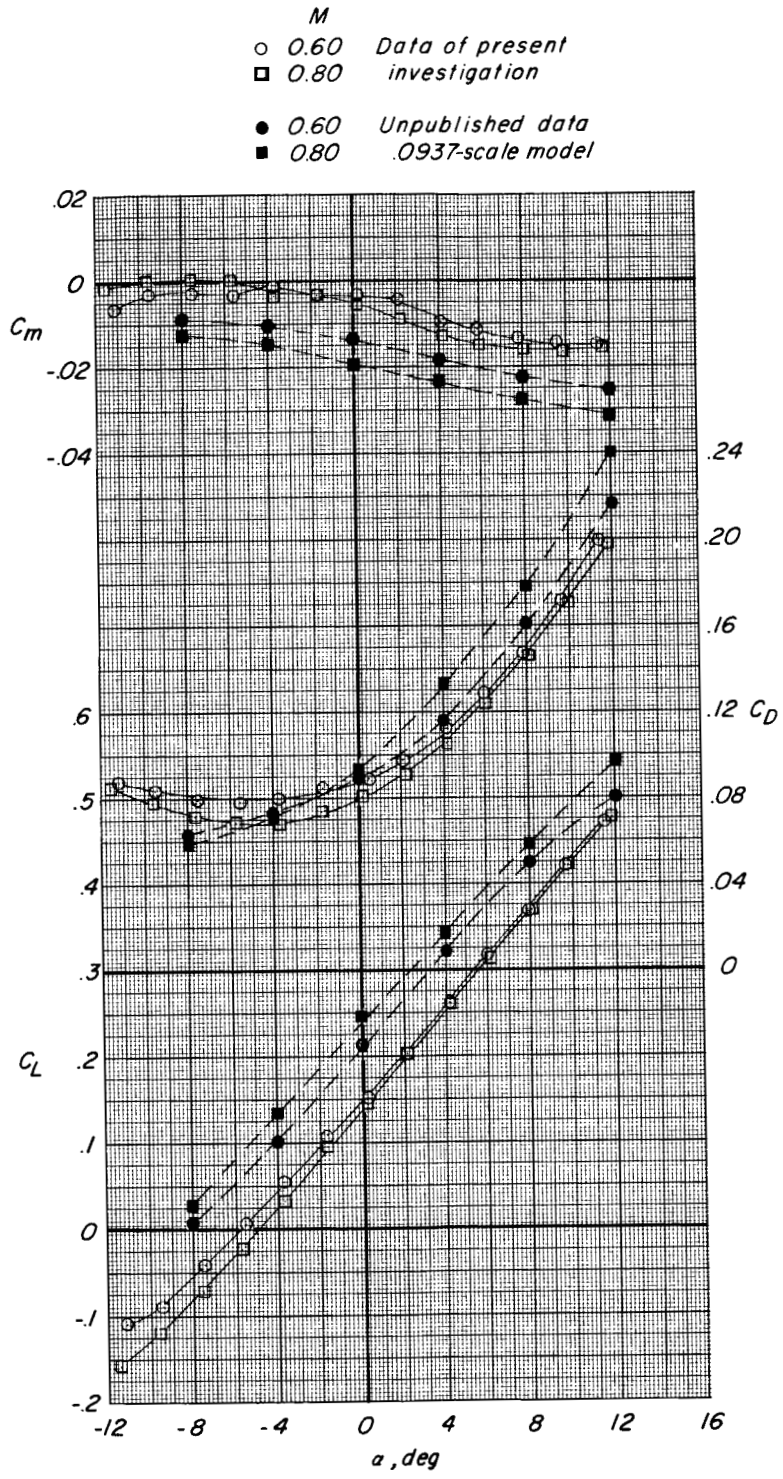

Figure 6.- Comparison of aerodynamic characteristics obtained on the 0.025-scale model of the M2-F2 in this study with unpublished data obtained on a 0.0937-scale model of the M2-F2. $\delta_\ell = 30^0$; $\delta_u = -10^0$; 10^0 rudder flare.

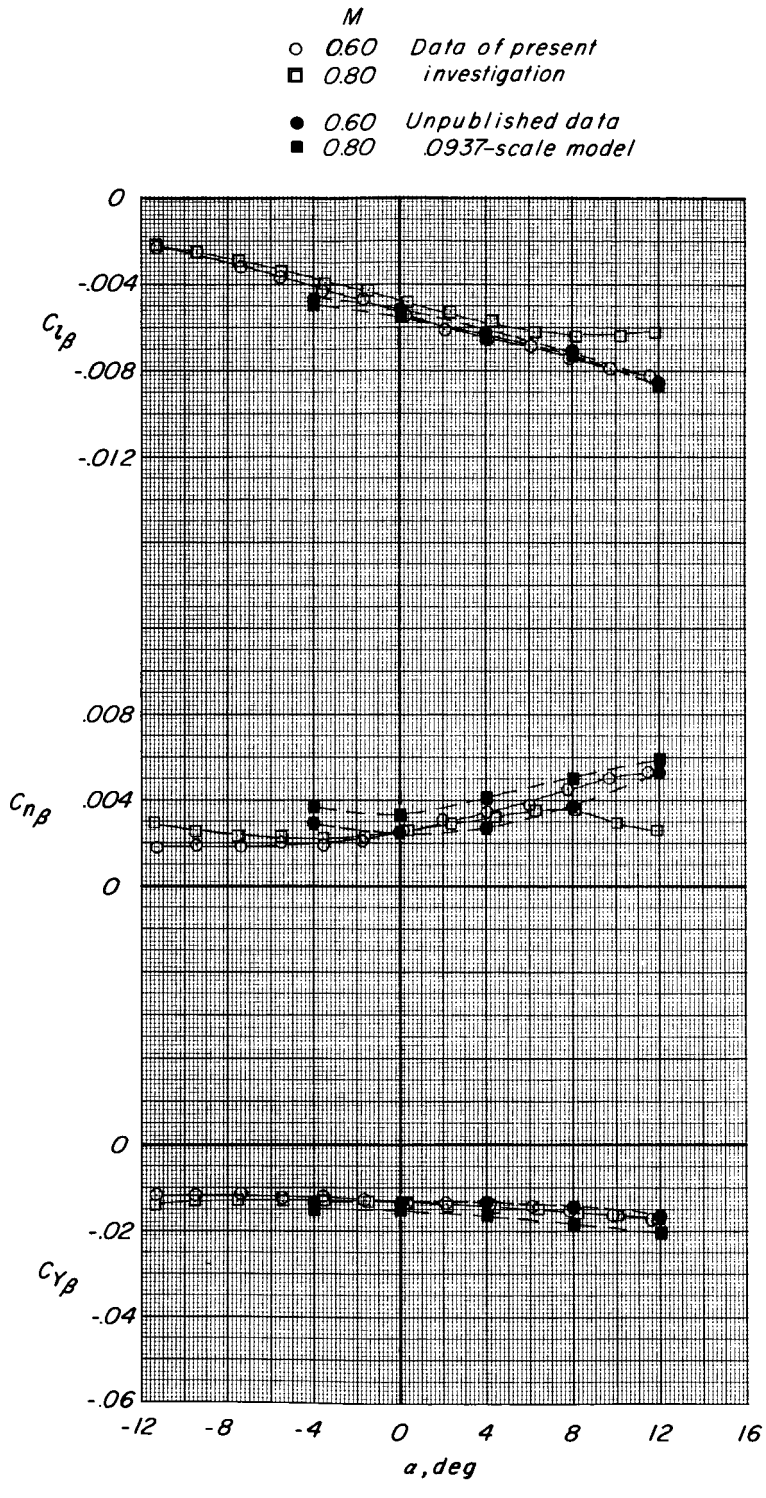

Figure 6.- Concluded.

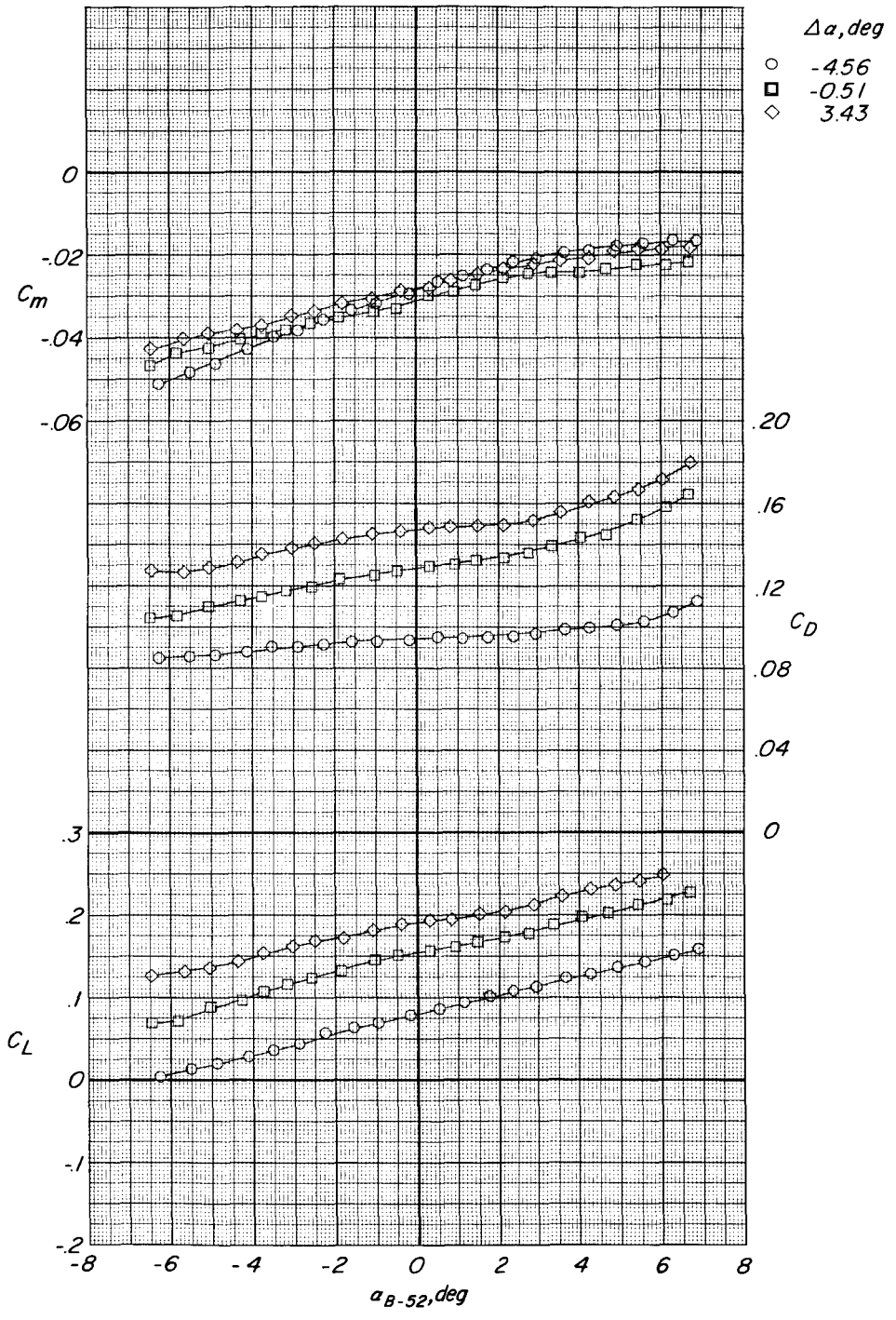

(a) z' = 0 feet (0 meters).

Figure 7.- Aerodynamic characteristics of M2-F2 model in presence of B-52 model. M = 0.60; $\Delta\beta = 0.75^0$; $\Phi = 0^0$; $\delta_l = 30^0$; $\delta_u = -10^0$; 10^0 rudder flare.

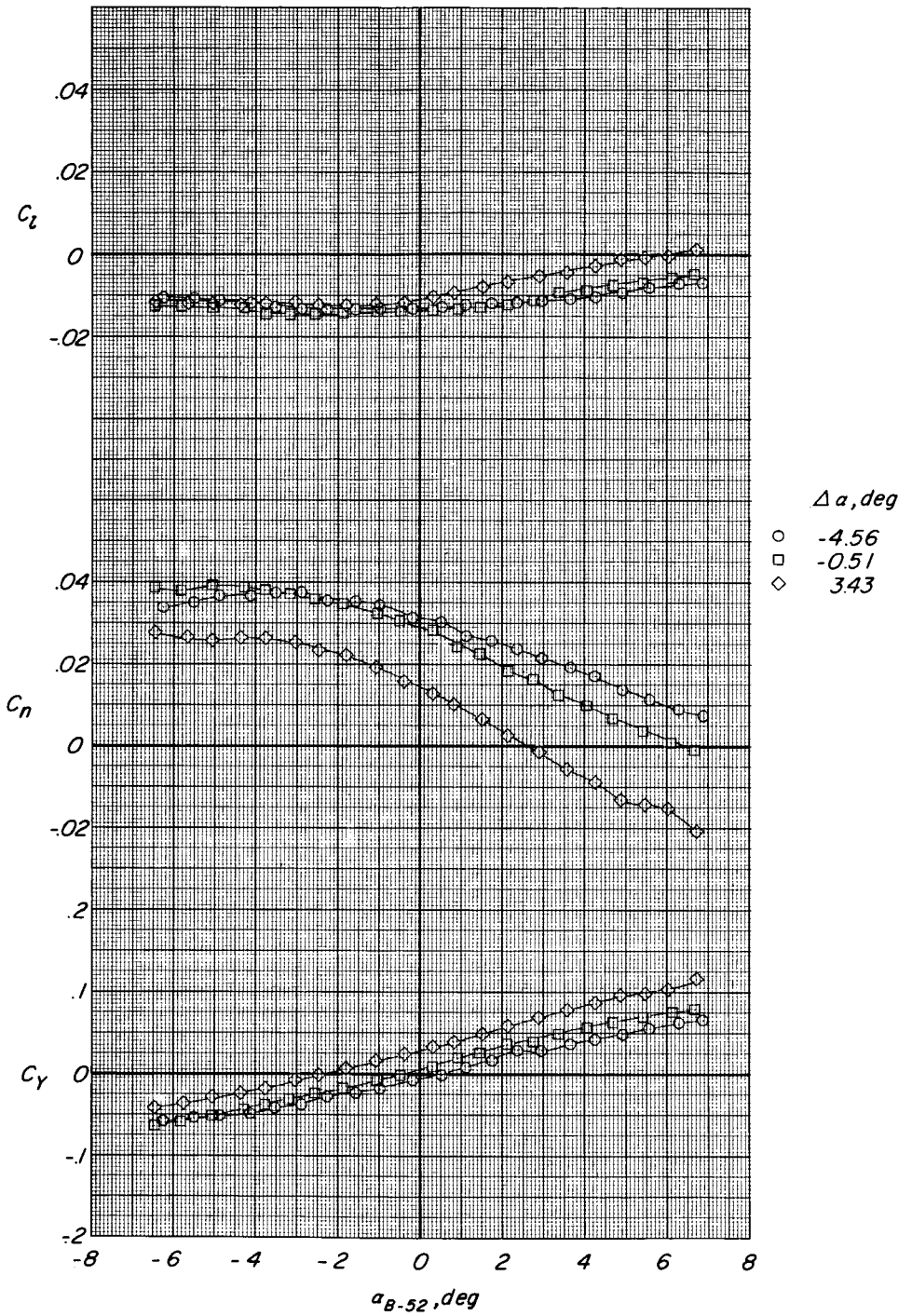

(a) Concluded.

Figure 7.- Continued.

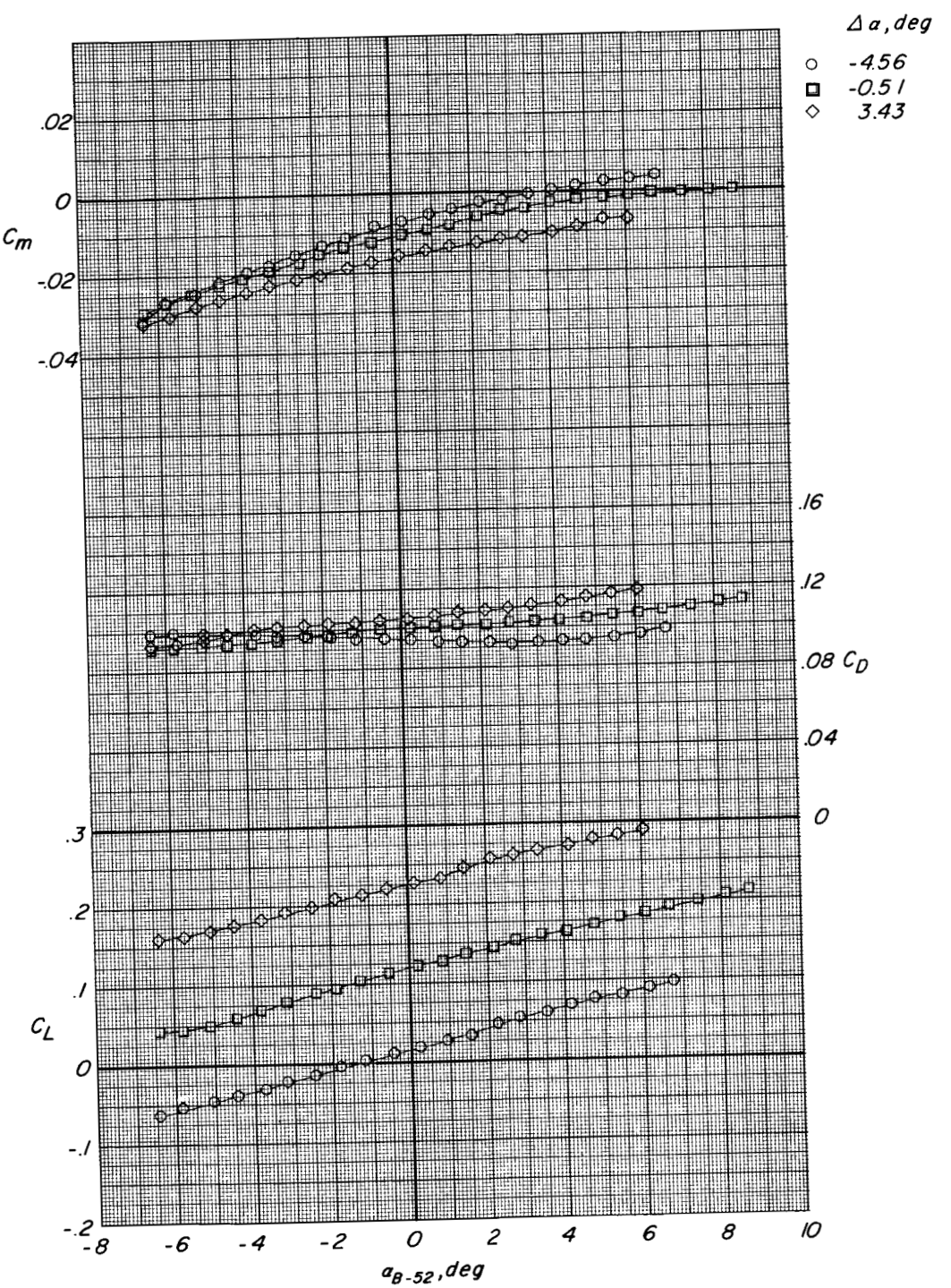

(b) z' = 4.0 feet (1.22 m) full scale.

Figure 7. Continued.

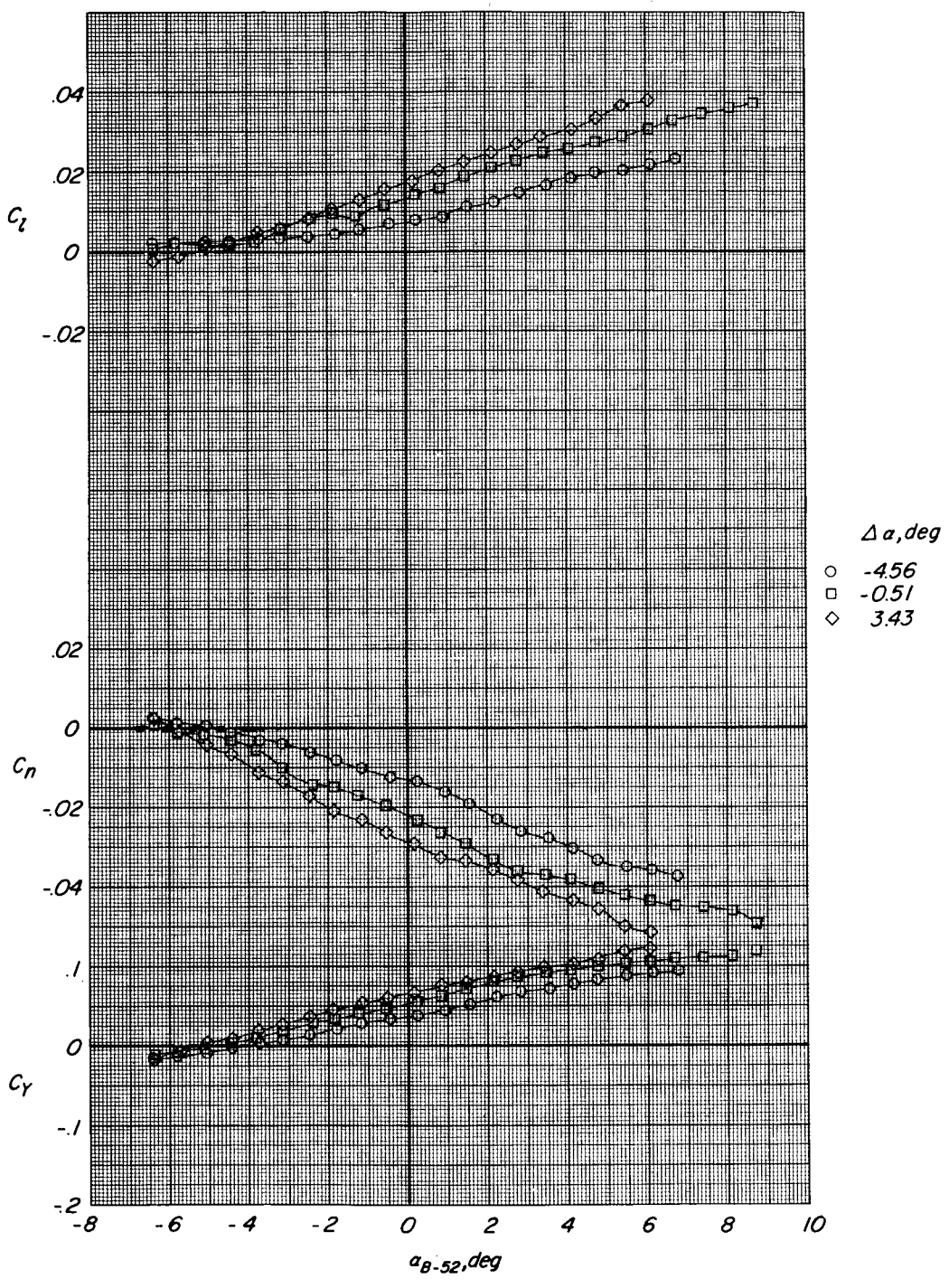

(b) Concluded.

Figure 7.- Continued.

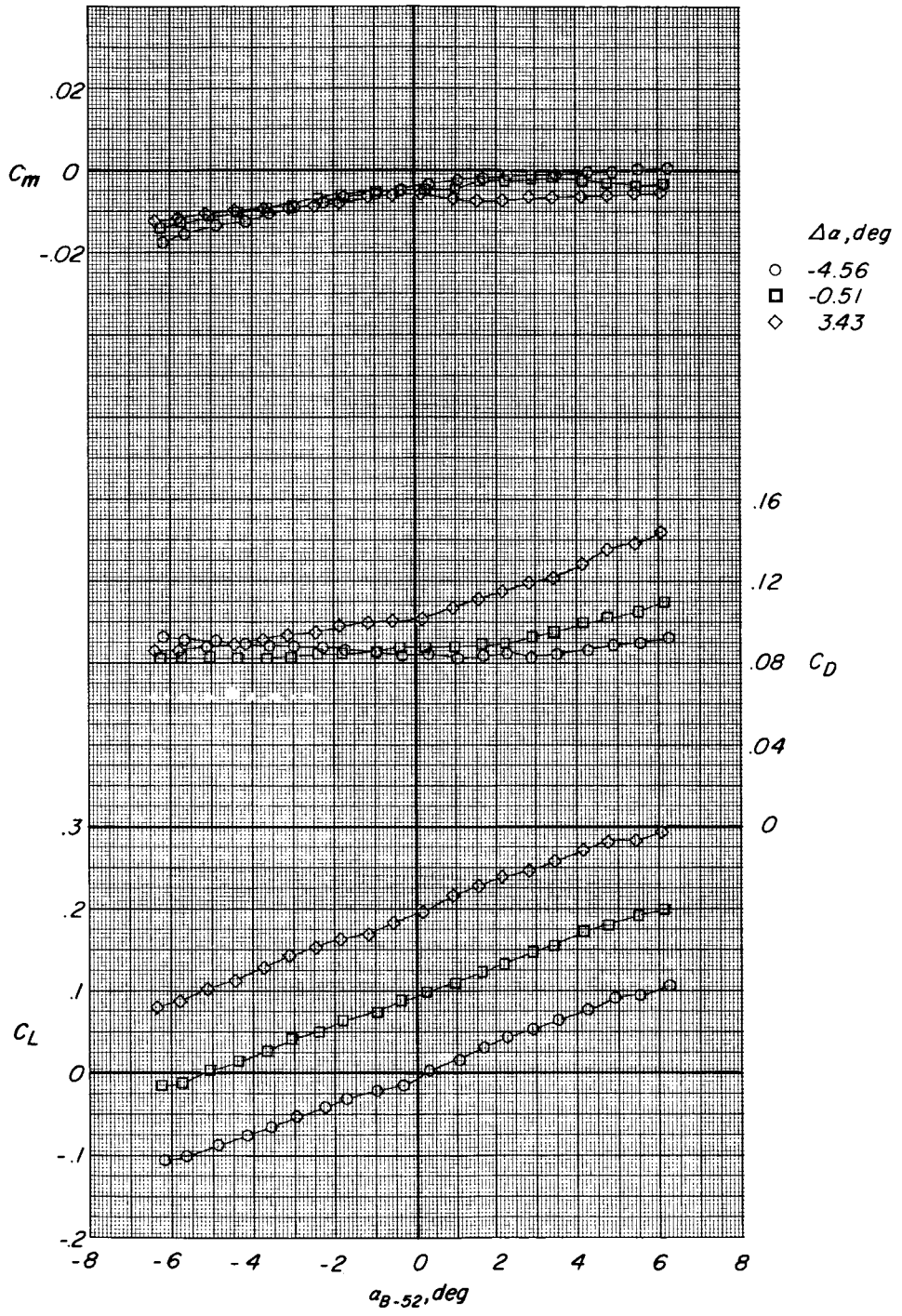

(c) z' = 10.0 feet (3.05 m) full scale.

Figure 7.- Continued.

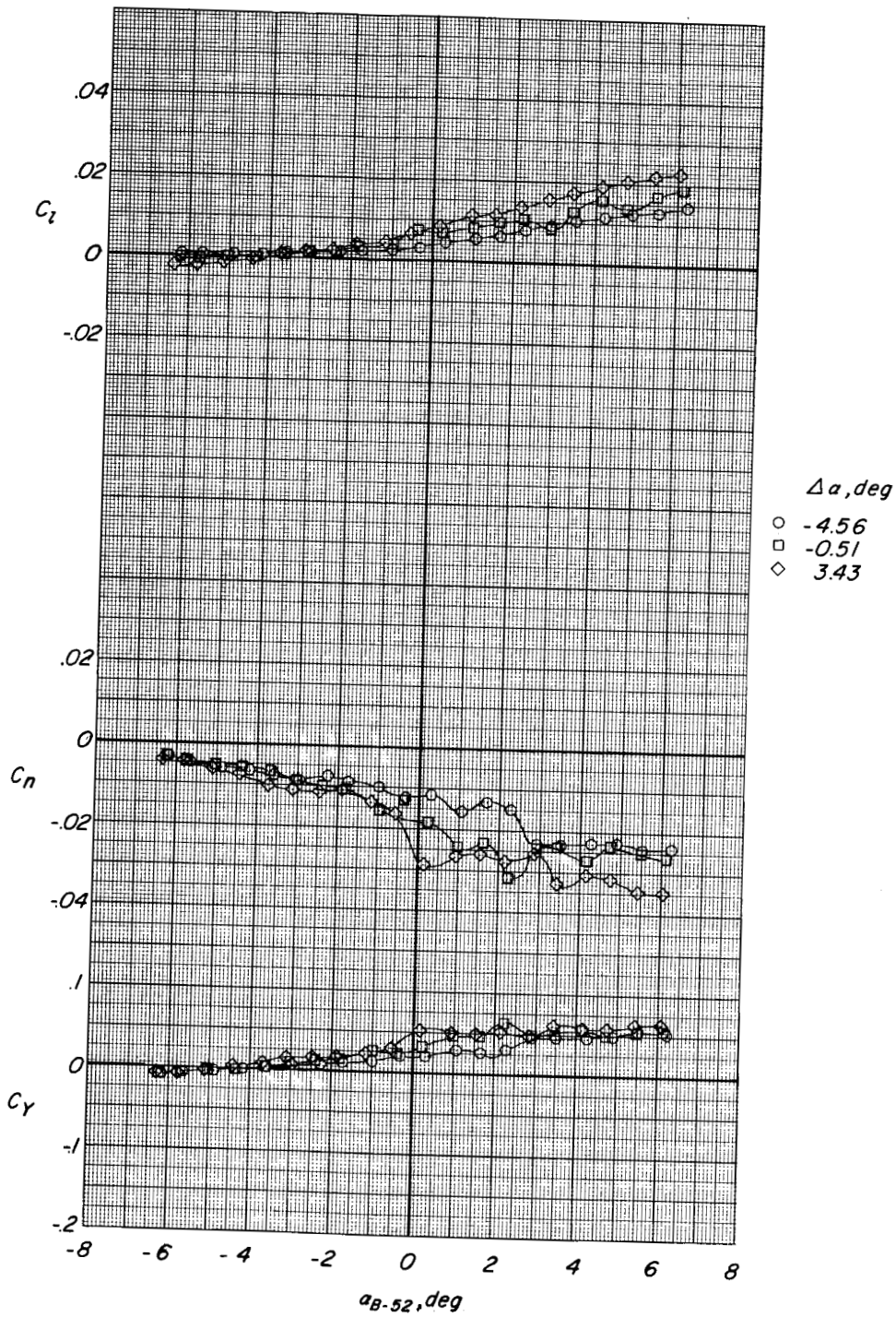

(c) Concluded.

Figure 7.- Concluded.

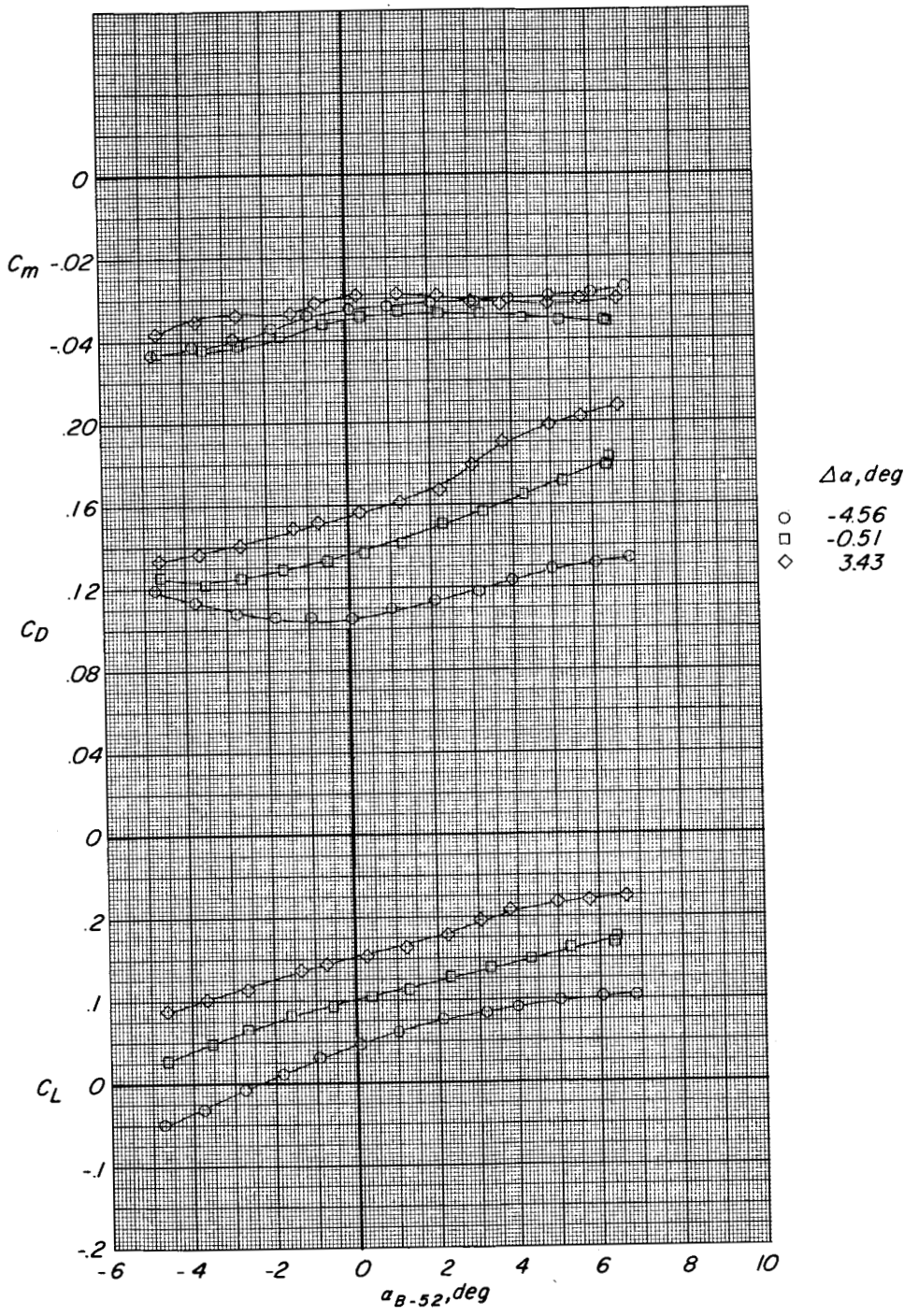

(a) z' = 0 feet (0 meters).

Figure 8.- Aerodynamic characteristics of M2-F2 model in presence of B-52 model. M = 0.80; $\Delta\beta = 0.75^0$; $\Phi = 0^0$; $\delta_\ell = 30^0$; $\delta_u = -10^0$; 10^0 rudder flare.

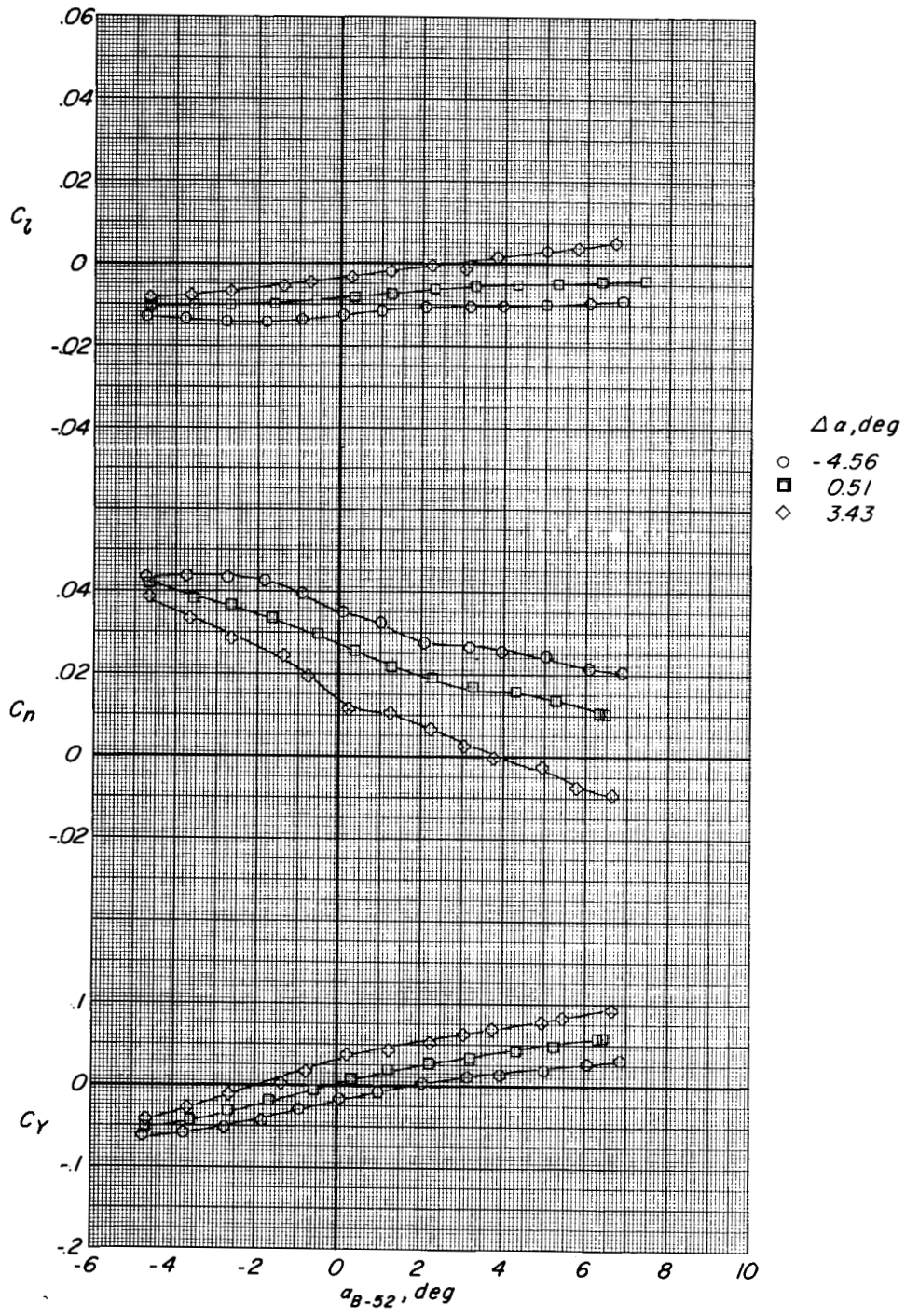

(a) Concluded.

Figure 8.- Continued.

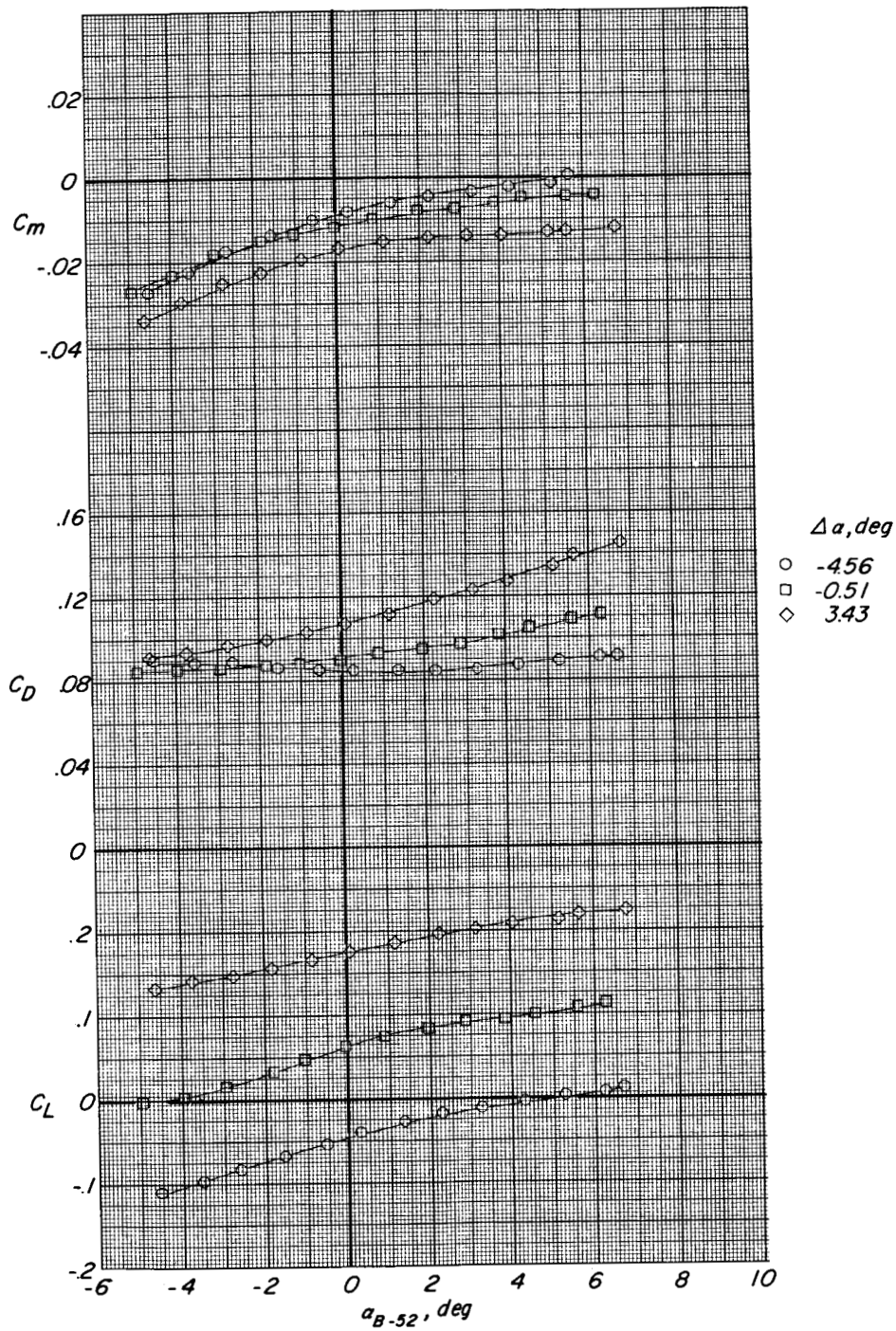

(b) $z' = 4.0$ feet (1.22 m) full scale.

Figure 8.- Continued.

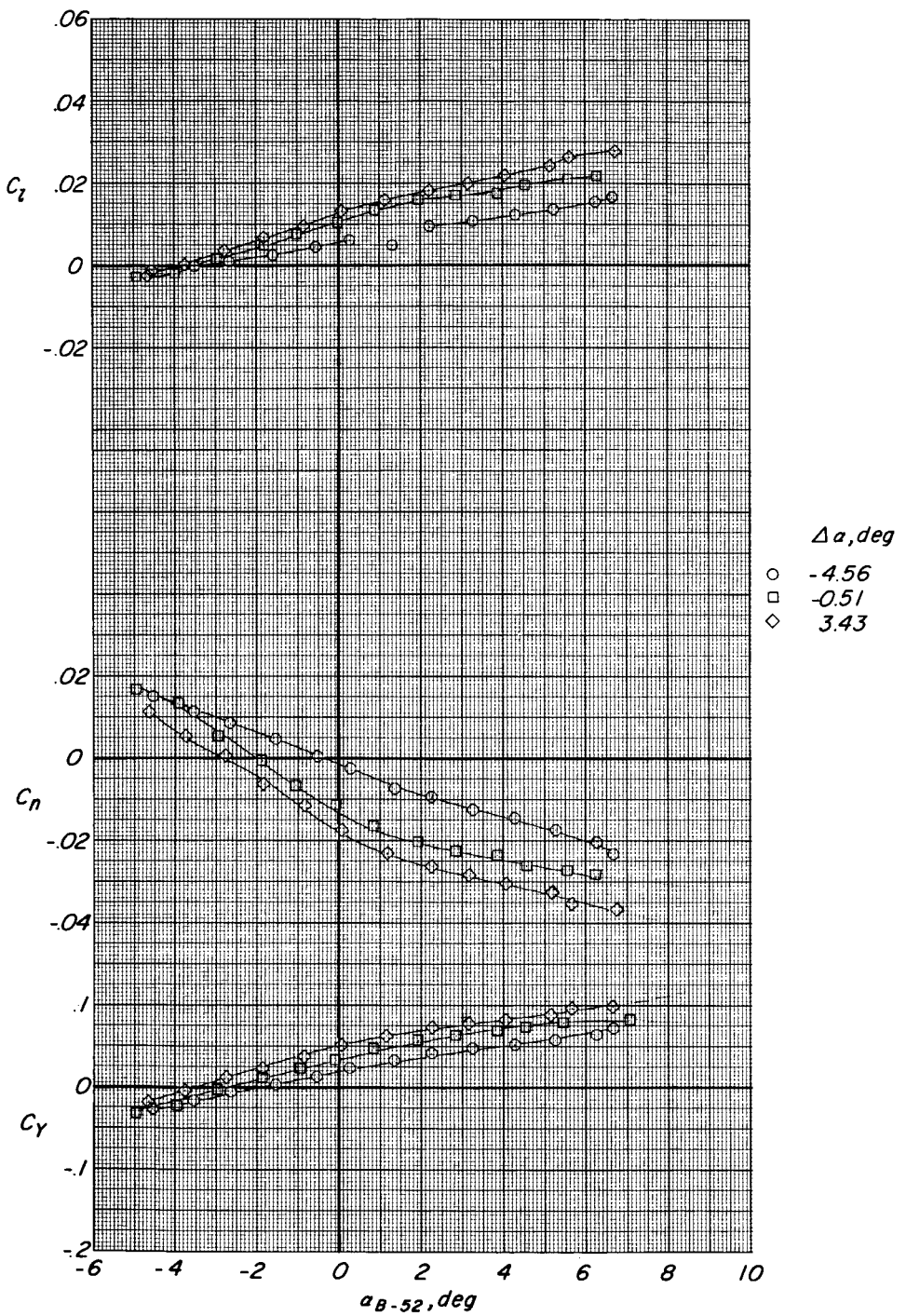

(b) Concluded.

Figure 8.- Continued.

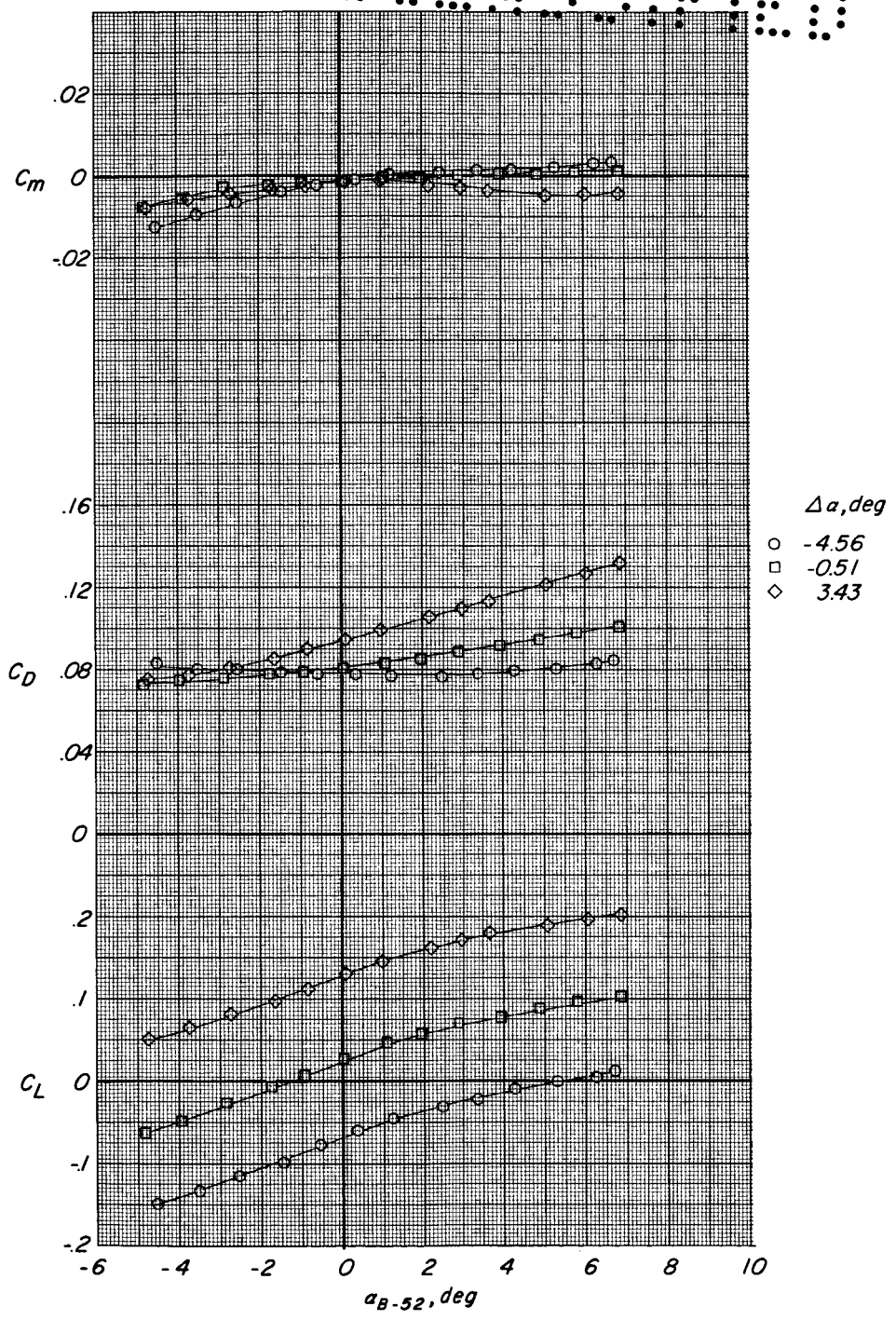

(c) z' = 10.0 feet (3.05 m) full scale.

Figure 8.- Continued.

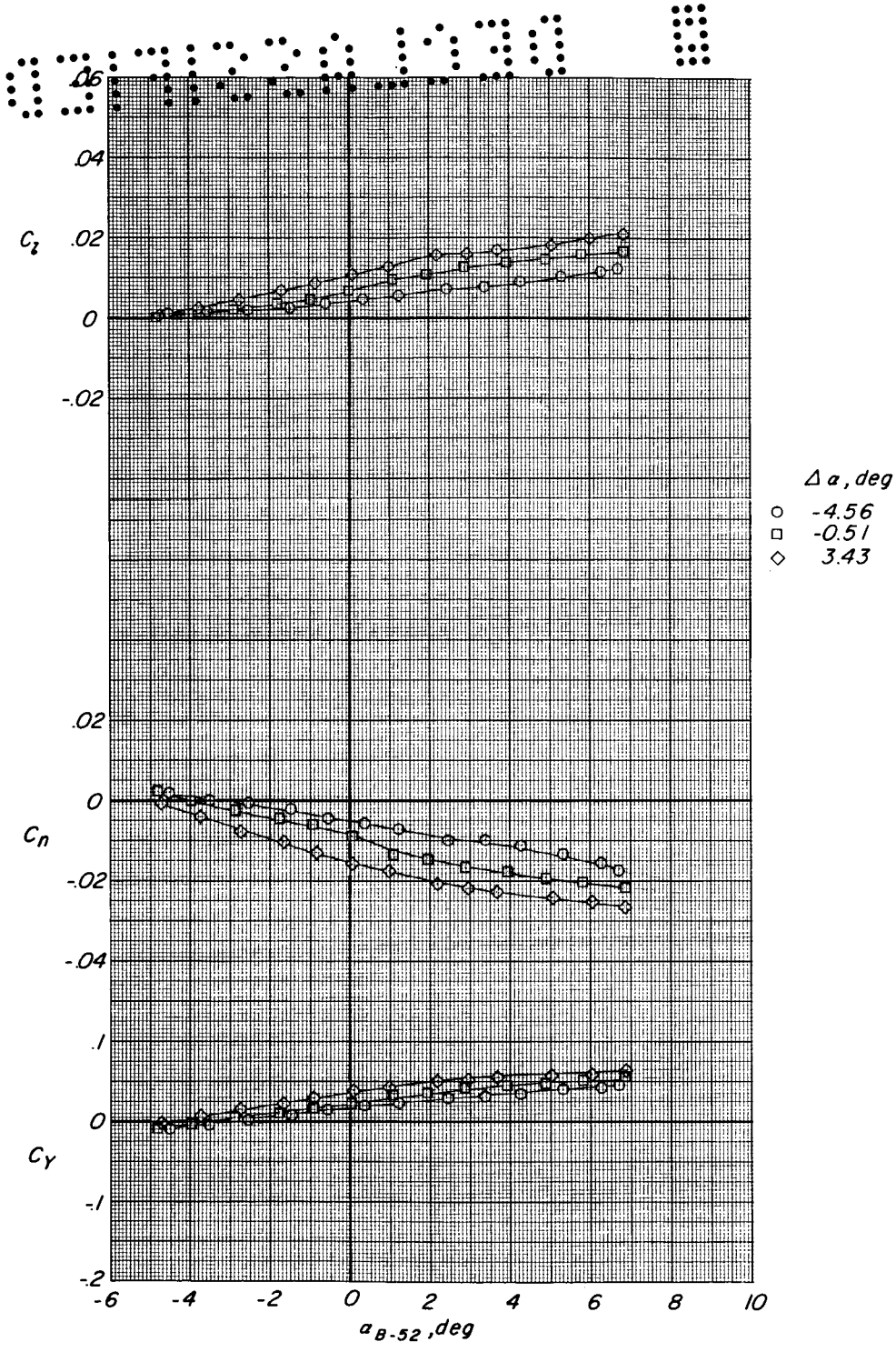

(c) Concluded.

Figure 8.- Concluded.

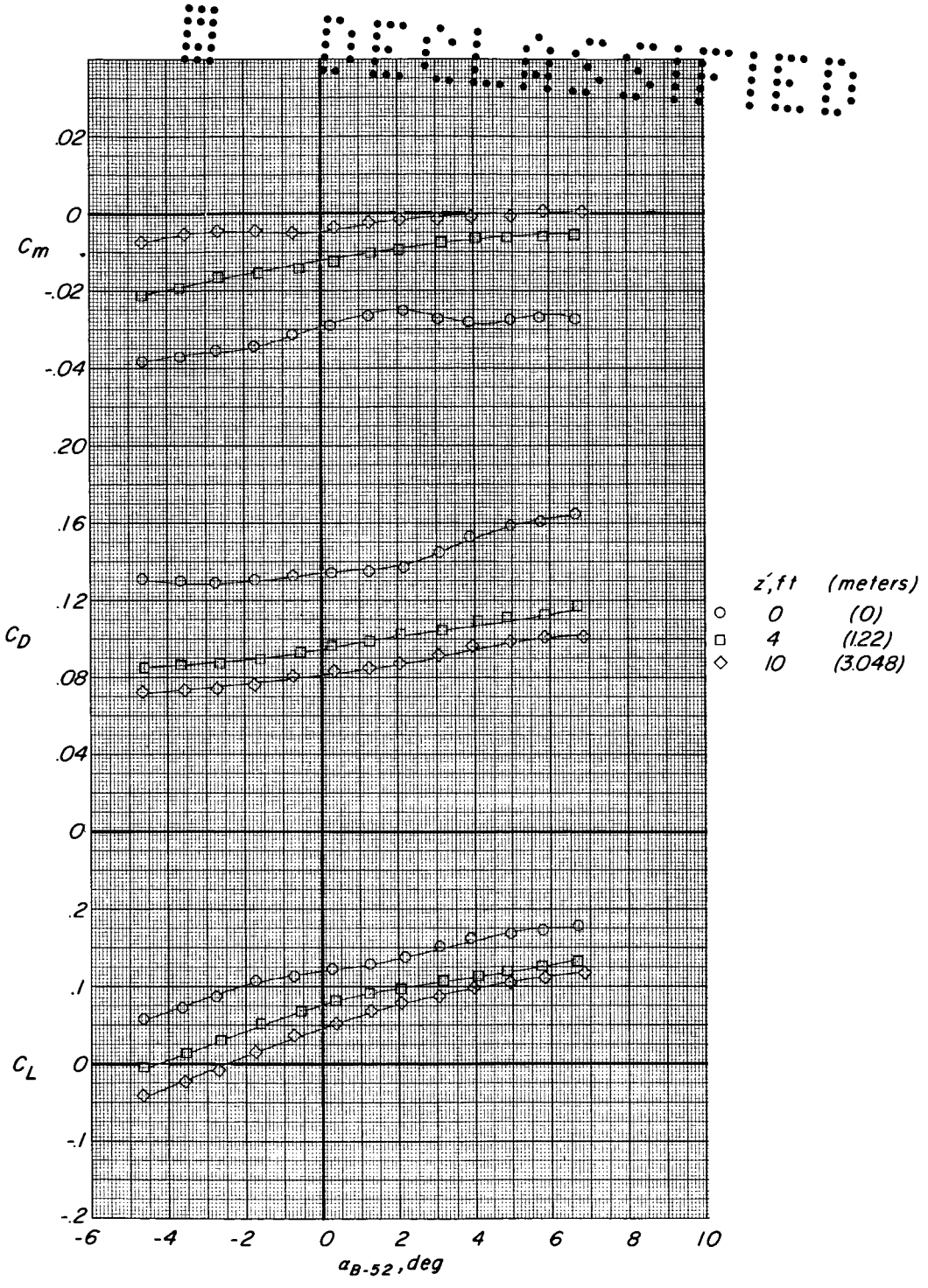

(a) $\Delta\beta = 6.40^{0}$.

Figure 9.- Effect of sideslipping of M2-F2 model in presence of B-52 model. $M = 0.80$; $\Delta\alpha = 0^{0}$; $\Phi = 0^{0}$; $\delta_{\ell} = 30^{0}$; $\delta_{u} = -10^{0}$; 10^{0} rudder flare.

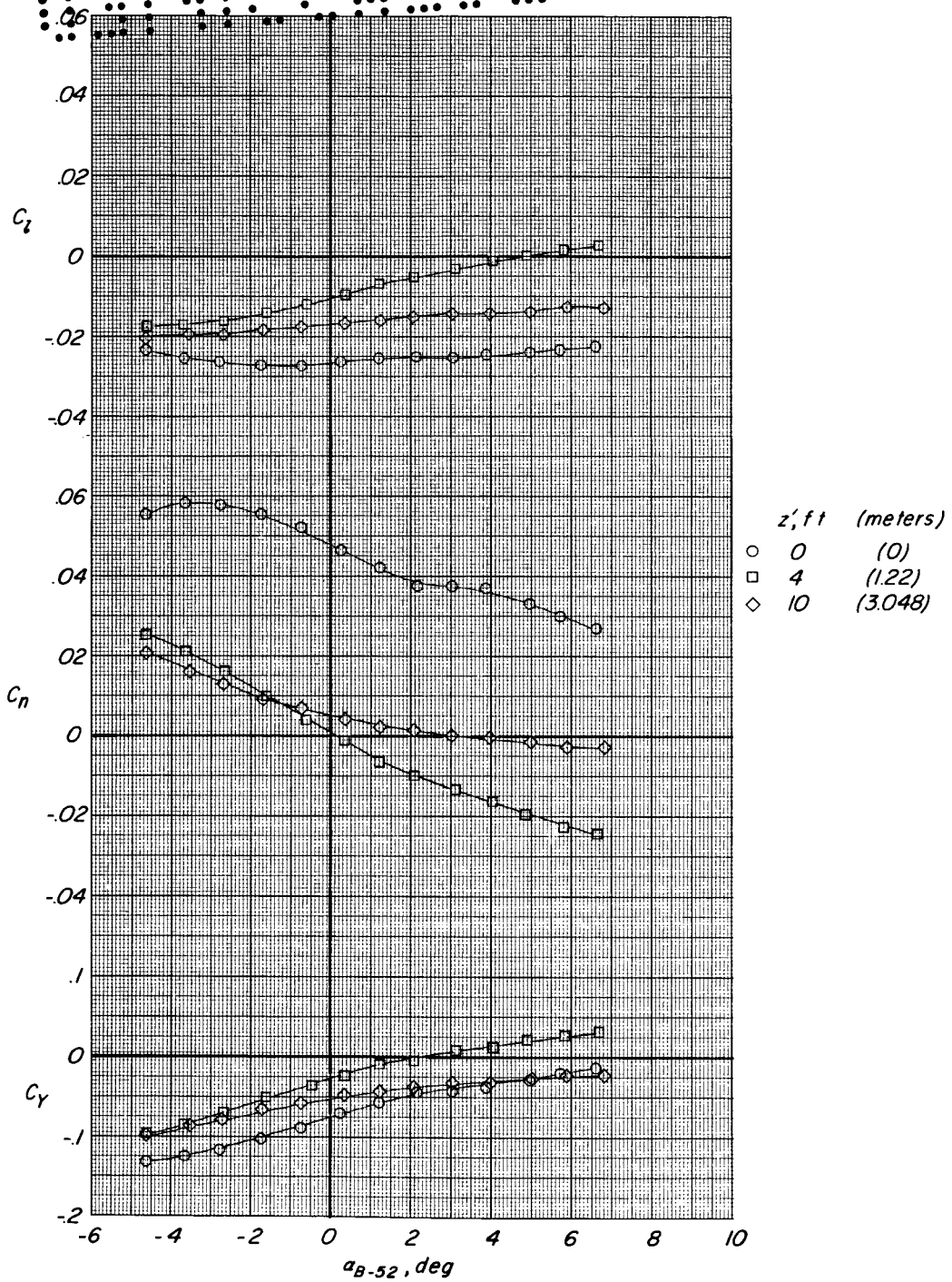

(a) Concluded.

Figure 9.- Continued.

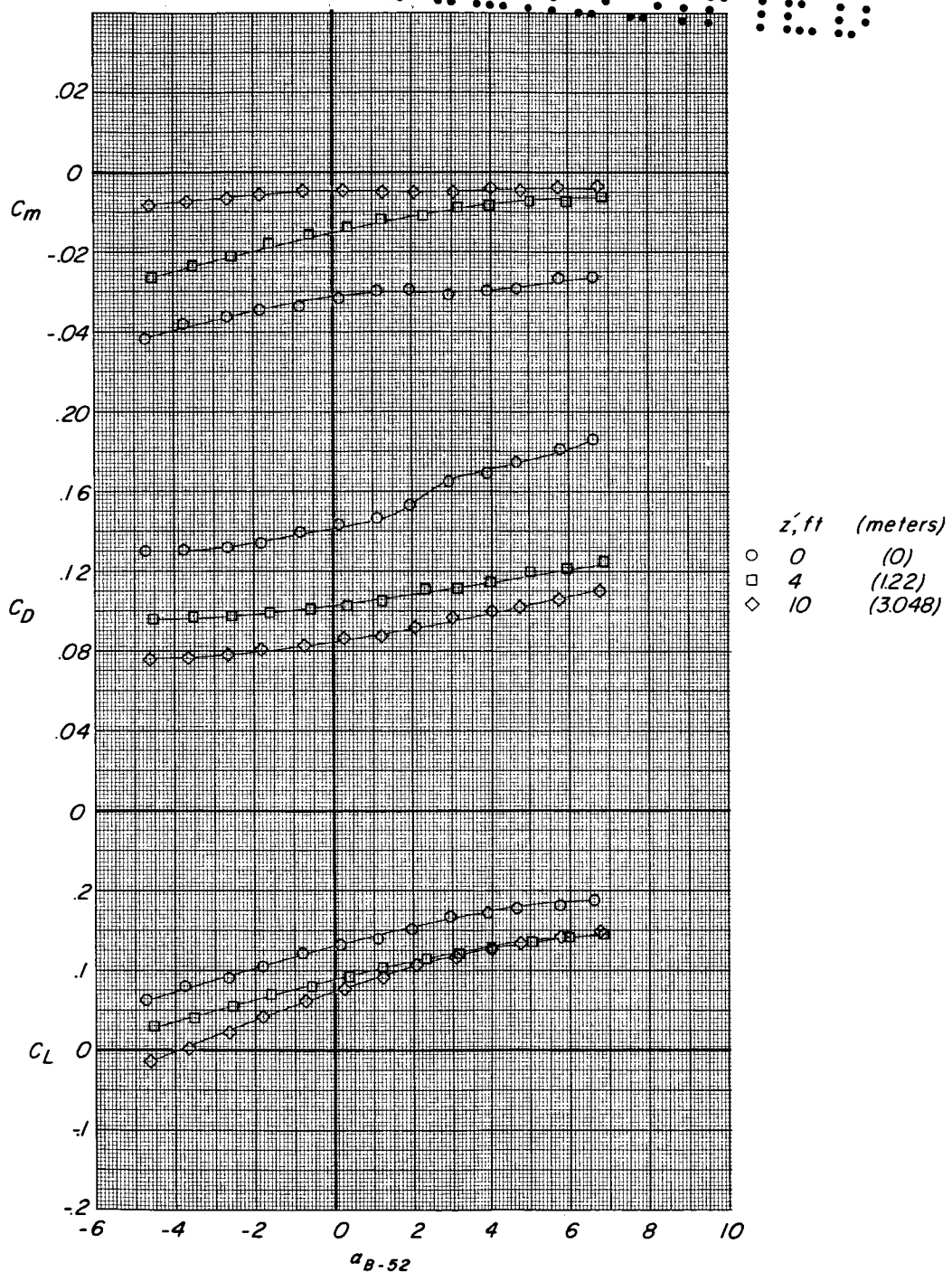

(b) $\Delta\beta = -3.92^{o}$.

Figure 9.- Continued.

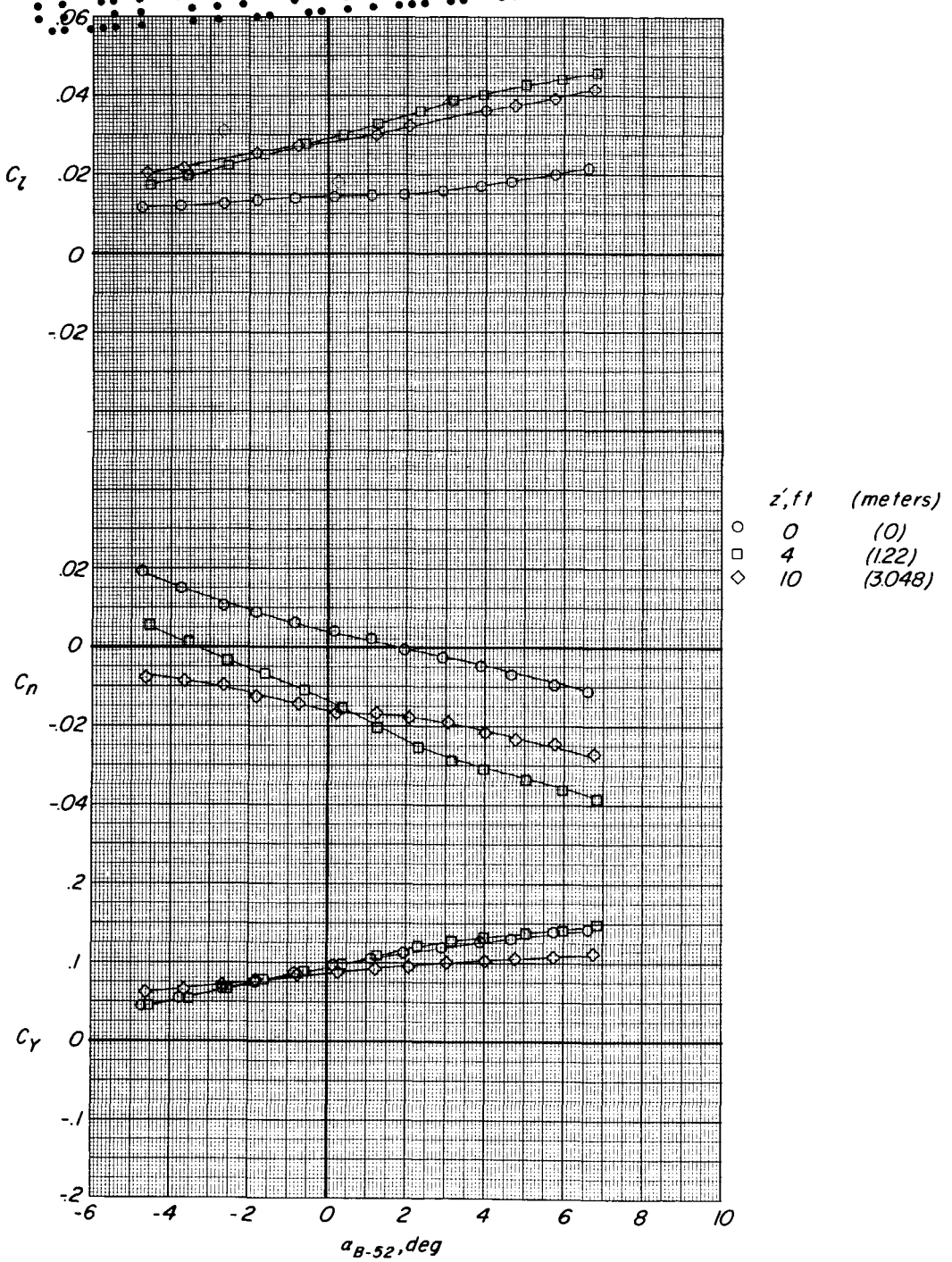

(b) Concluded.

Figure 9.- Concluded.

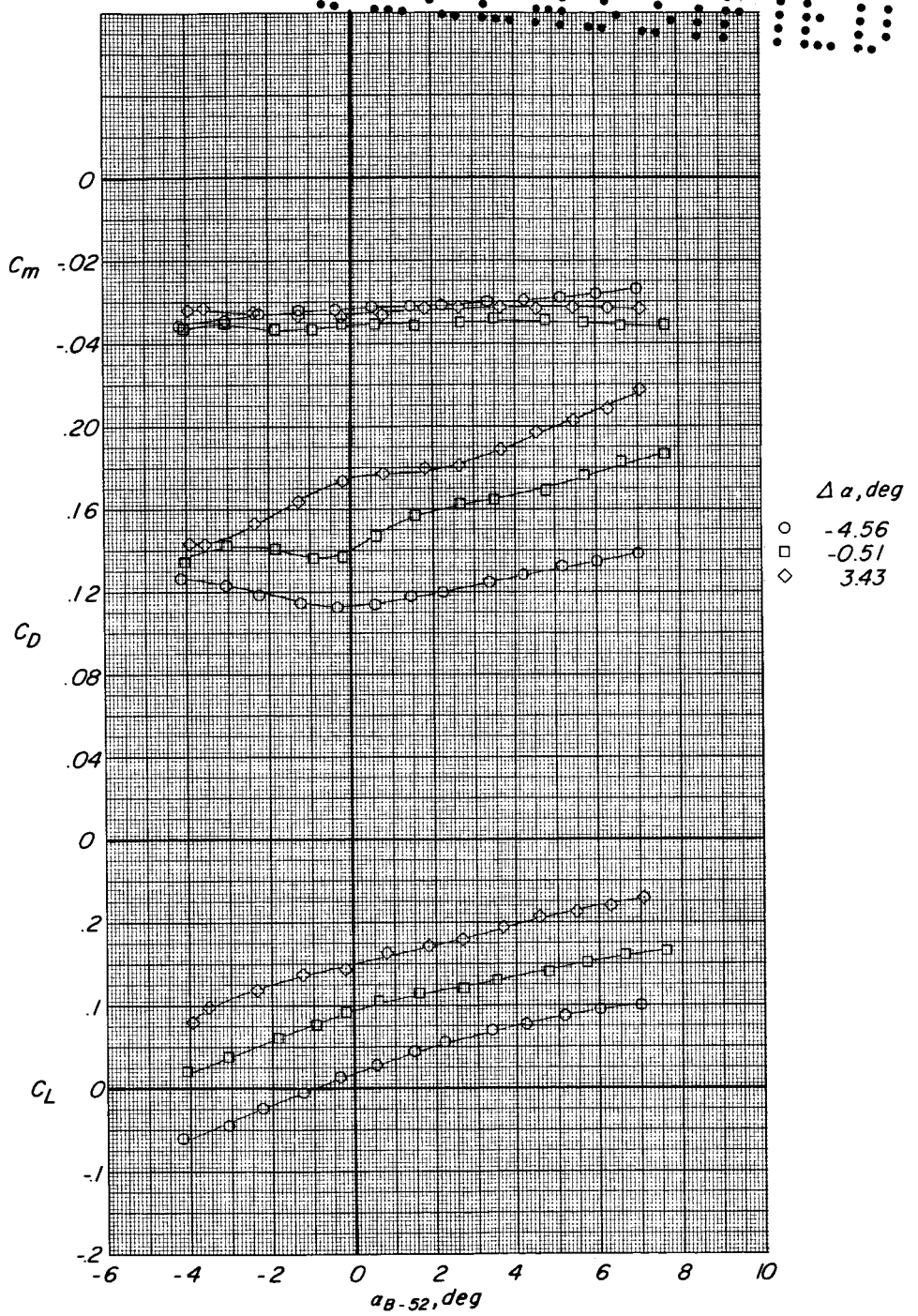

(a) $z' = 0$ feet (0 meters).

Figure 10.- Aerodynamic characteristics of M2-F2 model in presence of B-52 model. $M = 0.85$; $\Delta\beta = 0.75^0$; $\Phi = 0^0$; $\delta_l = 30^0$; $\delta_u = -10^0$; 10^0 rudder flare.

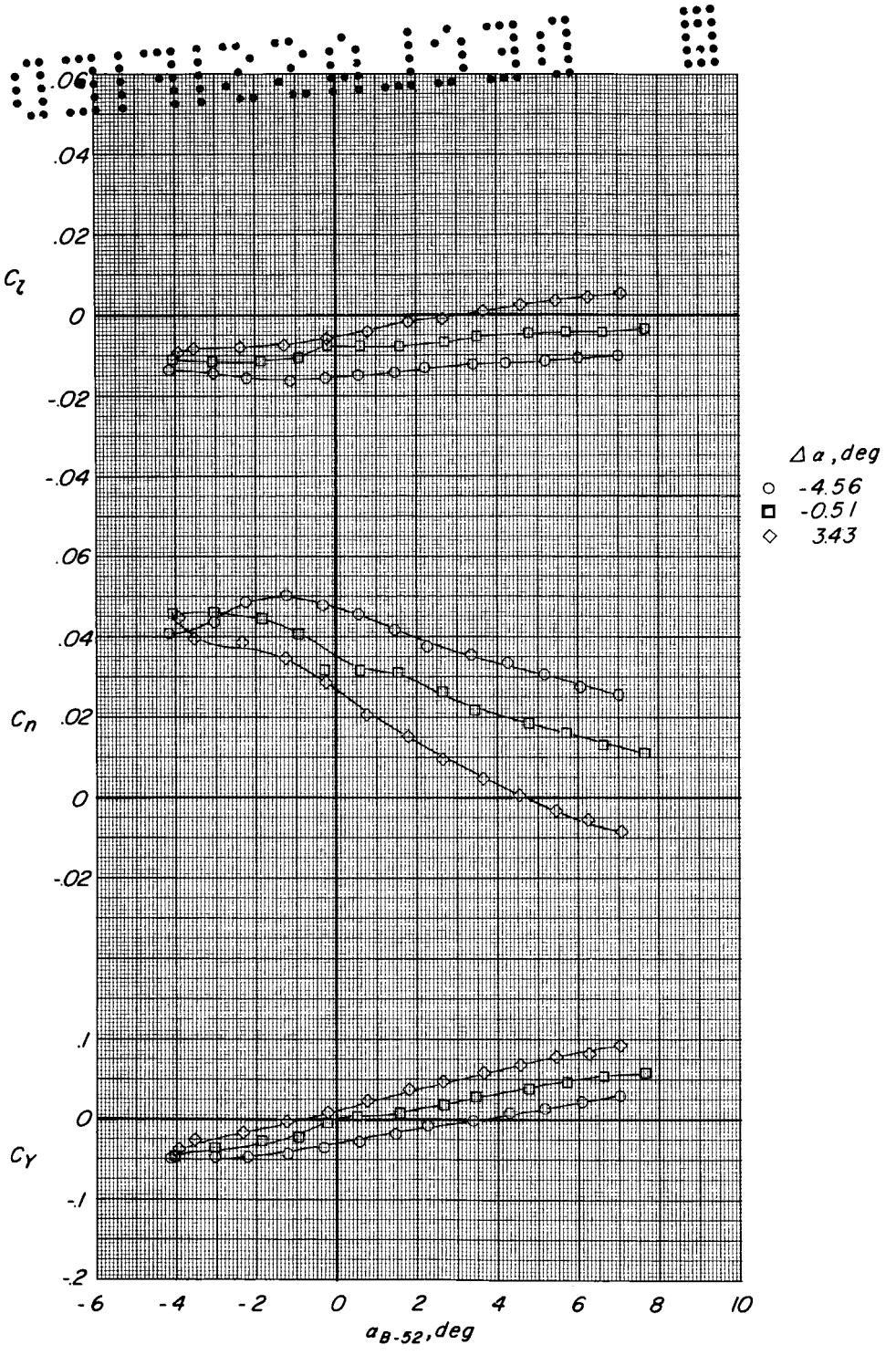

(a) Concluded.

Figure 10.- Continued.

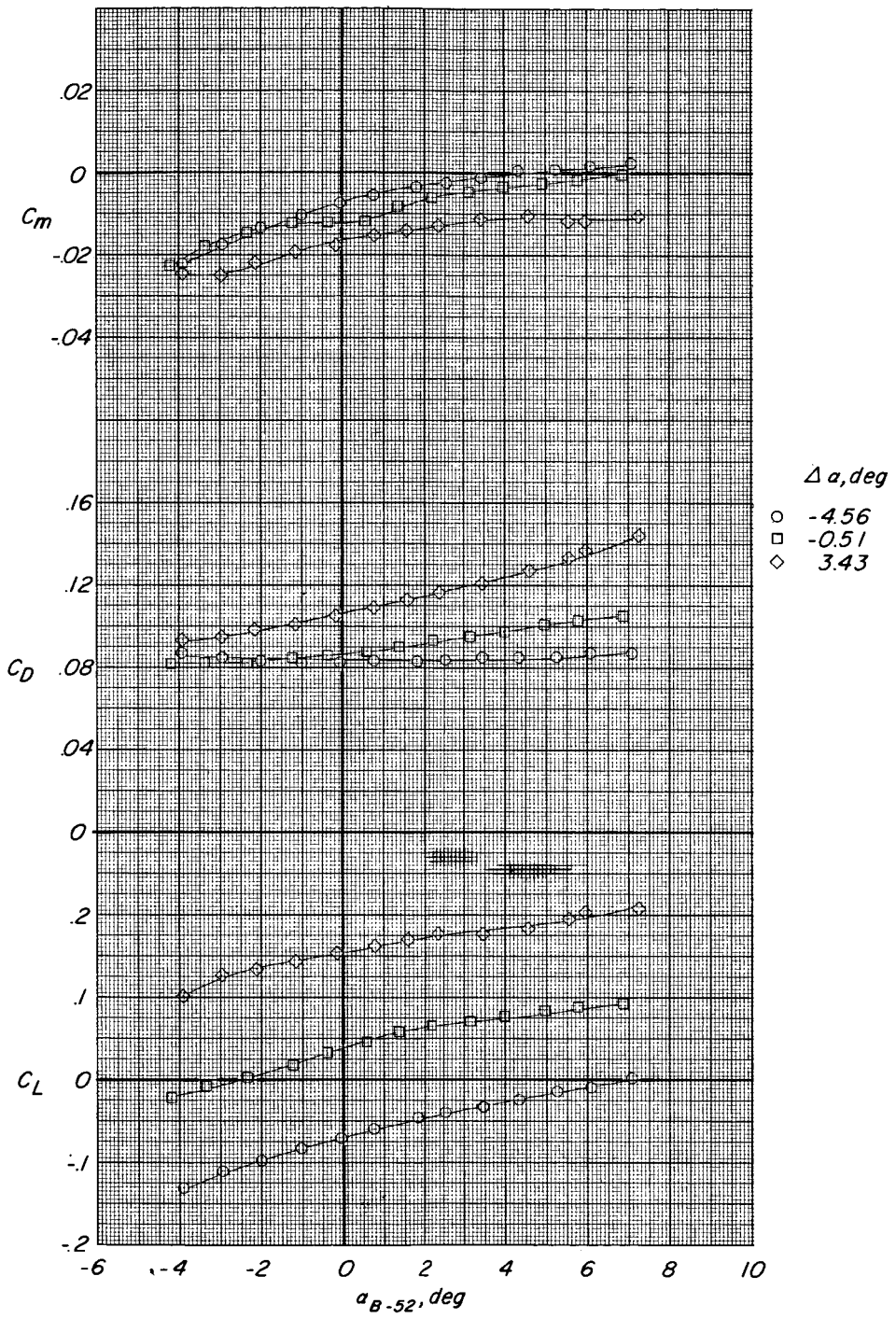

(b) z' = 4.0 feet (1.22 m) full scale.

Figure 10.- Continued.

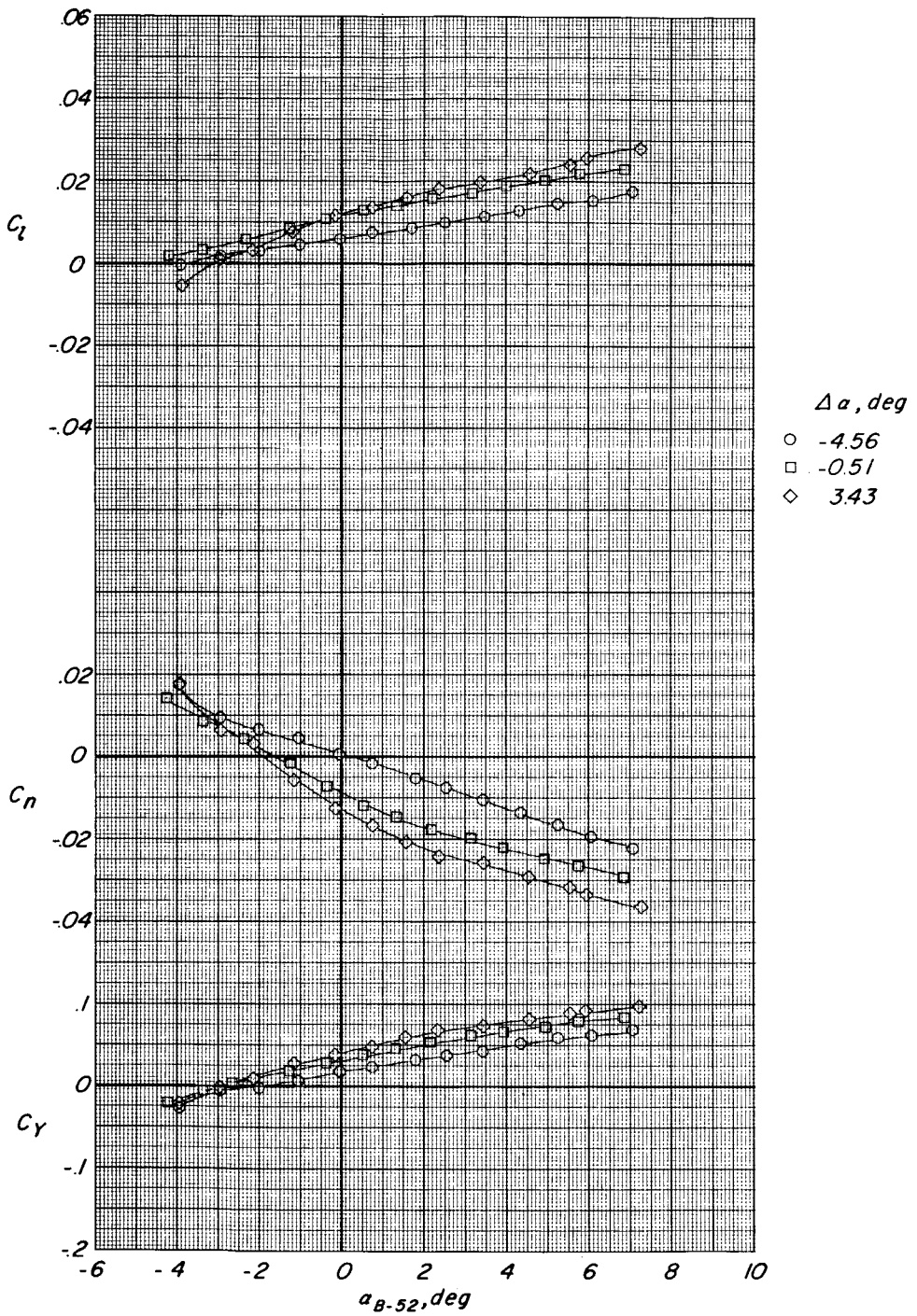

(b) Concluded.

Figure 10.- Continued.

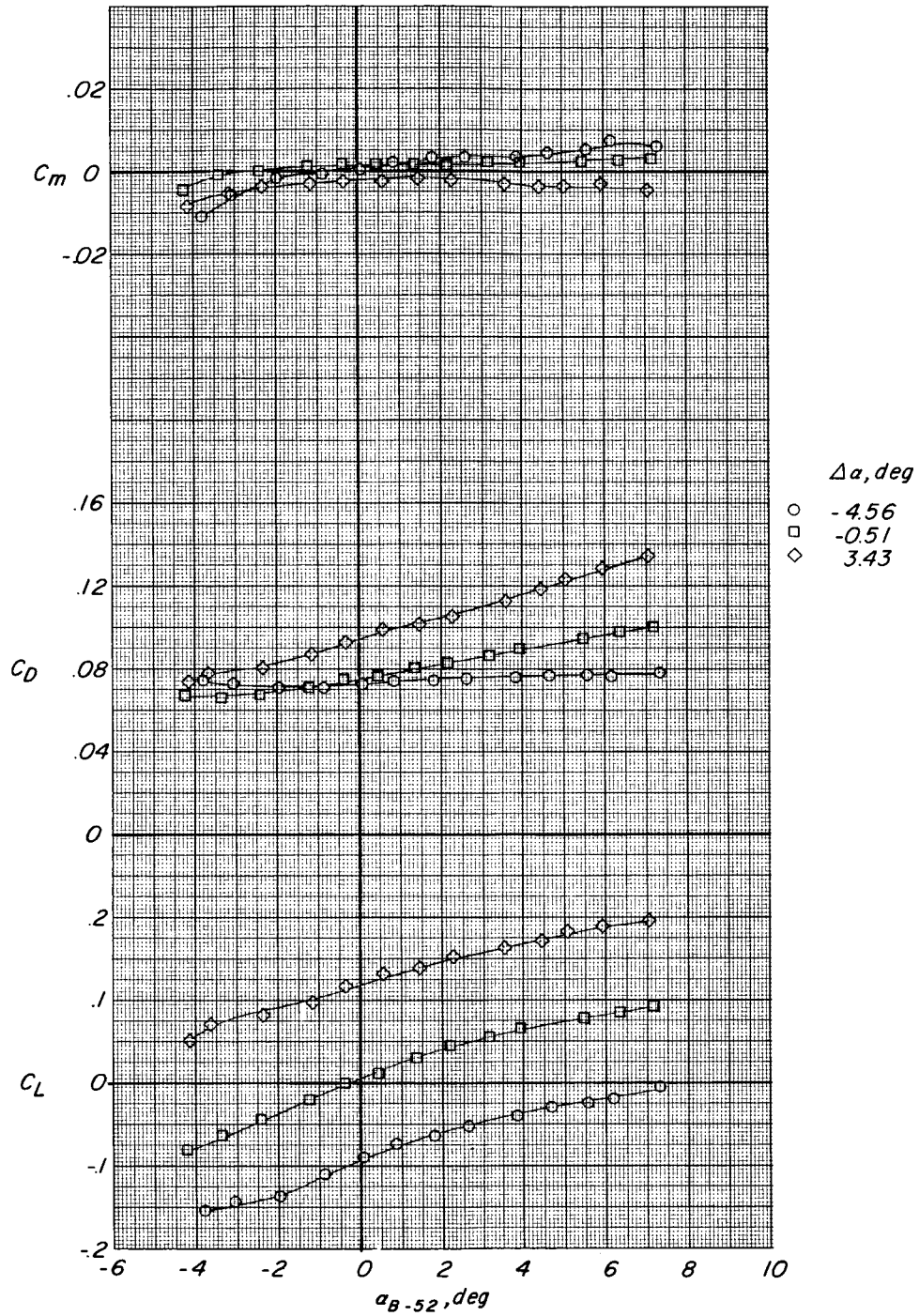

(c) z' = 10.0 feet (3.05 m) full scale.

Figure 10.- Continued.

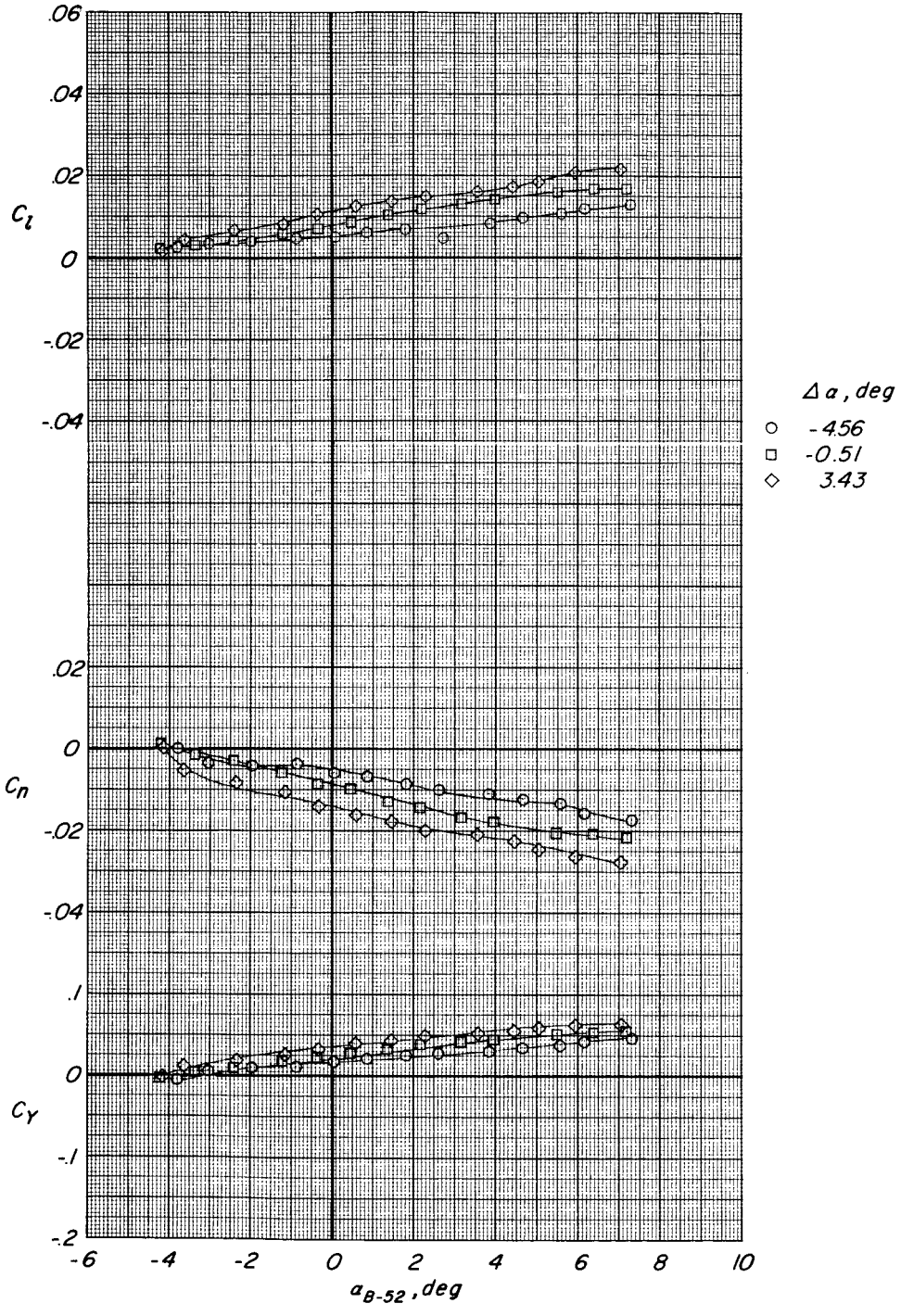

(c) Concluded.

Figure 10.- Concluded.

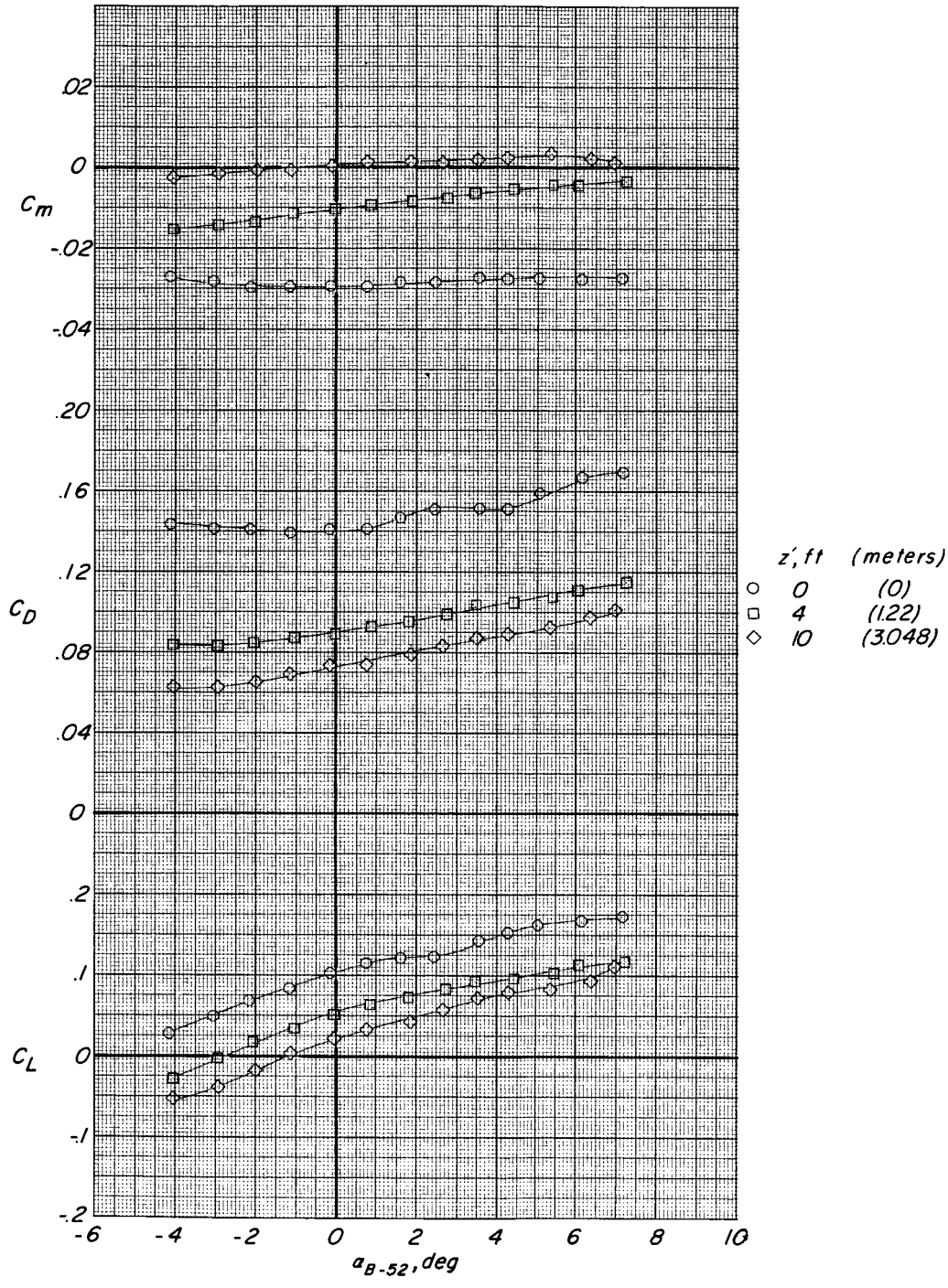

(a) $\Delta\beta = 6.40^0$.

Figure 11.- Effect of sideslipping of M2-F2 model in presence of B-52 model. $M = 0.85$; $\Delta\alpha = 0^0$; $\Phi = 0^0$; $\delta_l = 30^0$; $\delta_u = -10^0$; 10^0 rudder flare.

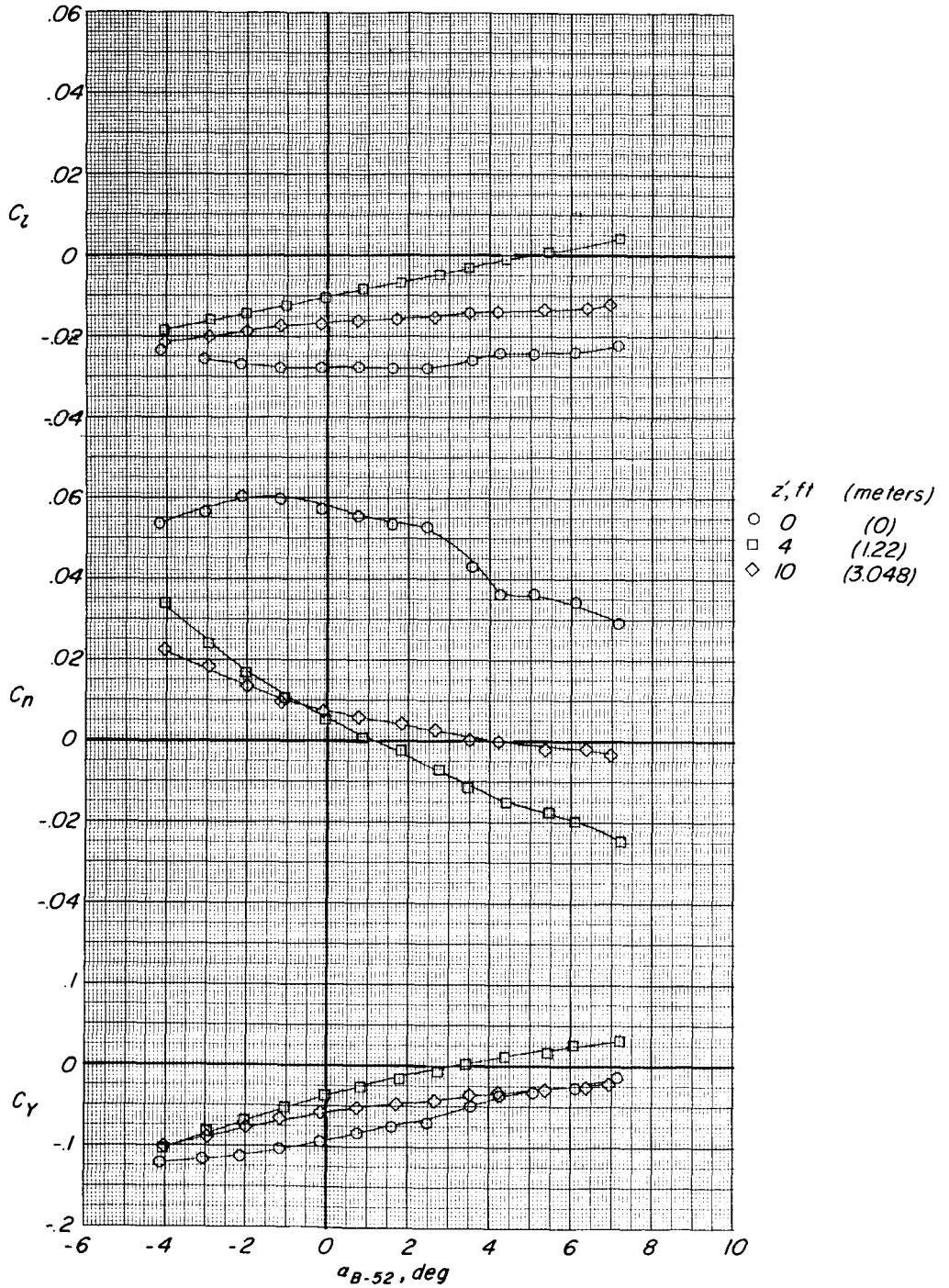

(a) Concluded.

Figure 11.- Continued.

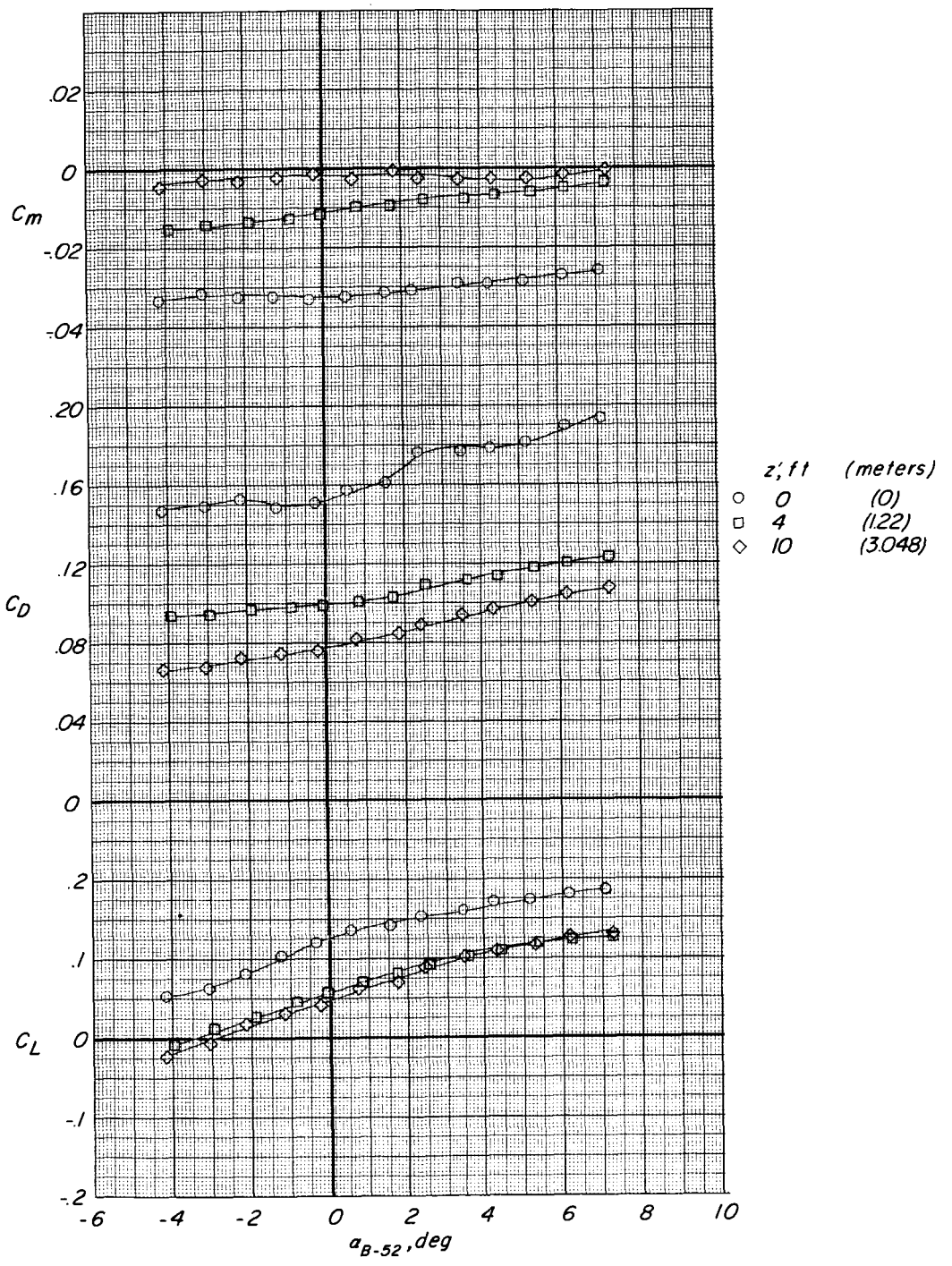

(b) $\Delta\beta = -3.92^{o}$.

Figure 11.- Continued.

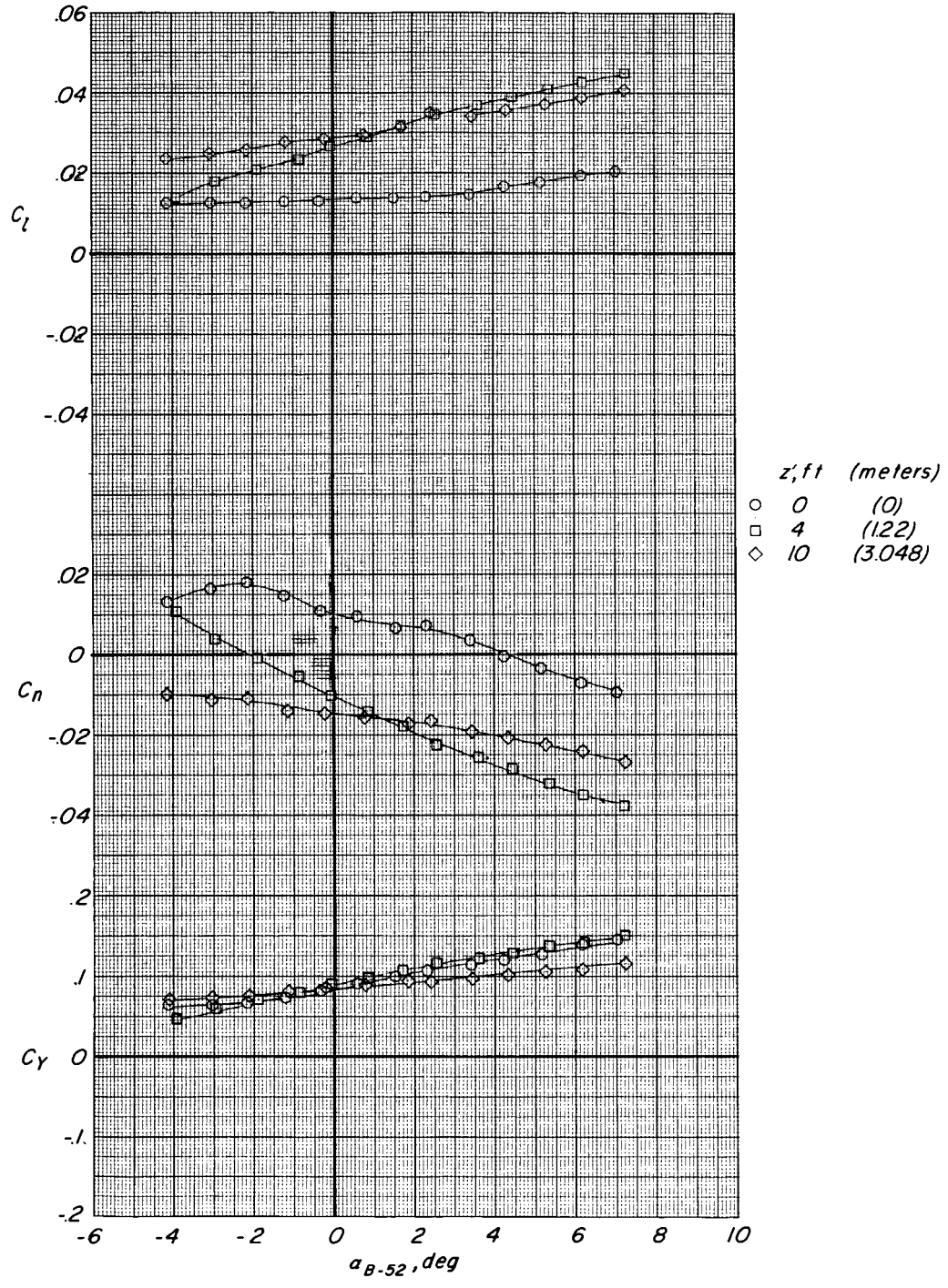

(b) Concluded.

Figure 11.- Concluded.

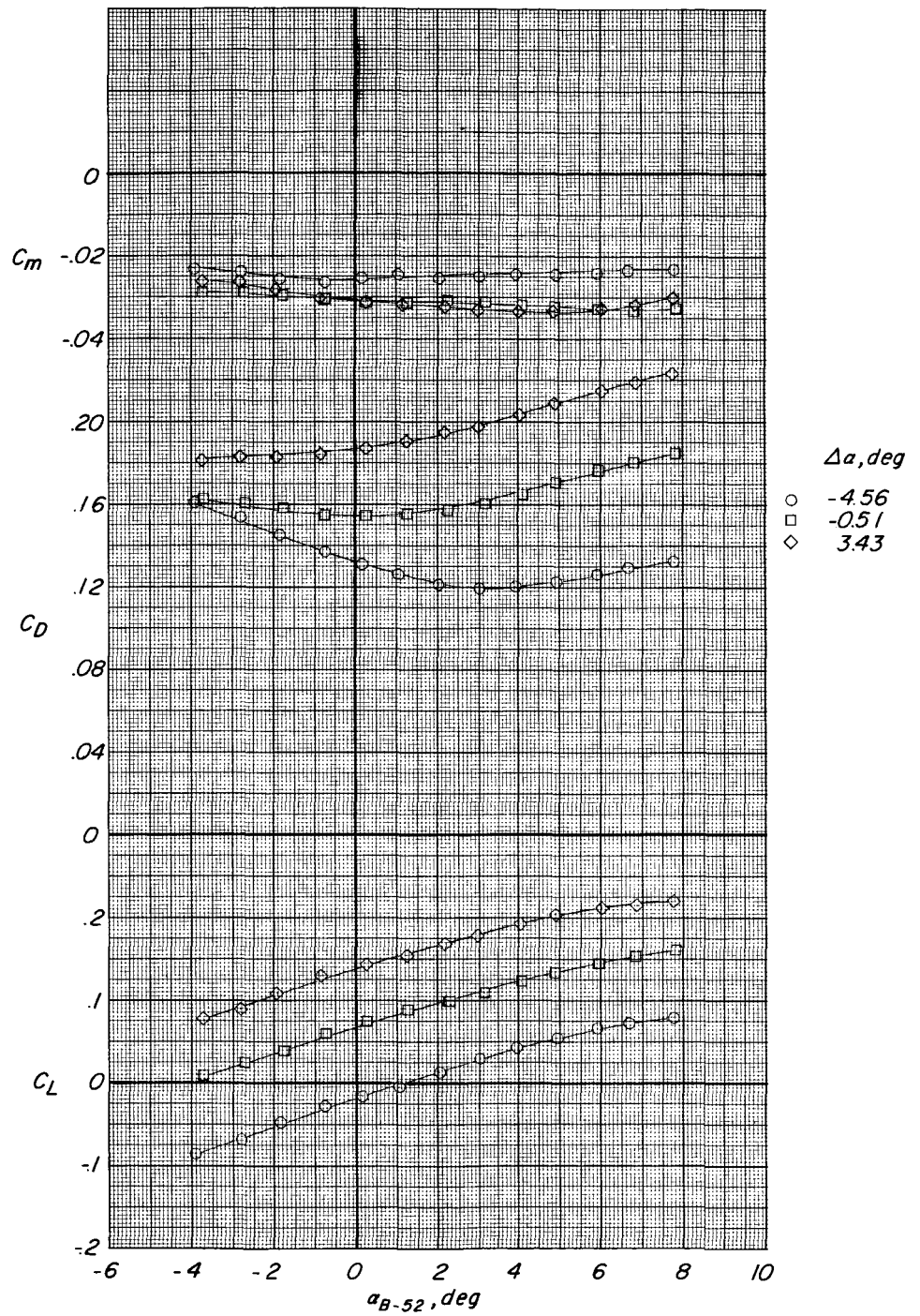

(a) z' = 0 feet (0 meters).

Figure 12.- Aerodynamic characteristics of M2-F2 model in presence of B-52 model. M = 0.90; $\Delta\beta = 0.75^0$; $\Phi = 0^0$; $\delta_\ell = 30^0$; $\delta_U = -10^0$; 10^0 rudder flare.

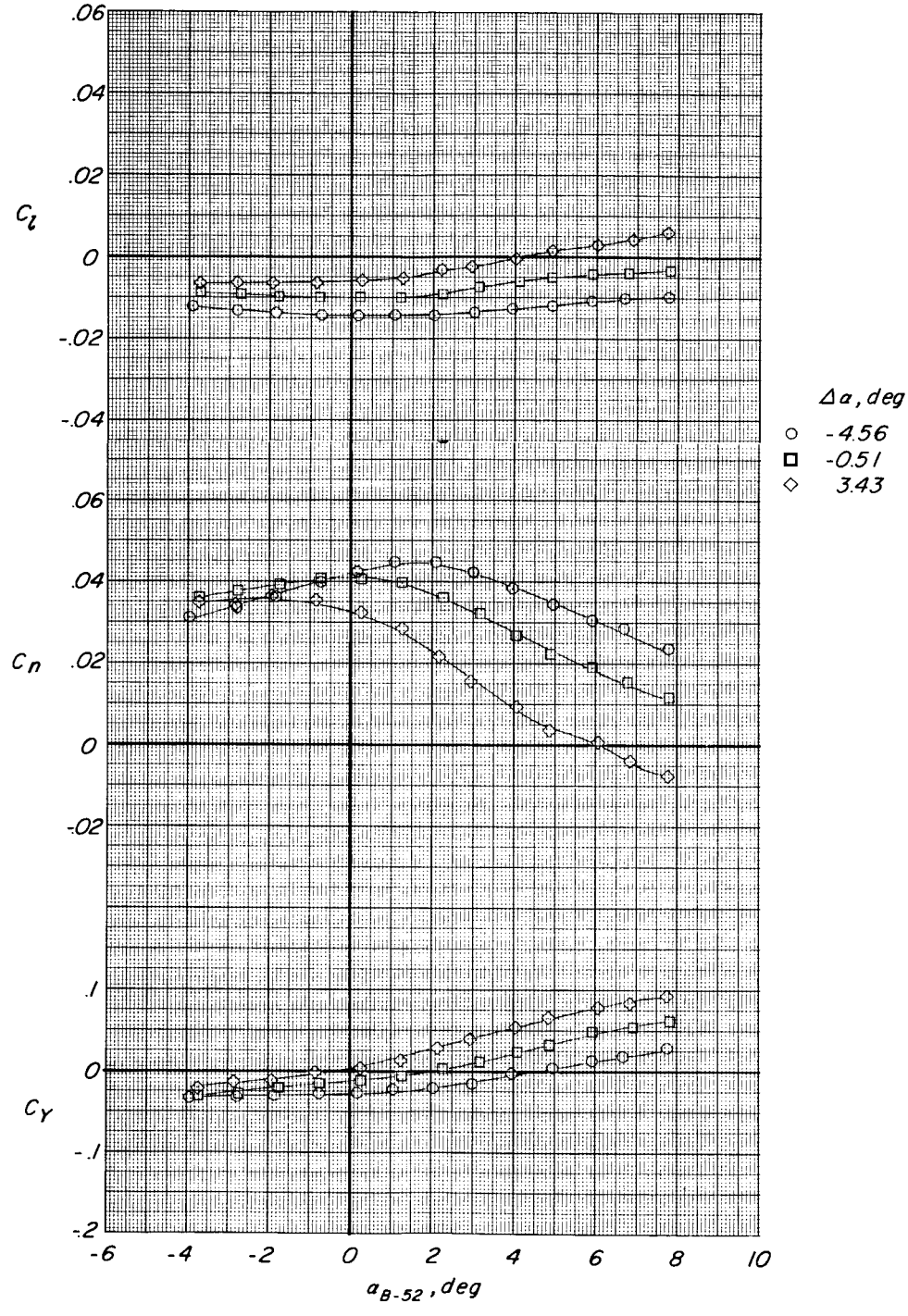

(a) Concluded.

Figure 12.- Continued.

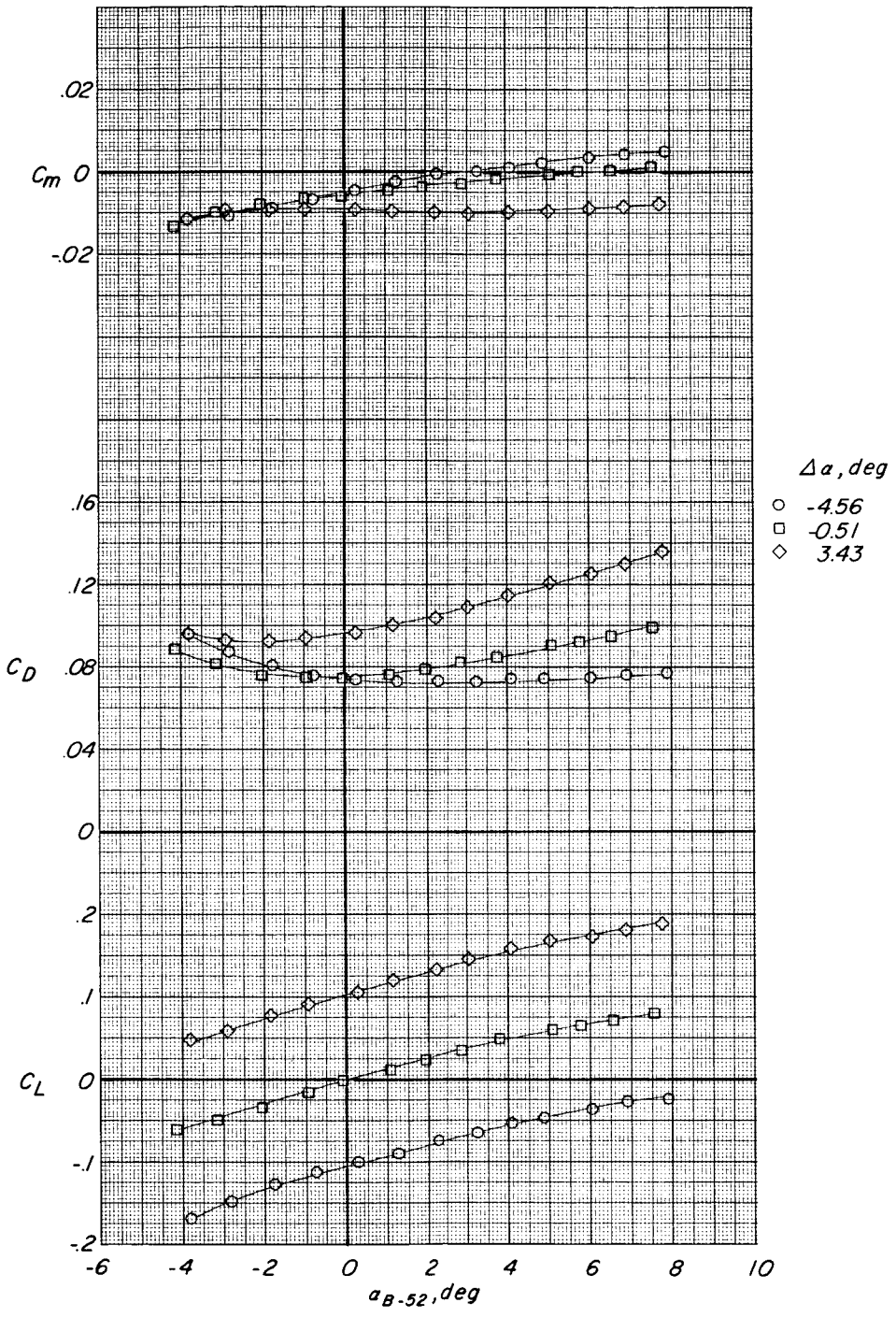

(b) z' = 4.0 feet (1.22 m) full scale.

Figure 12.- Continued.

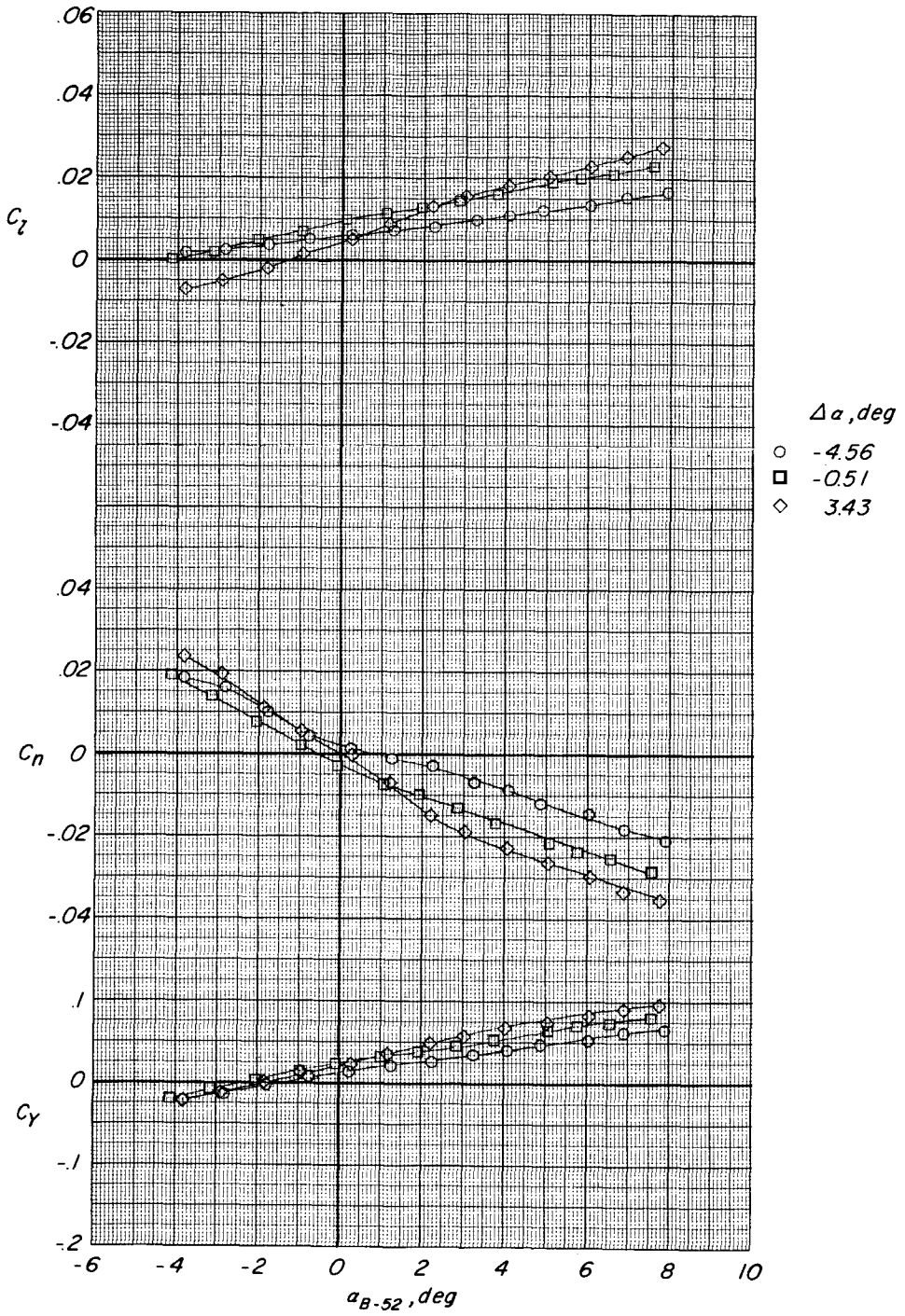

(b) Concluded.

Figure 12.- Continued.

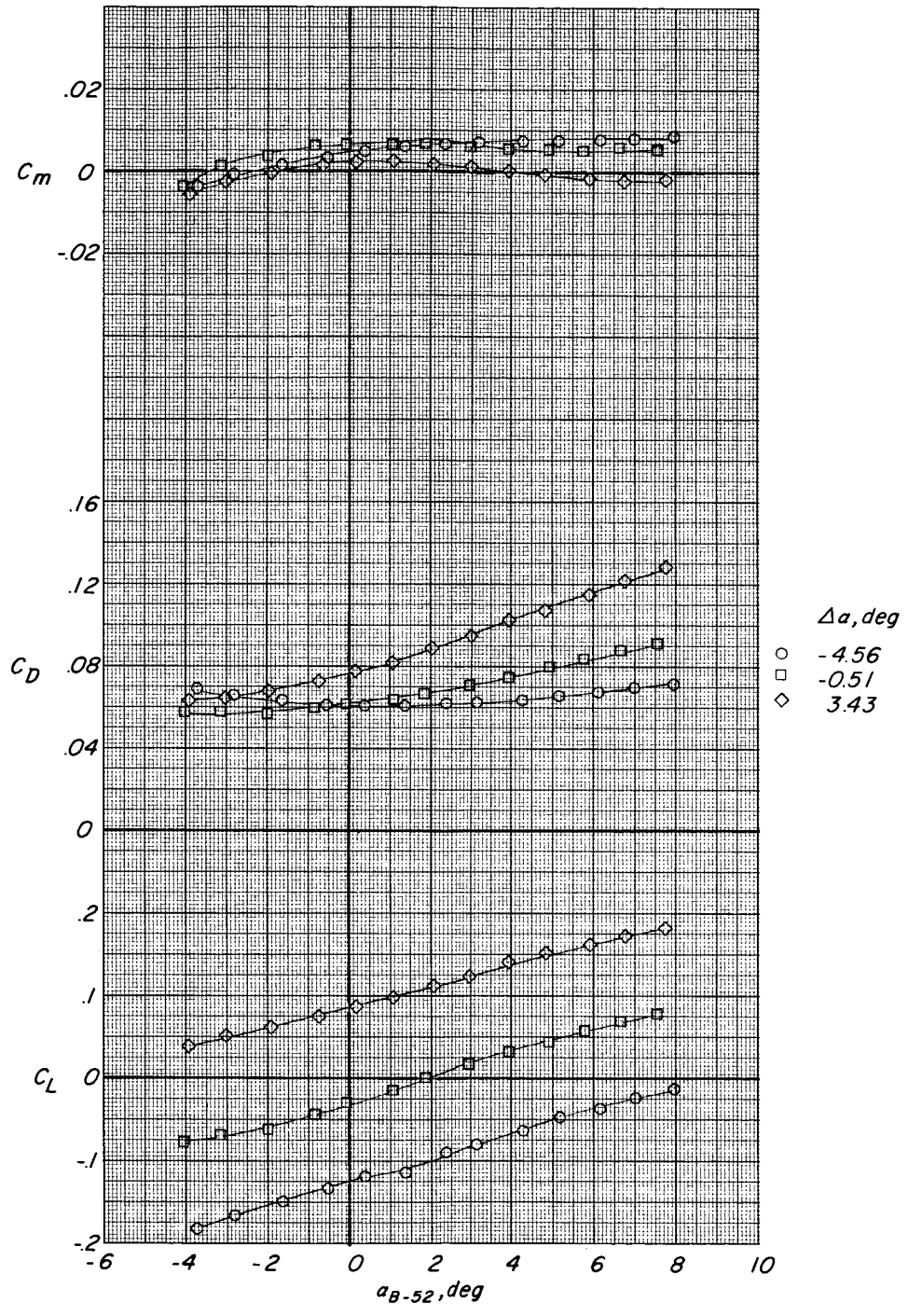

(c) z' = 10.0 feet (3.05 m) full scale.

Figure 12.- Continued.

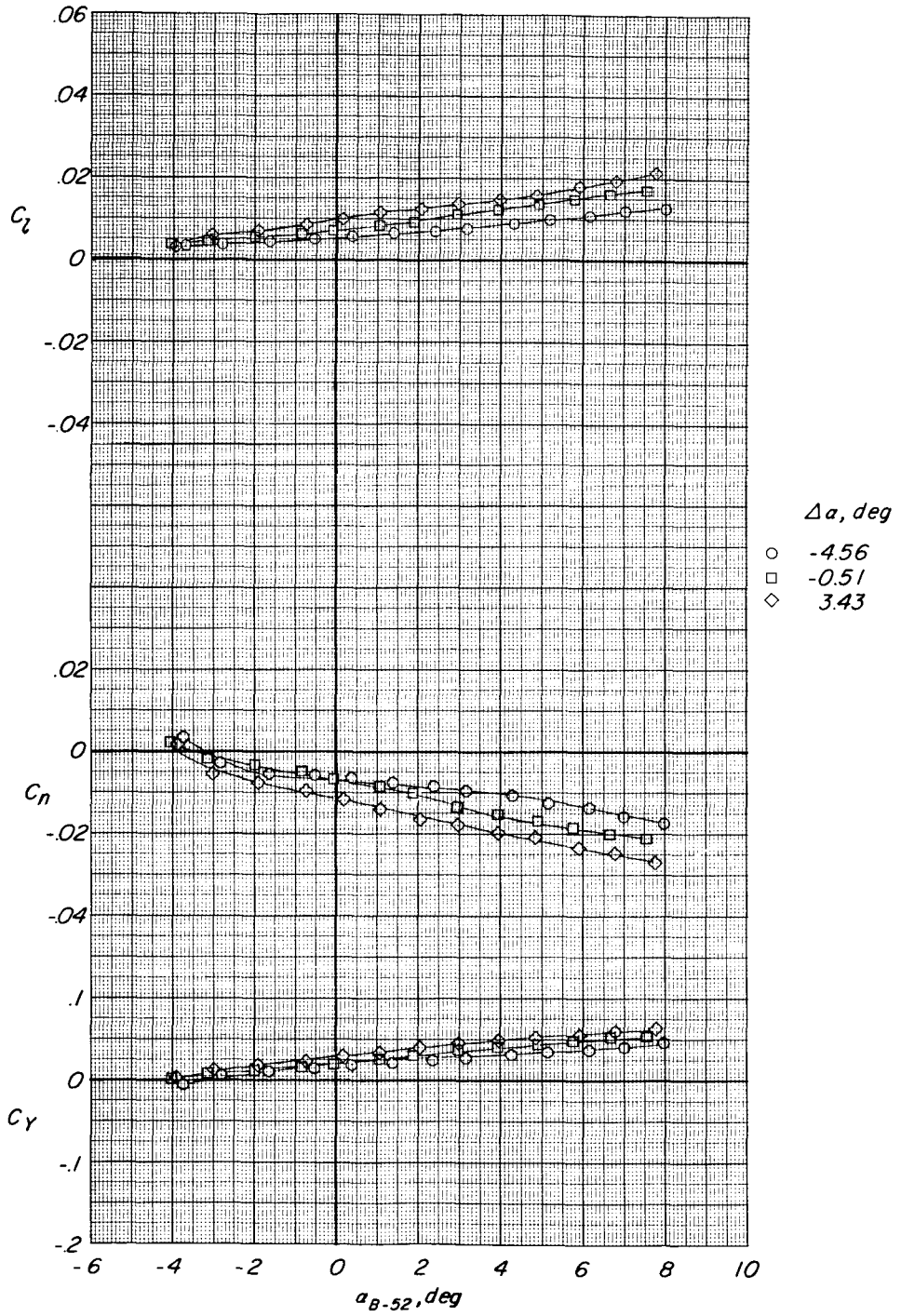

(c) Concluded.

Figure 12.- Concluded.

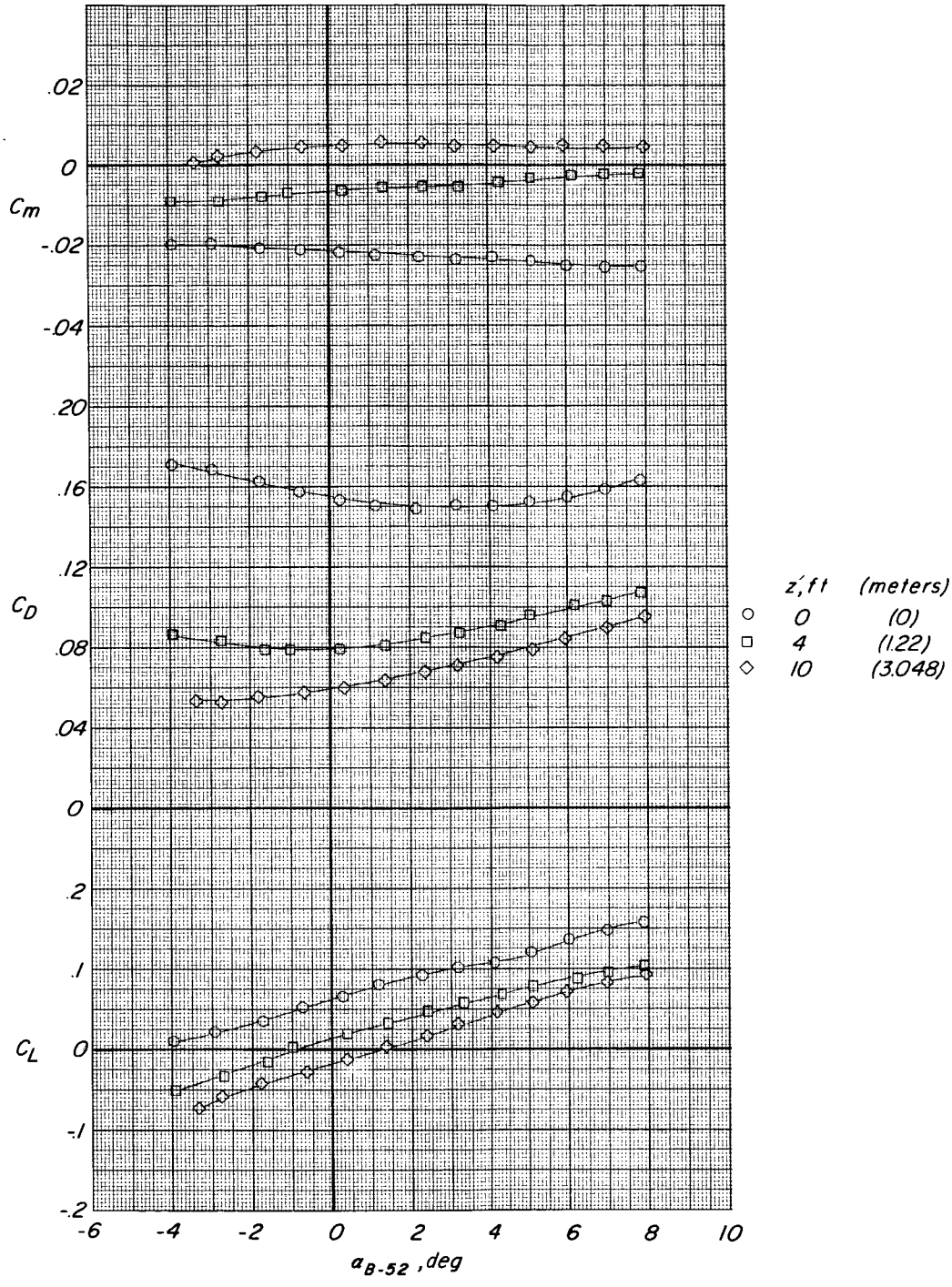

(a) $\Delta\beta = 6.40^0$.

Figure 13.- Effect of sideslipping of M2-F2 model in presence of B-52 model. M = 0.90; $\Delta\alpha = 0^0$; $\Phi = 0^0$; $\delta_l = 30^0$; $\delta_u = -10^0$; 10^0 rudder flare.

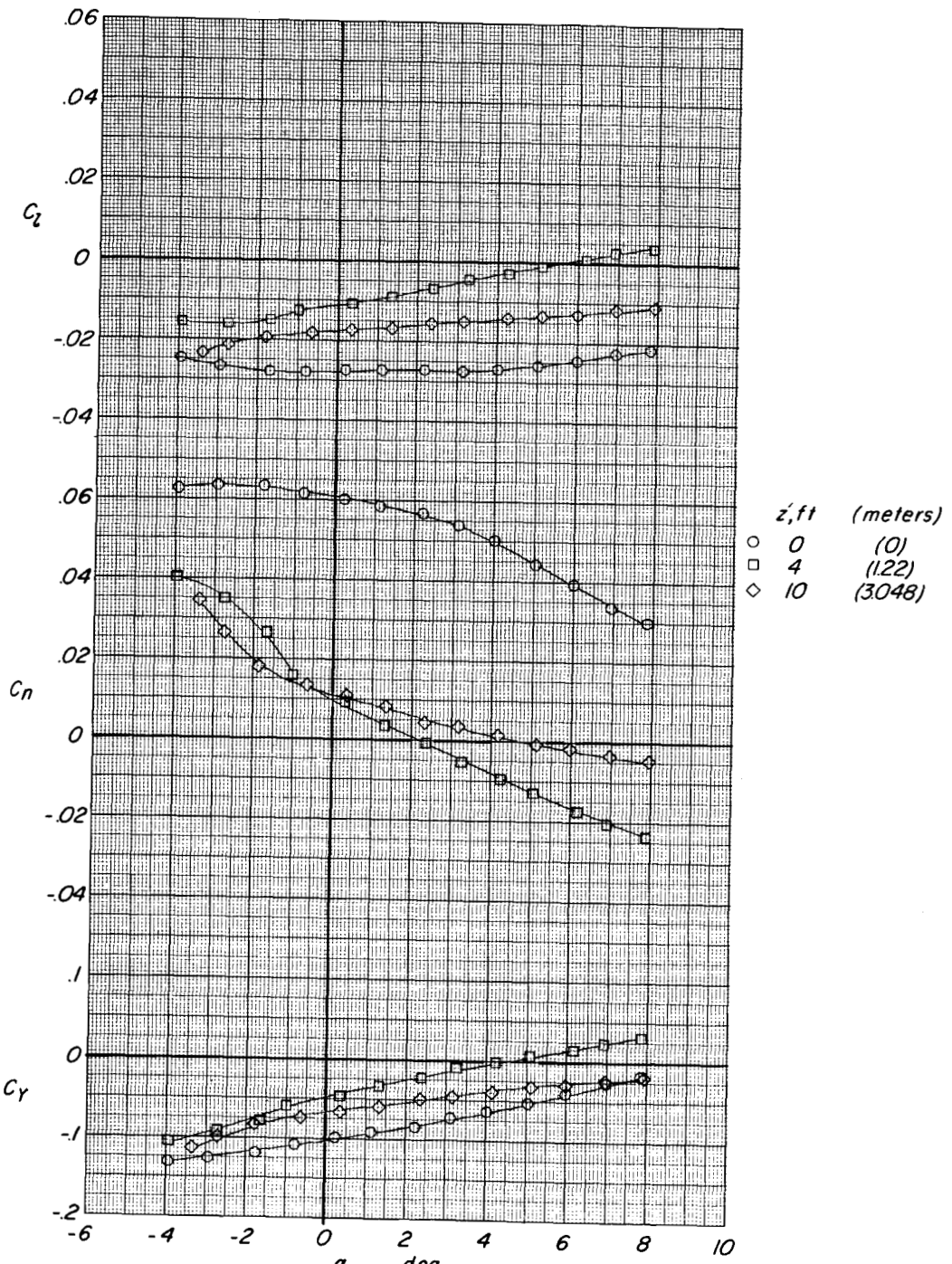

(a) Concluded.

Figure 13.- Continued.

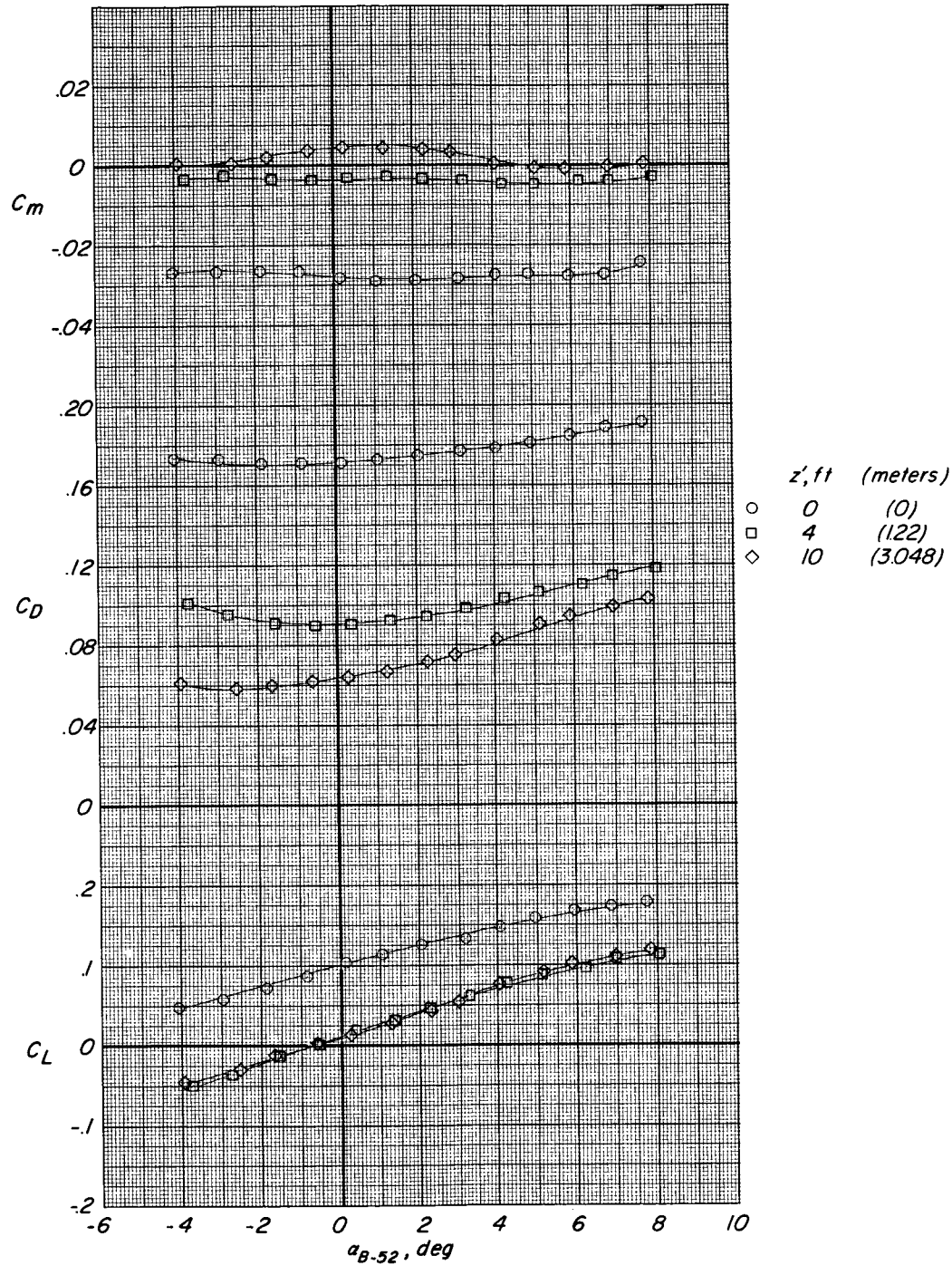

(b) $\Delta\beta = -3.92^0$.

Figure 13.- Continued.

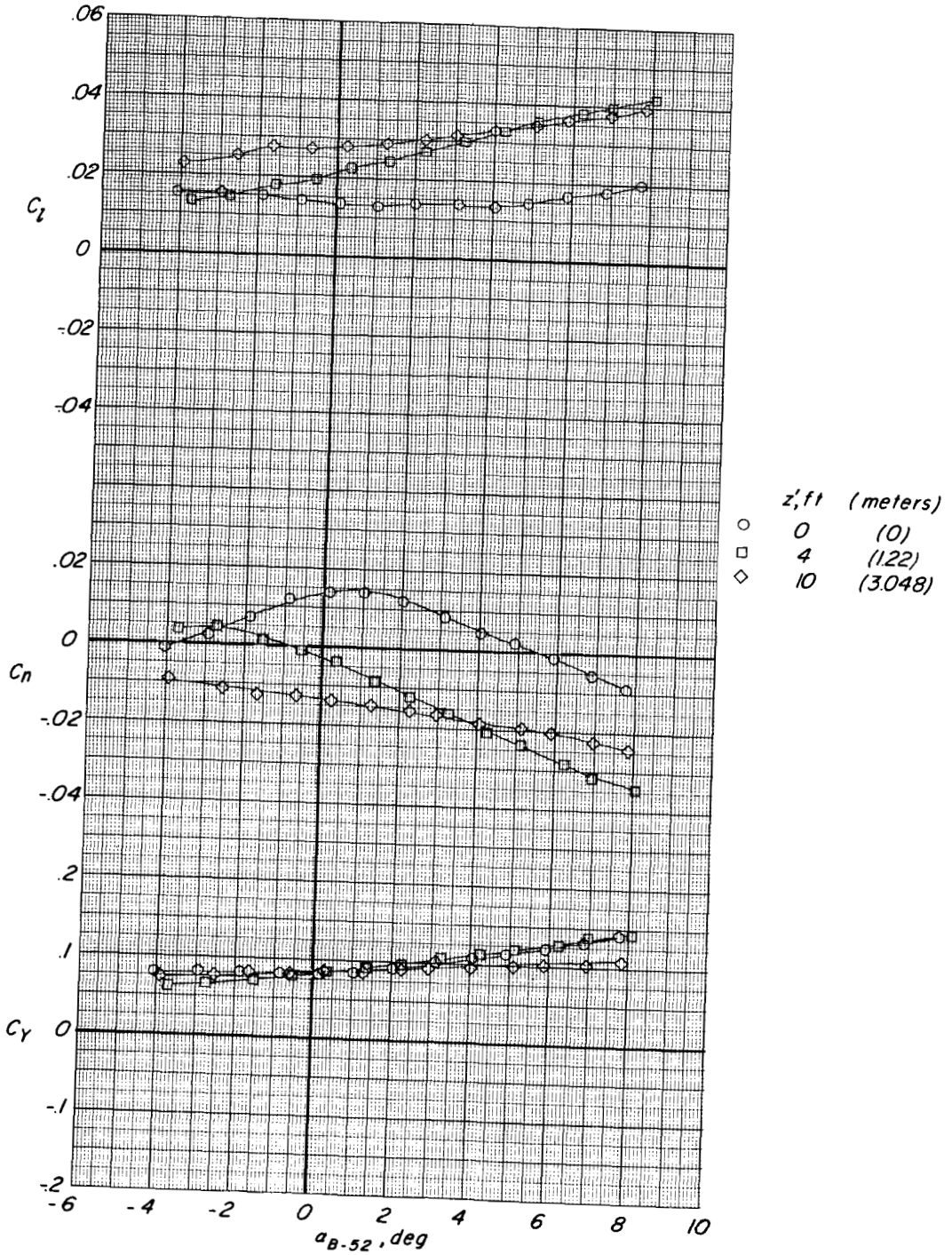

(b) Concluded.

Figure 13.- Concluded.

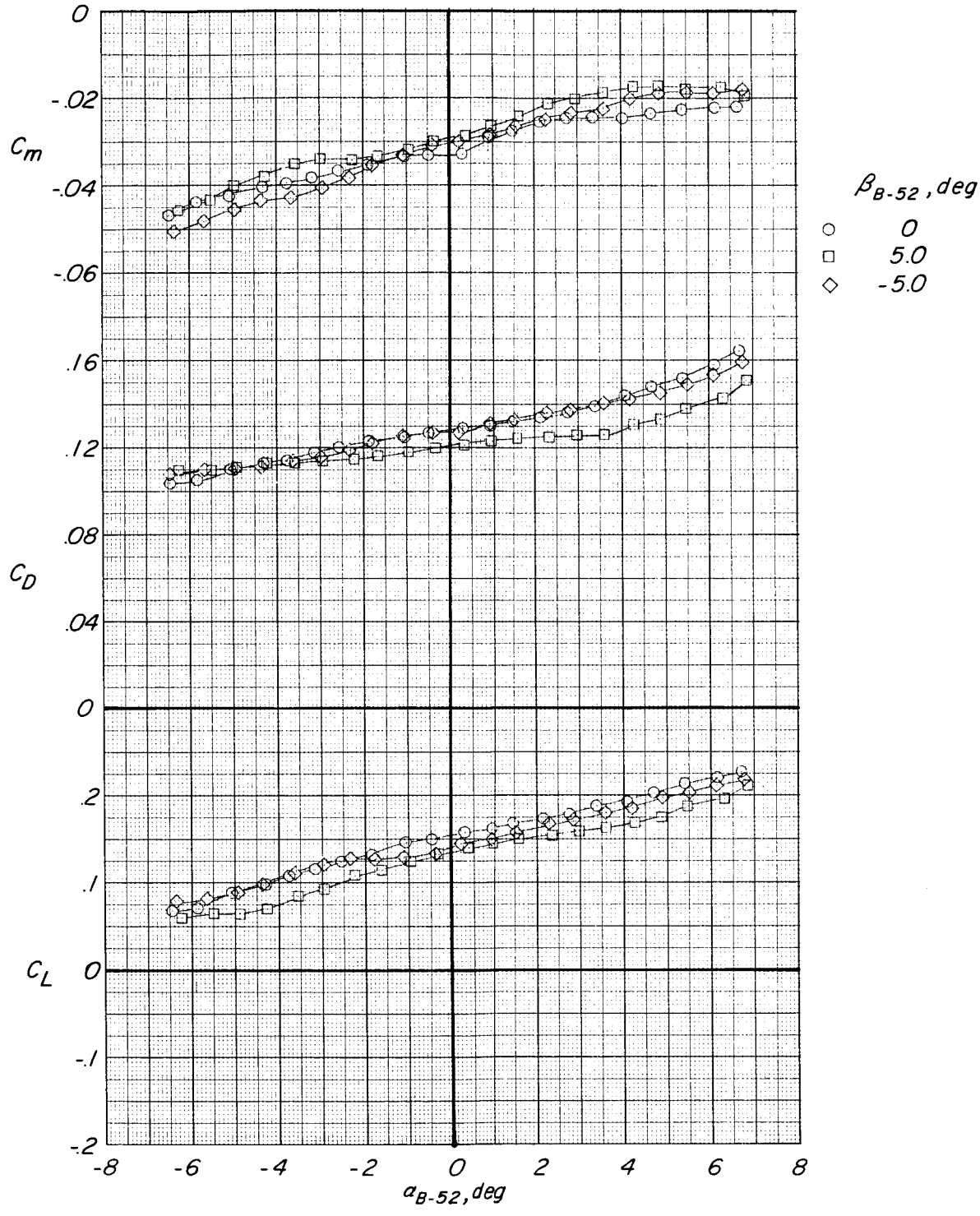

Figure 14.- Aerodynamic characteristics of M2-F2 model in presence of B-52 model. Effect of sideslip of M2-F2/B-52 combination. M = 0.60; $\Delta\beta = 0.75^0$; $\Phi = 0^0$; $\delta_l = 30^0$; $\delta_u = -10^0$; 10^0 rudder flare.

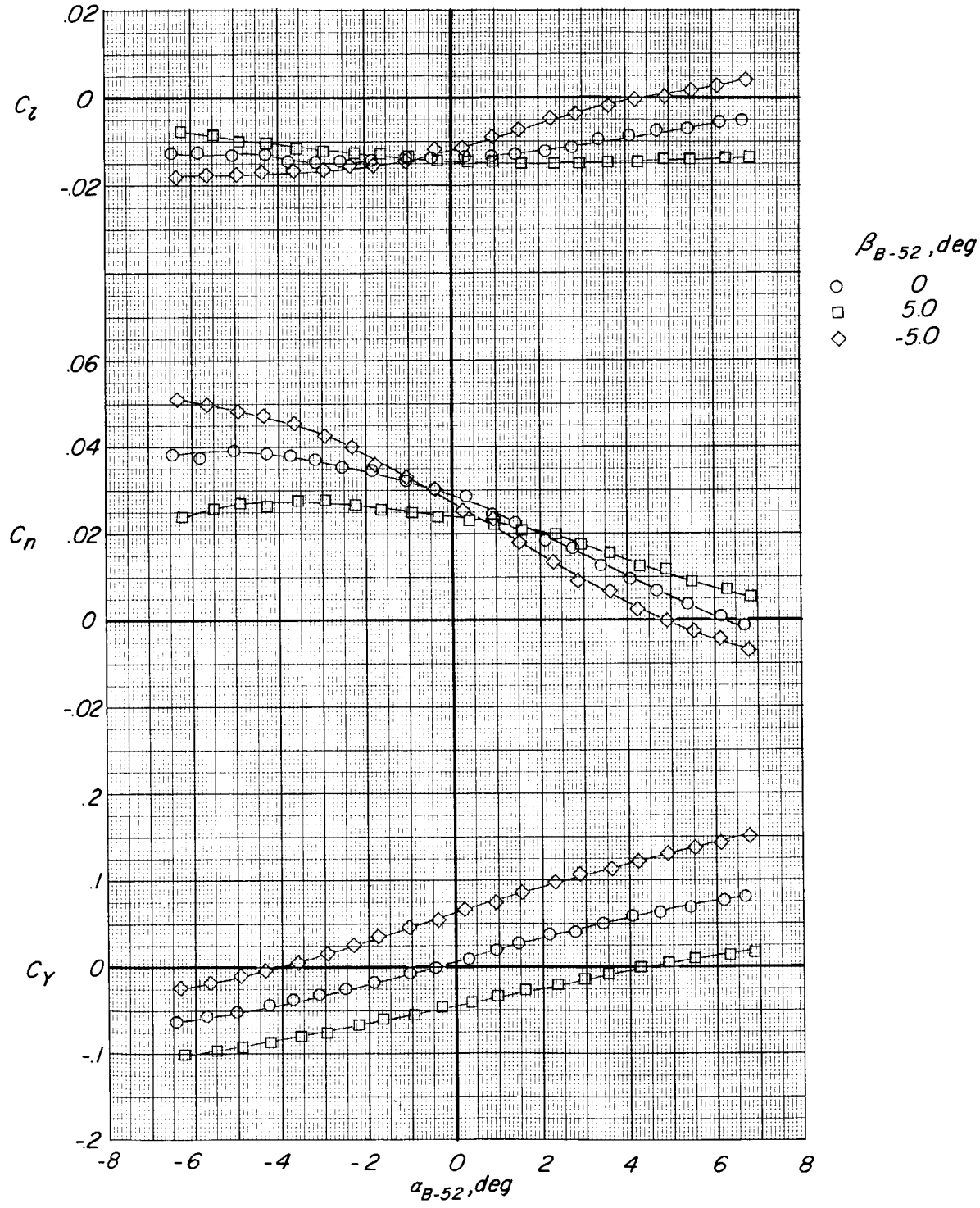

Figure 14.- Concluded.

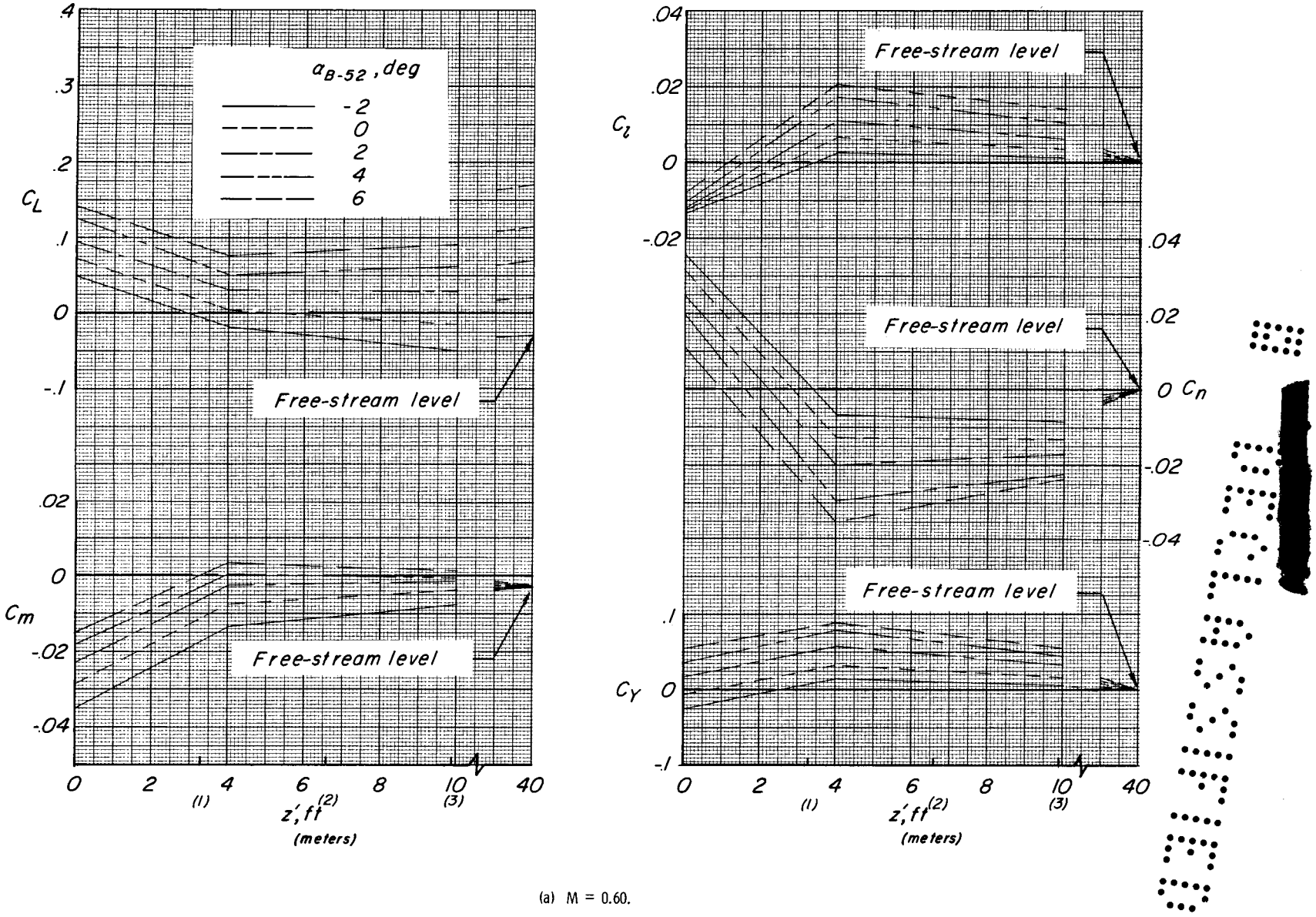

(a) M = 0.60.

Figure 15.- Variation of force and moment coefficients with z'; $\Delta\alpha = -5^0$.

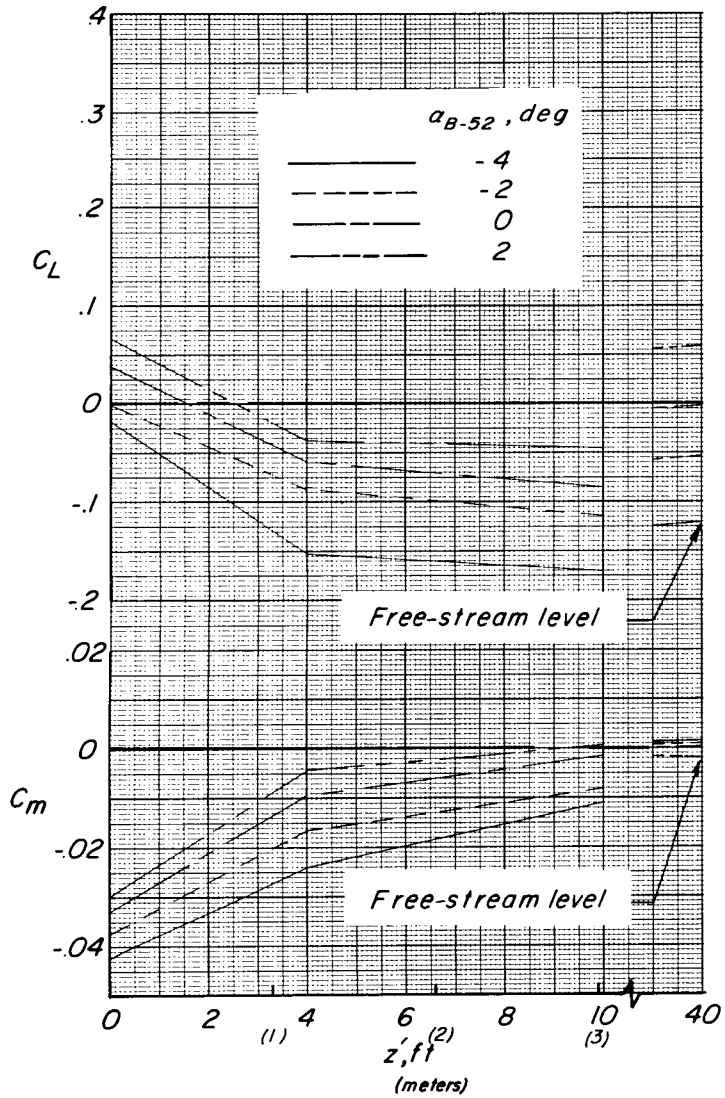

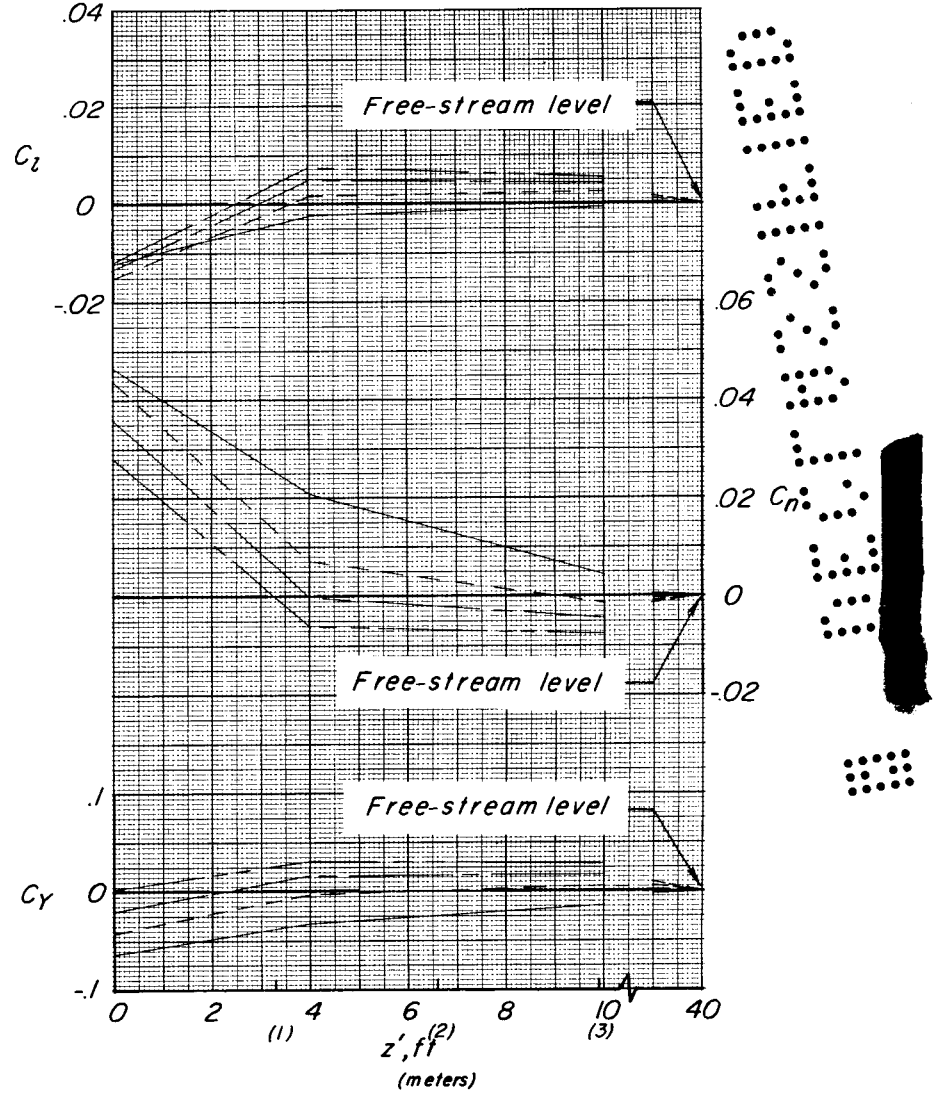

(b) M = 0.80.

Figure 15.- Continued.

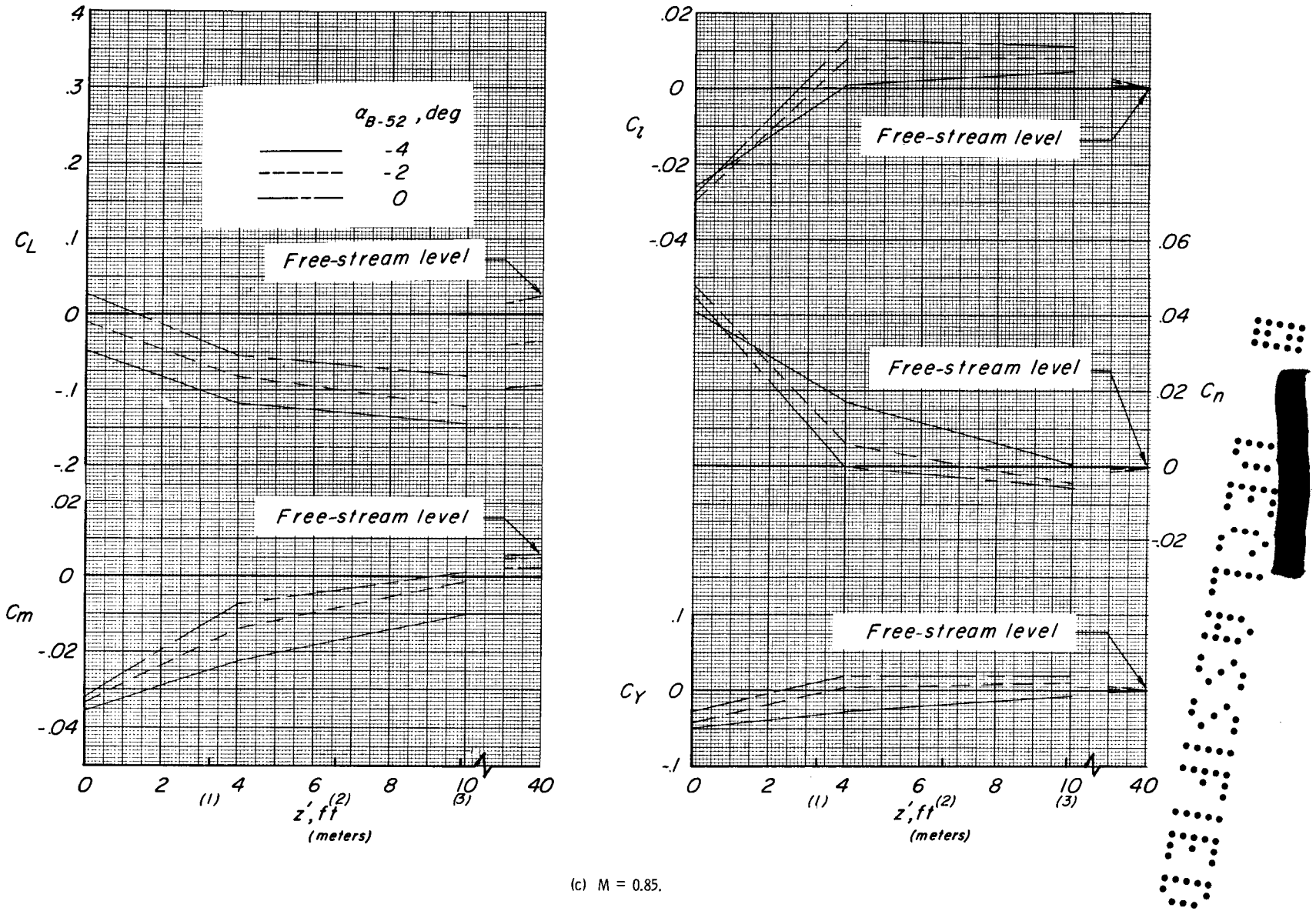

(c) M = 0.85.

Figure 15.- Concluded.

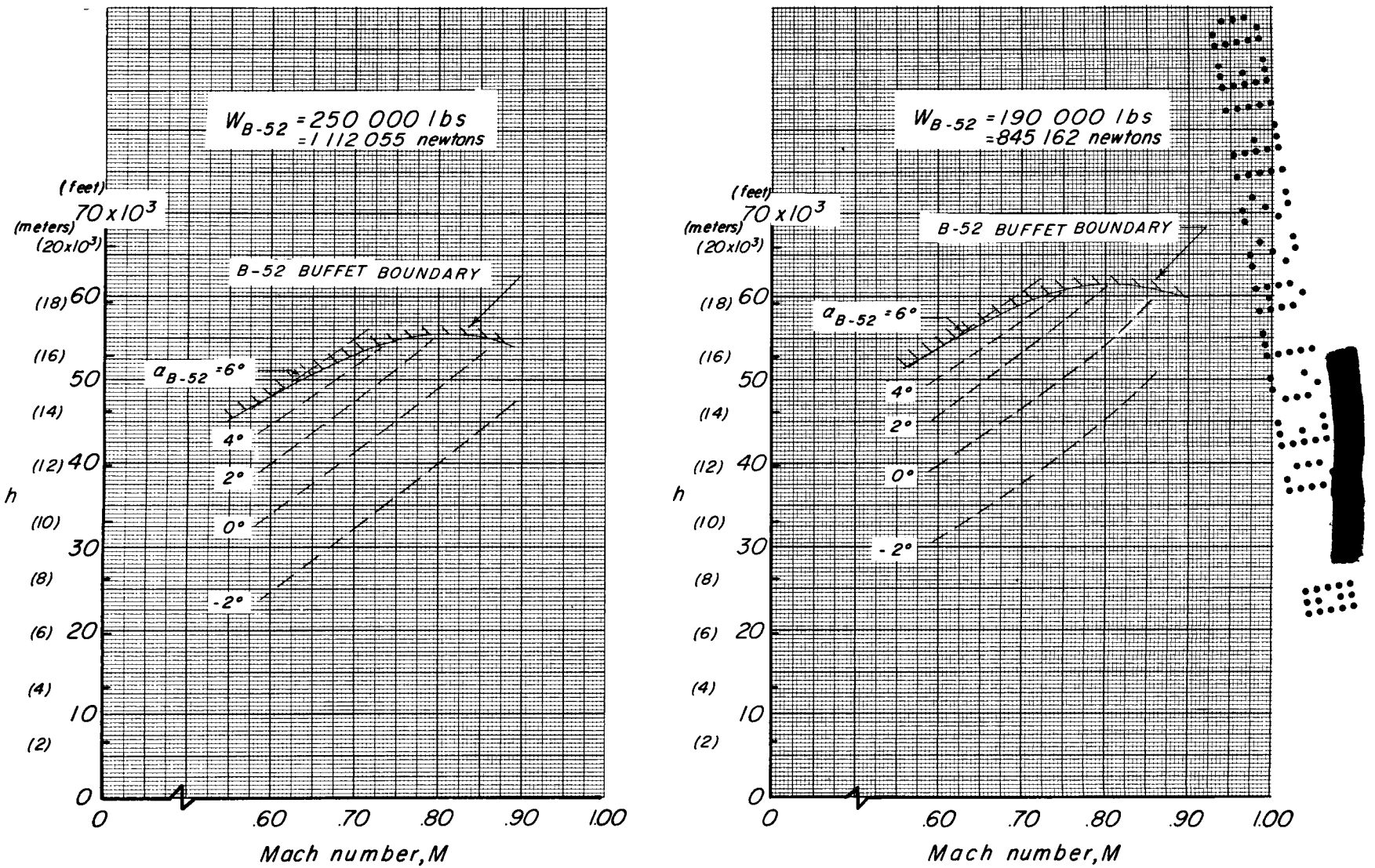

Figure 16.- B-52 buffet boundary.

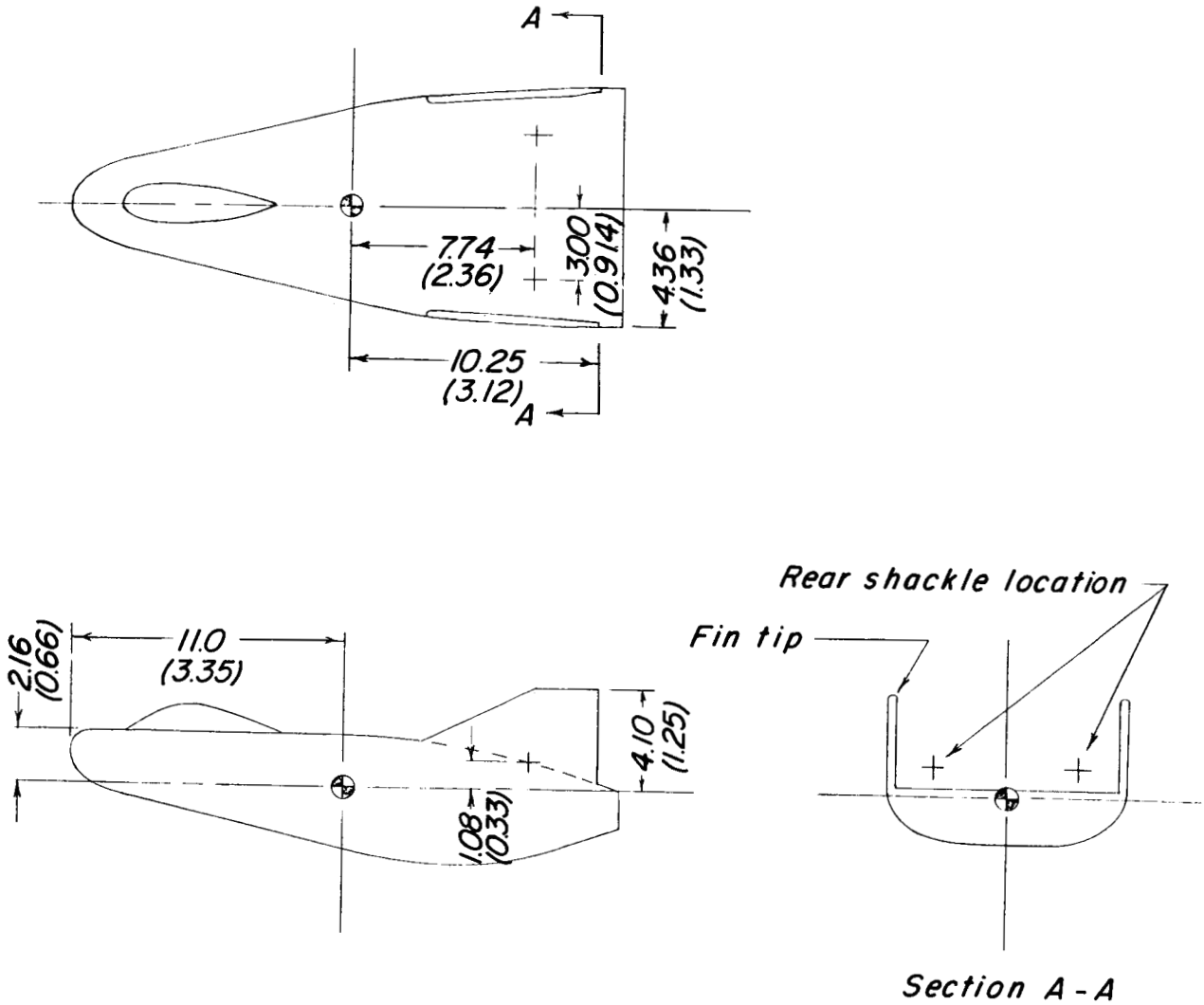

Figure 17.- Reference section of M2-F2 used in motion studies. All dimensions are given first in feet and parenthetically in meters.

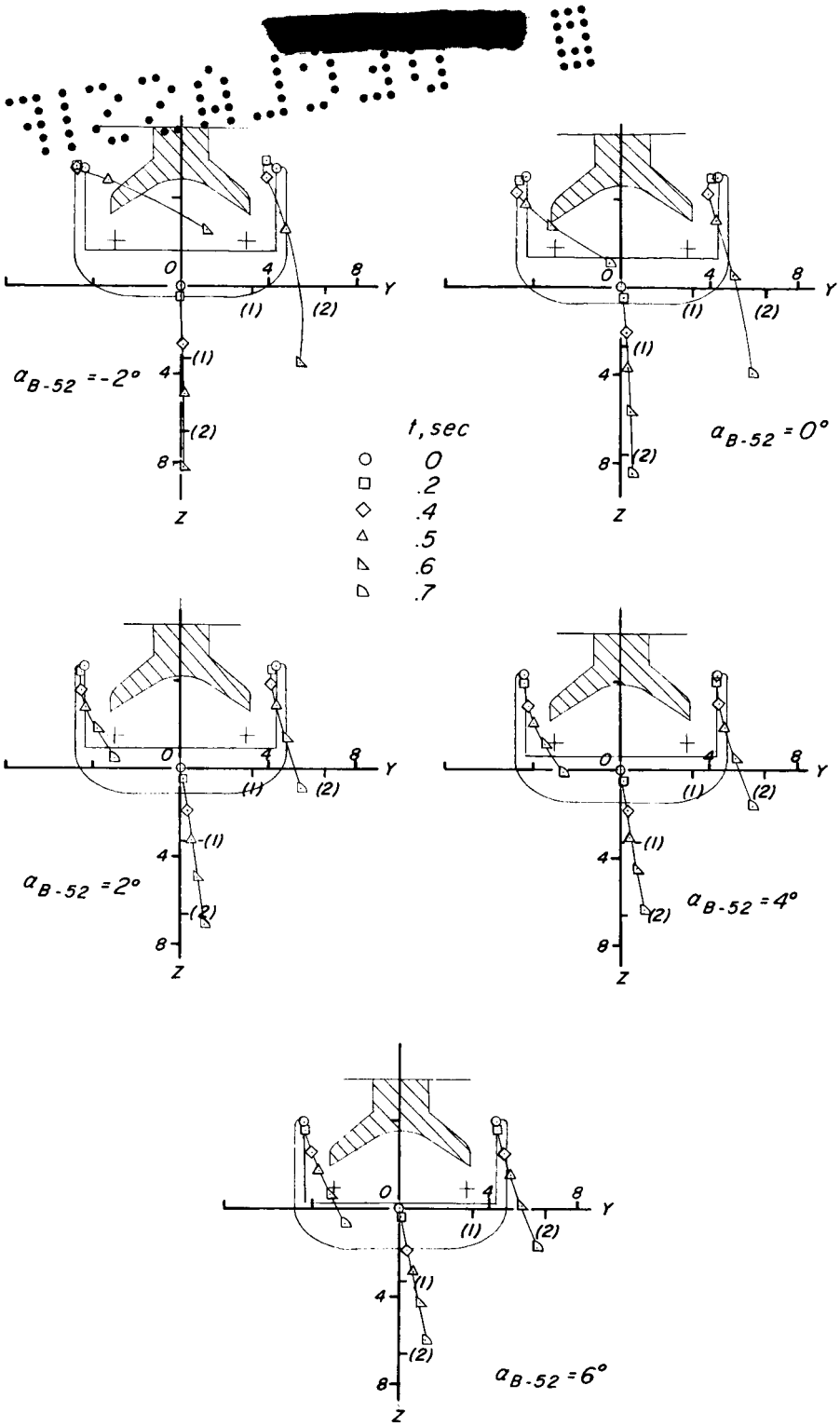

(a) Fin-tip and center-of-gravity paths. (Values along the coordinate scales are given in feet and parenthetically in meters.)

Figure 18.- Effect of variation in B-52 angle of attack (variation in altitude). Dampers off; $M = 0.60$; $\Delta\alpha = -5^{0}$; $W_{M2-F2} = 5576$ pounds (24 803 N); $W_{B-52} = 250\,000$ pounds (1 112 055 N).

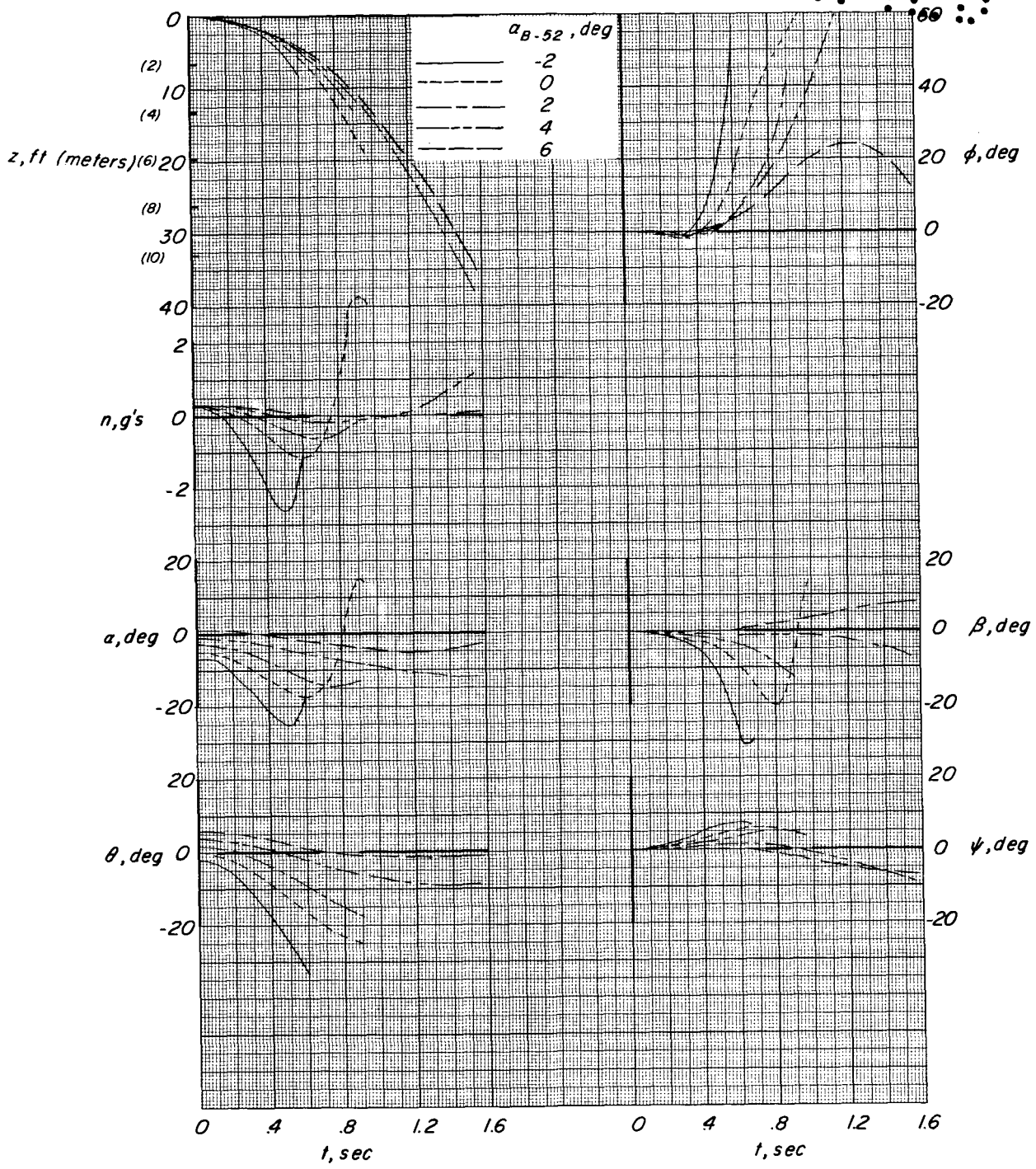

(b) Vehicle motions after launch.

Figure 18.- Concluded.

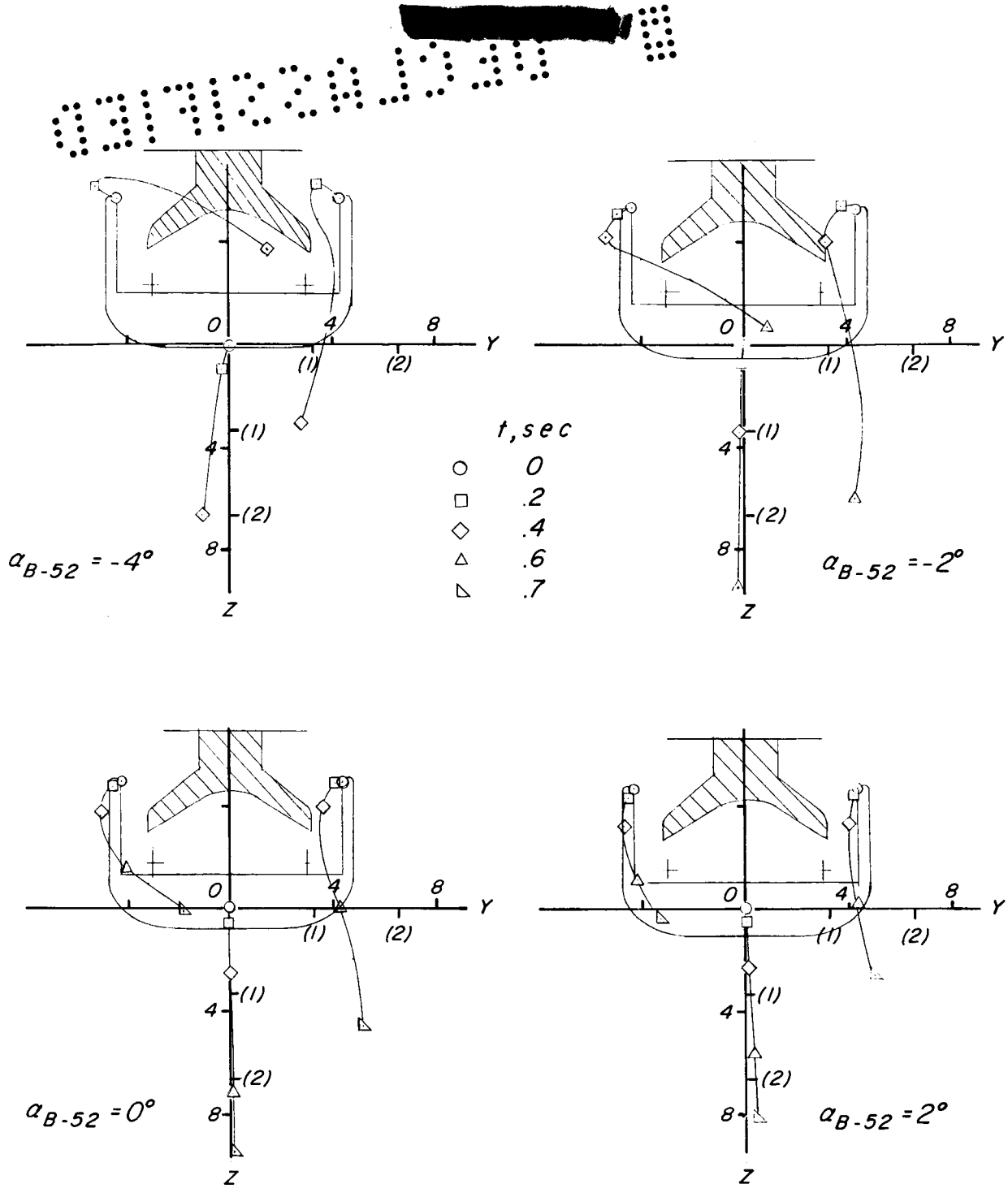

(a) Fin-tip and center-of-gravity paths. (Values along the coordinate scales are given in feet and parenthetically in meters.)

Figure 19.- Effect of variation in B-52 angle of attack (variation in altitude). Dampers off; $M = 0.80$; $\Delta\alpha = -5^{o}$; $W_{M2\text{-}F2} = 5576$ pounds (24 803 N); $W_{B\text{-}52} = 250\,000$ pounds (1 112 055 N).

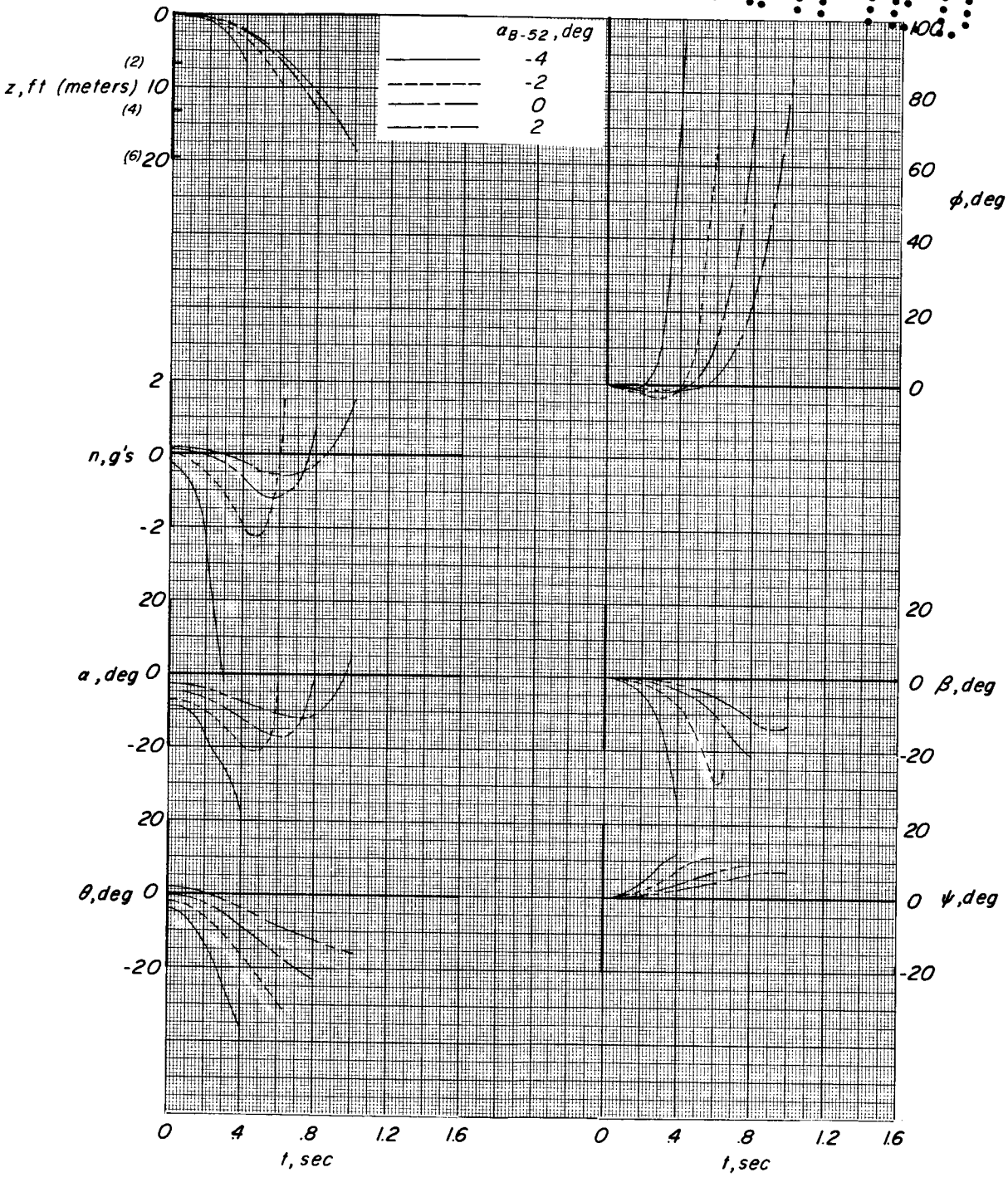

(b) Vehicle motions after launch.

Figure 19.- Concluded.

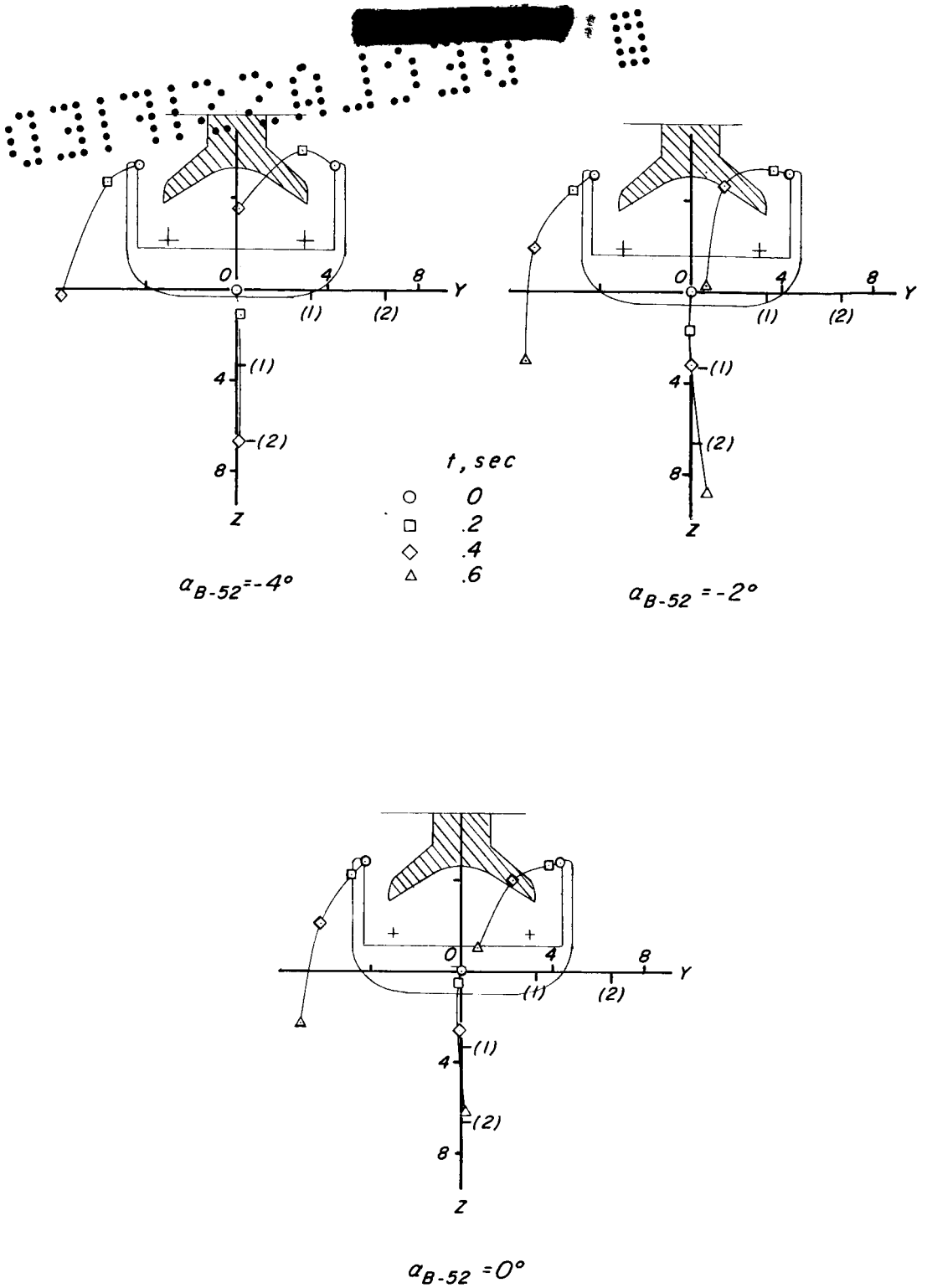

(a) Fin-tip and center-of-gravity paths. (Values along the coordinate scales are given in feet and parenthetically in meters.)

Figure 20.- Effect of variation in B-52 angle of attack (variation in altitude). Dampers off; $M = 0.85$; $\Delta\alpha = -4^{0}$; $W_{M2\text{-}F2} = 5576$ pounds (24 803 N); $W_{B\text{-}52} = 250\,000$ pounds (1 112 055 N).

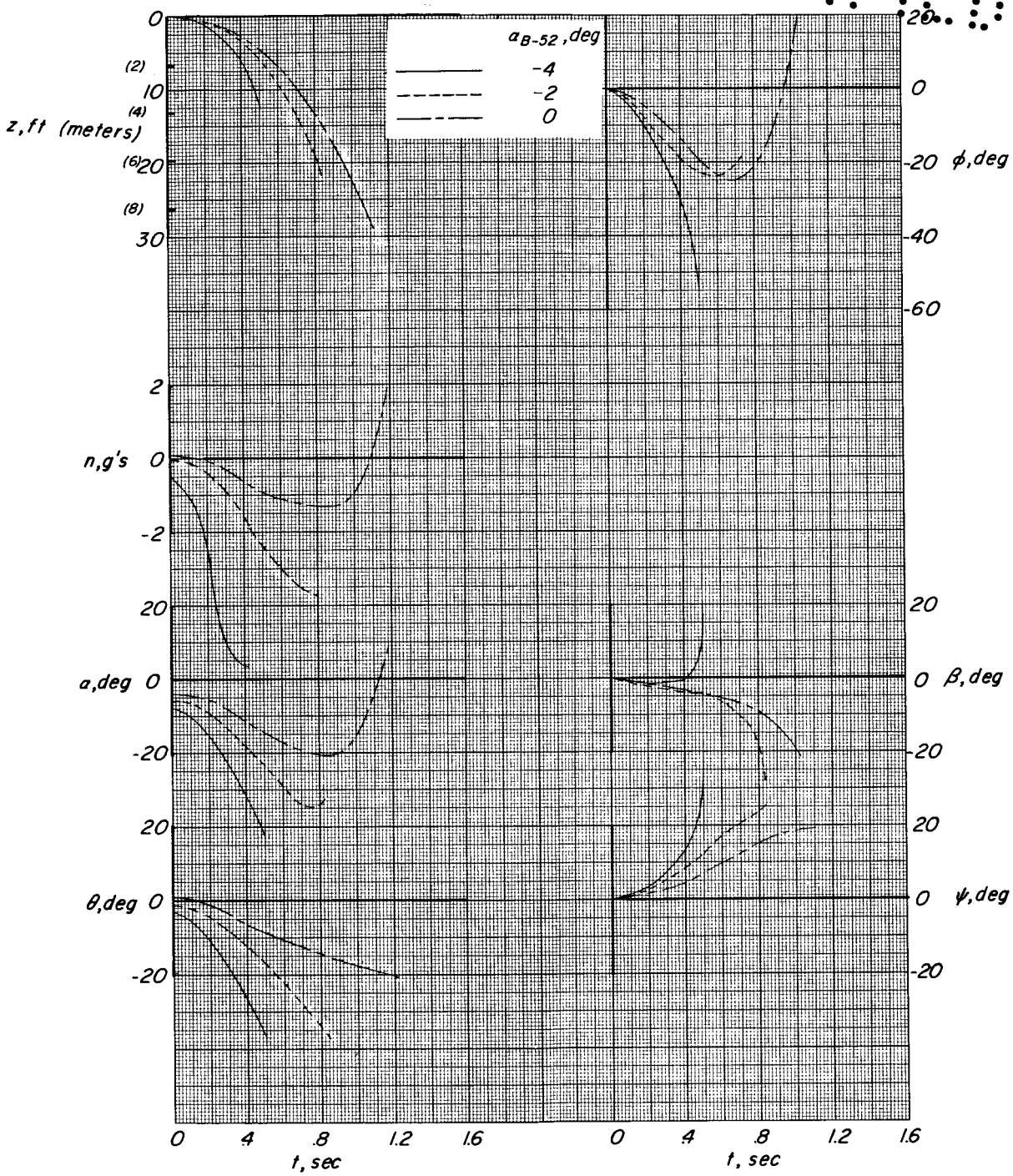

(b) Vehicle motions after launch.

Figure 20.- Concluded.

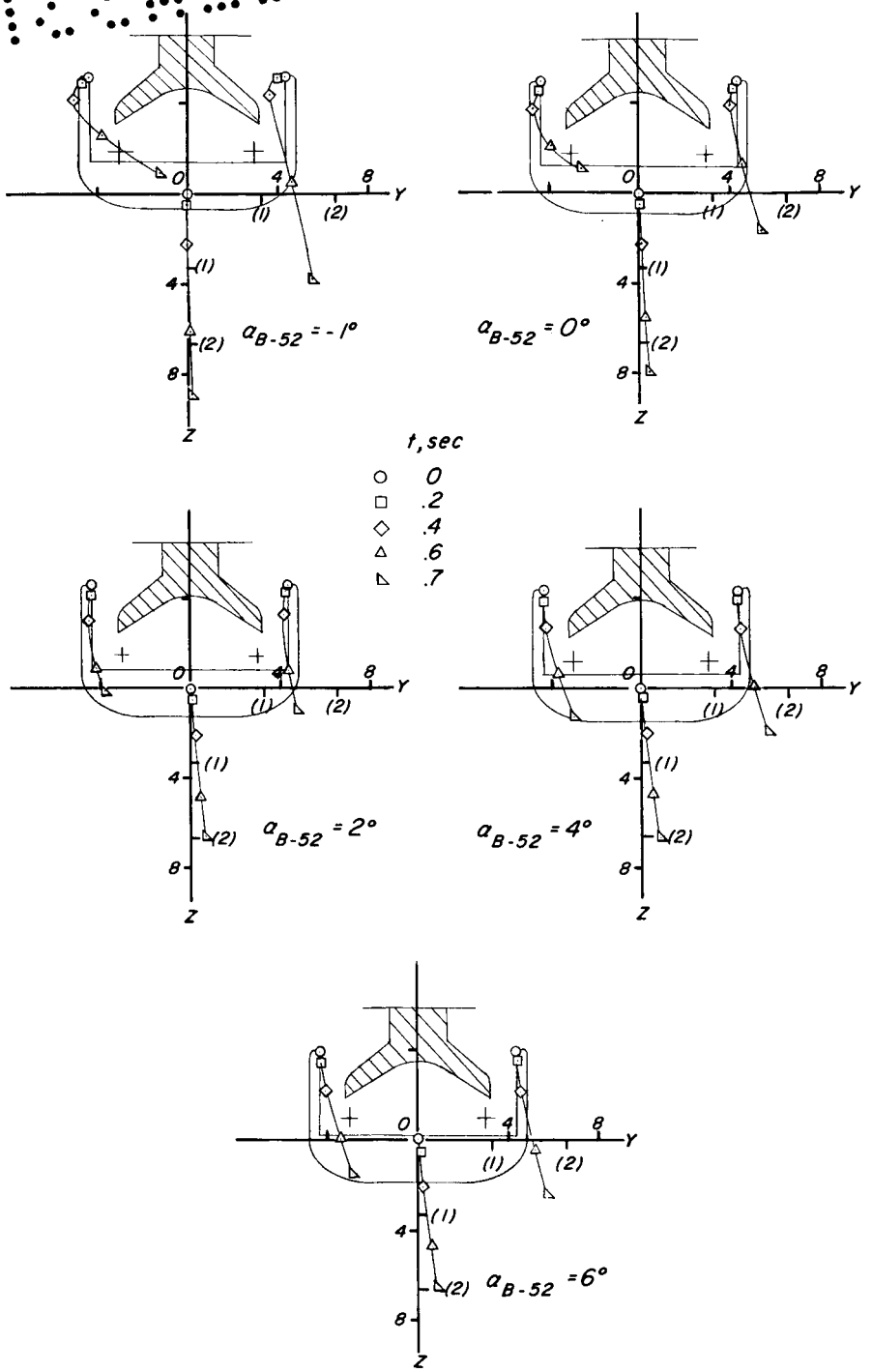

(a) Fin-tip and center-of-gravity paths. (Values along the coordinate scales are given in feet and parenthetically in meters.)

Figure 21.- Effect of variation in B-52 angle of attack (variation in altitude). Dampers off; $M = 0.60$; $\Delta\alpha = -5^{0}$; $W_{M2\text{-}F2} = 5576$ pounds (24 803 N); $W_{B\text{-}52} = 190\,000$ pounds (845 162 N).

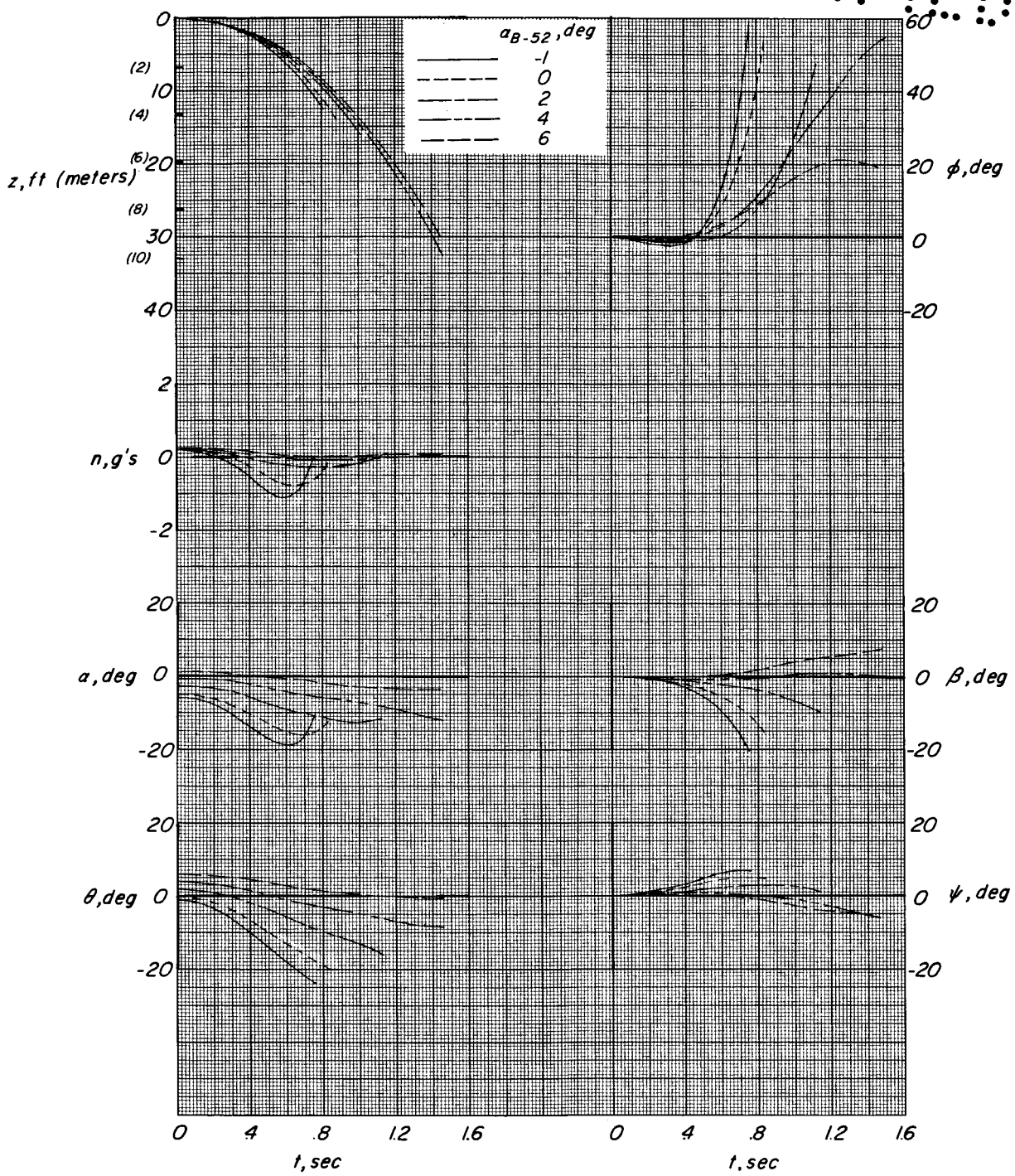

(b) Vehicle motions after launch.

Figure 21.- Concluded.

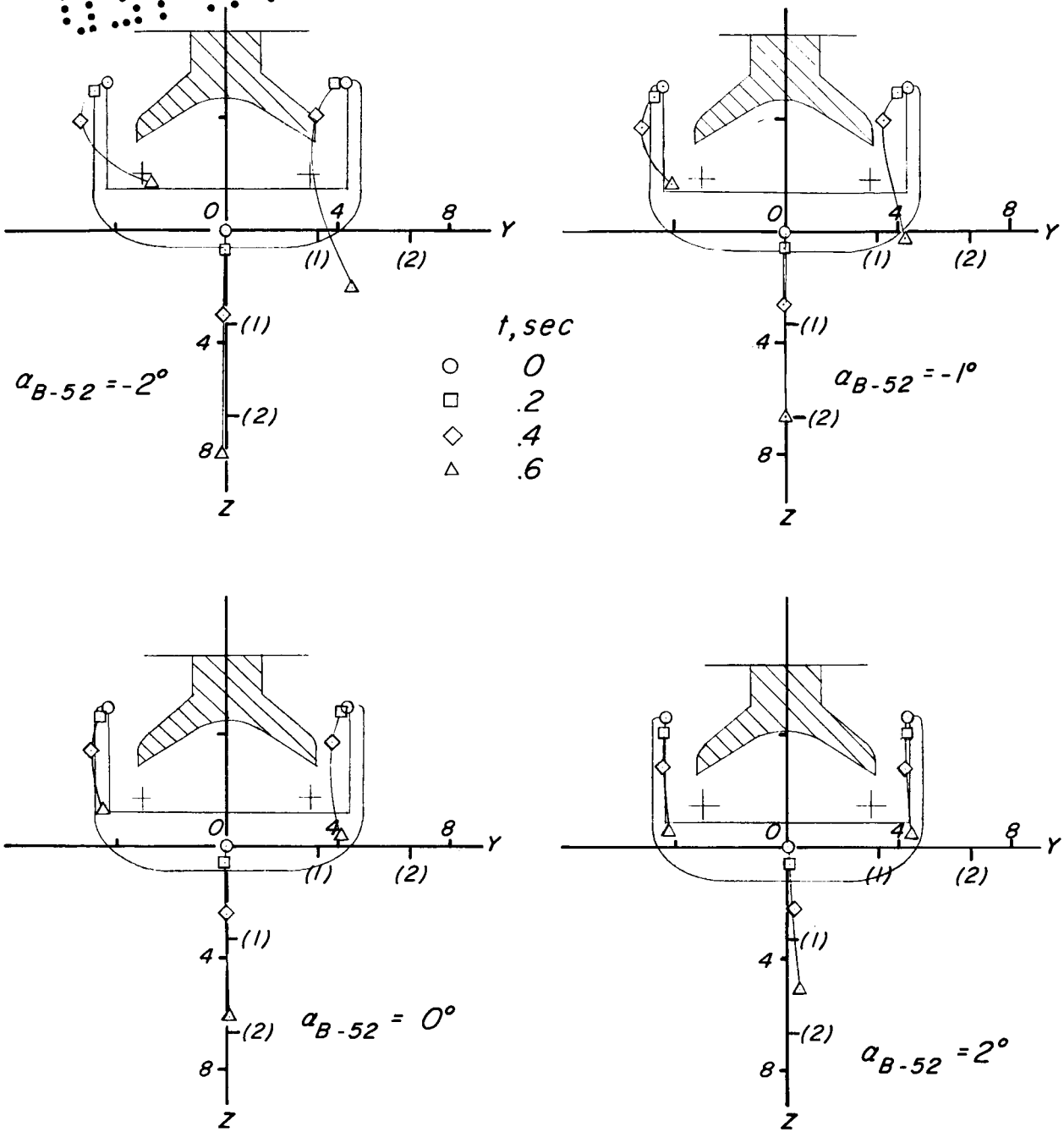

(a) Fin-tip and center-of-gravity paths. (Values along the coordinate scales are given in feet and parenthetically in meters.)

Figure 22.- Effect of variation in B-52 angle of attack (variation in altitude). Dampers off; $M = 0.80$; $\Delta\alpha = -5^{0}$; $W_{M2-F2} = 5576$ pounds (24 803 N); $W_{B-52} = 190\,000$ pounds (845 162 N).

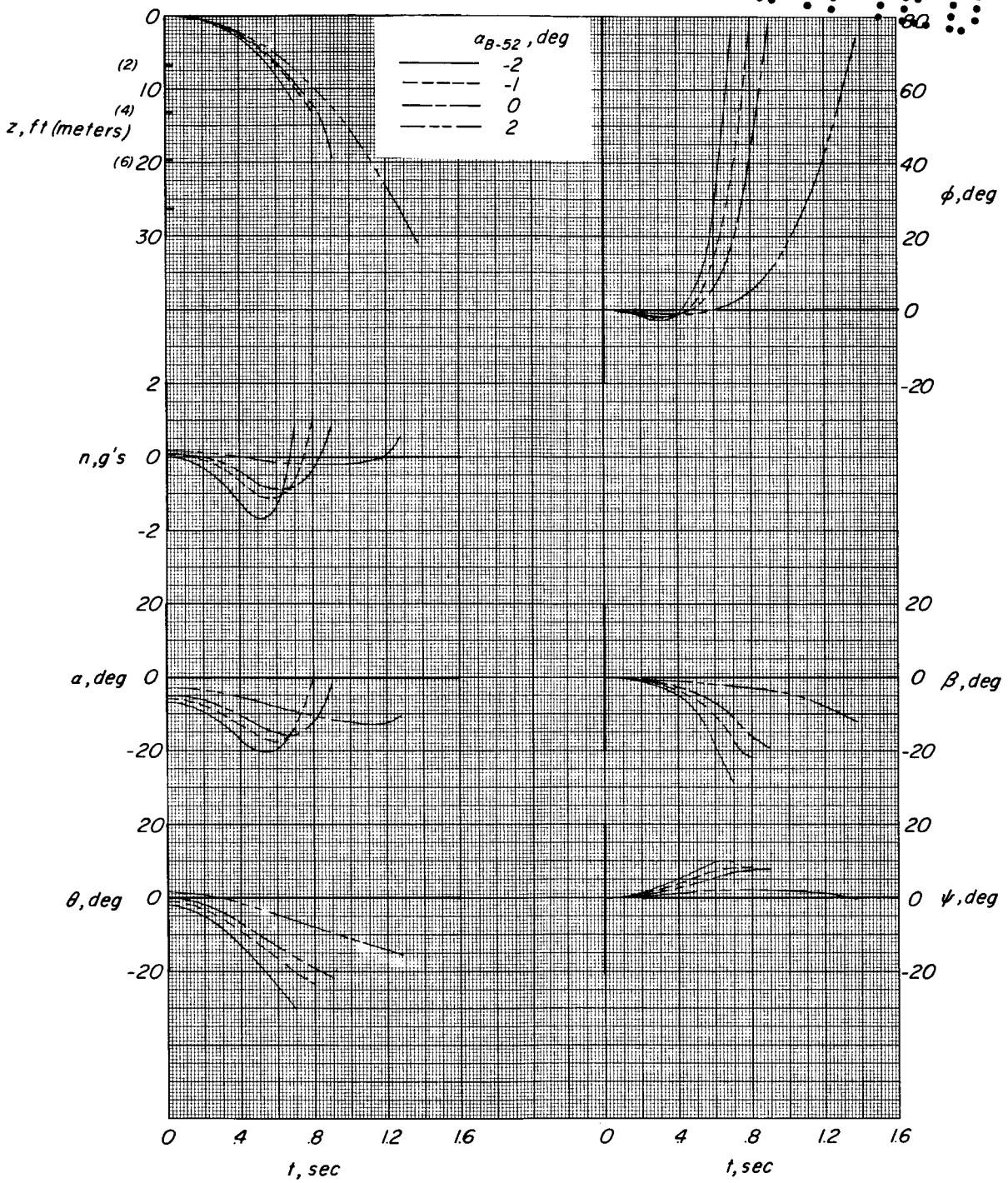

(b) Vehicle motions after launch.

Figure 22.- Concluded.

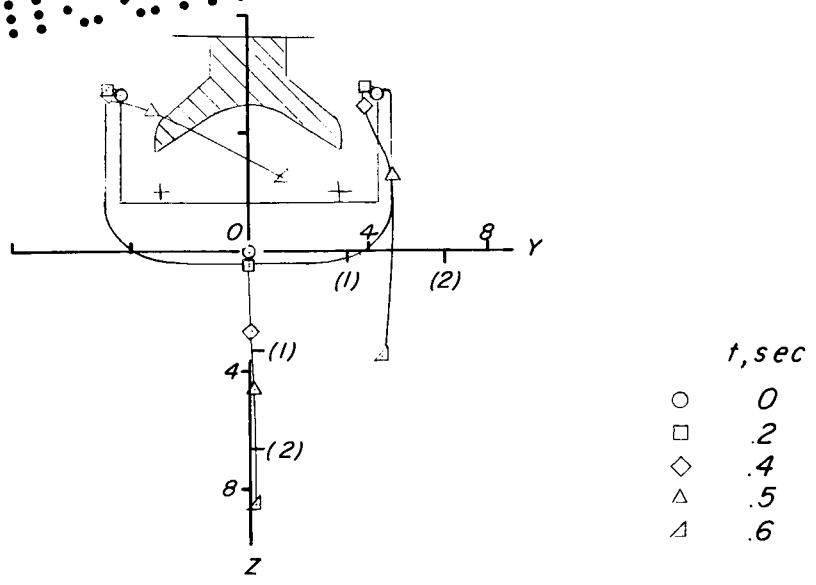

Damper off

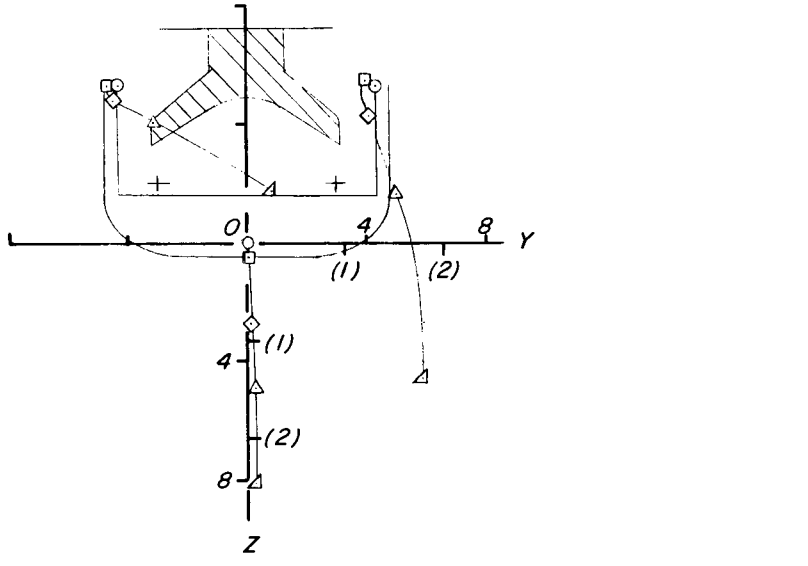

Damper on

(a) Fin-tip and center-of-gravity paths. (Values along the coordinate scales are given in feet and parenthetically in meters.)

Figure 23.- Effect of dampers. $M = 0.60$; $\alpha_{B-52} = -2^0$; $\Delta\alpha = -5^0$; $W_{M2-F2} = 5576$ pounds (24 803 N); $W_{B-52} = 250\,000$ pounds (1 112 055 N).

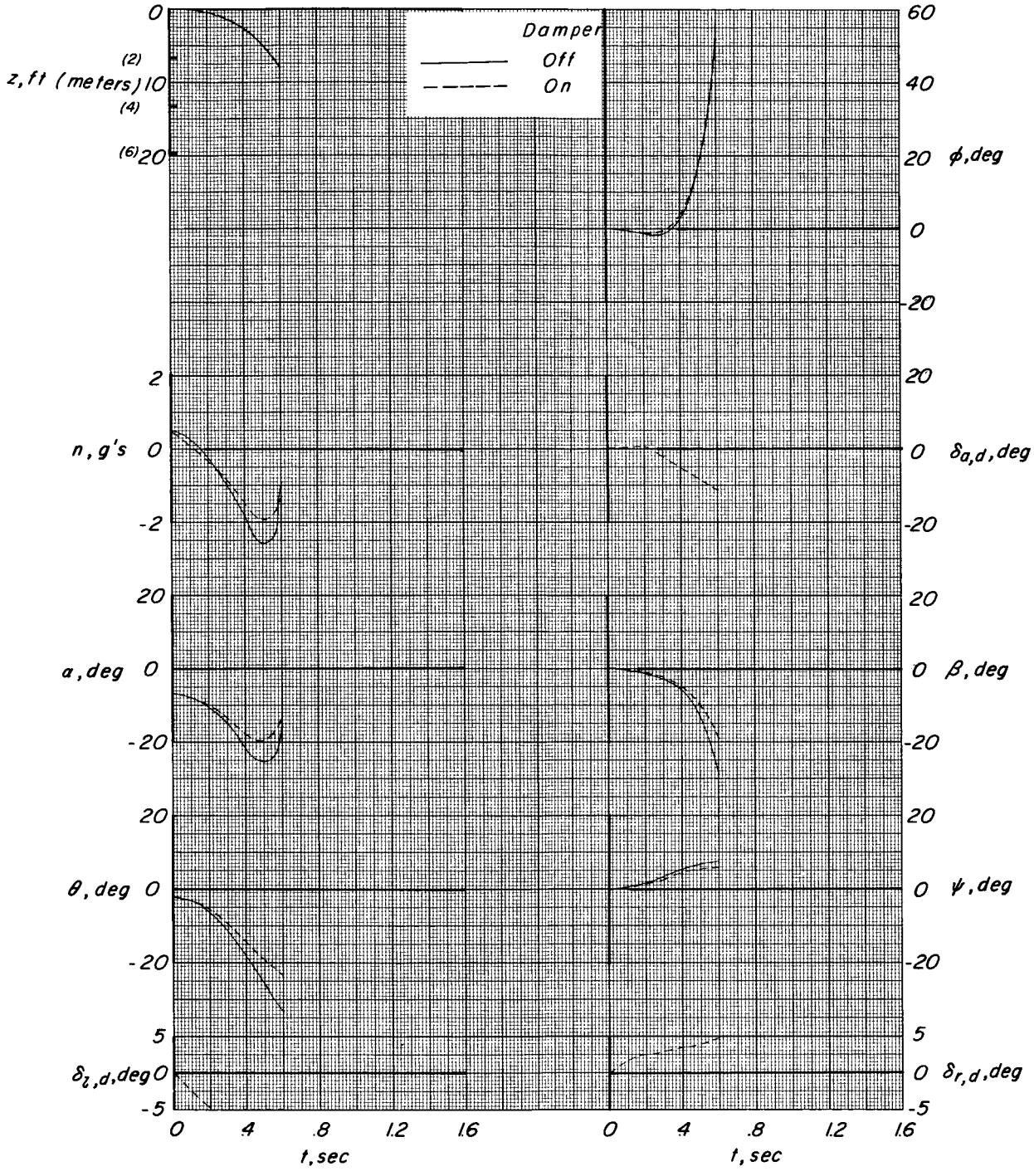

(b) Vehicle motions after launch.

Figure 23.- Concluded.

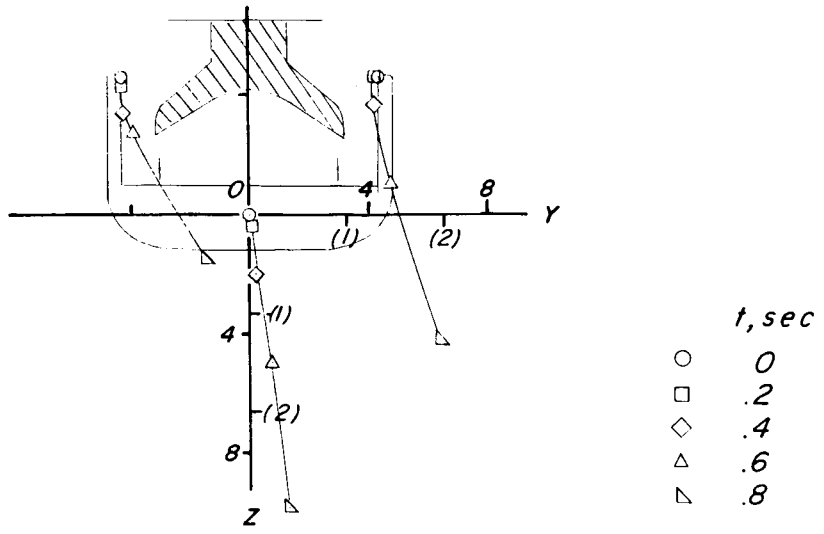

Damper off

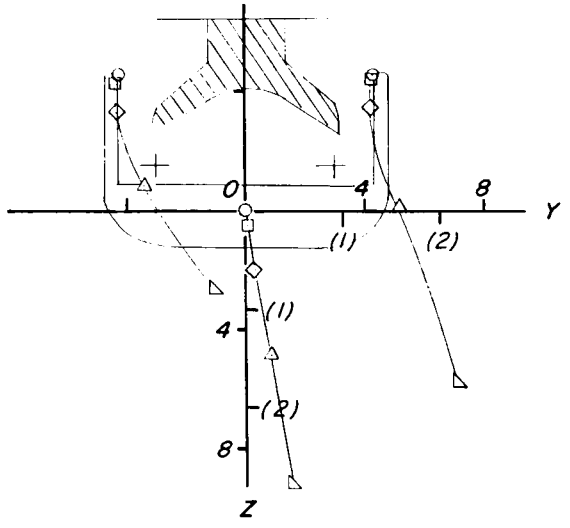

Damper on

(a) Fin-tip and center-of-gravity paths. (Values along the coordinate scales are given in feet and parenthetically in meters.)

Figure 24.- Effect of dampers. $M = 0.60$; $\alpha_{B-52} = 2^{o}$; $\Delta\alpha = -5^{o}$; $W_{M2-F2} = 5576$ pounds (24 803 N); $W_{B-52} = 250\,000$ pounds (1 112 055 N).

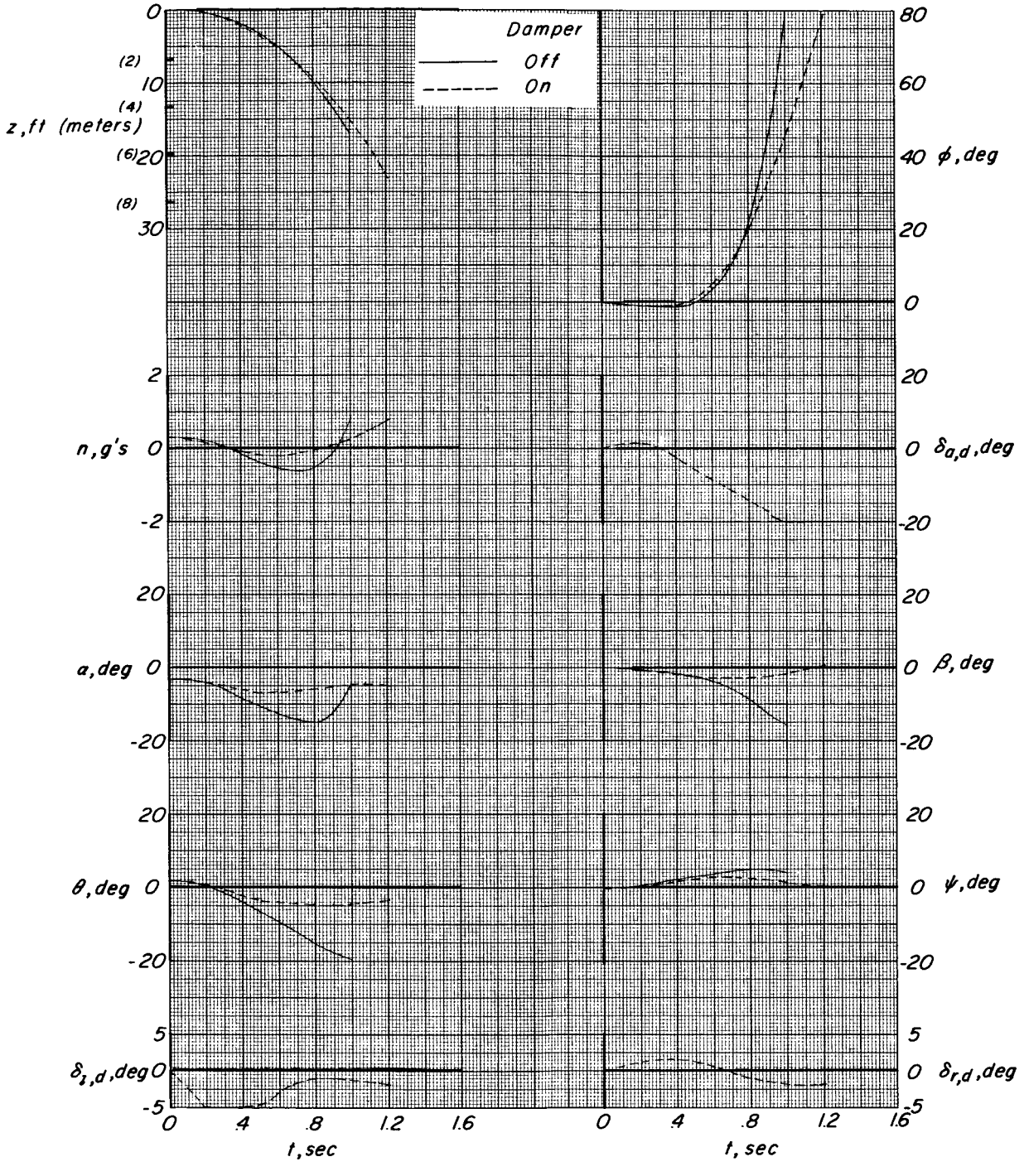

(b) Vehicle motions after launch.

Figure 24.- Concluded.

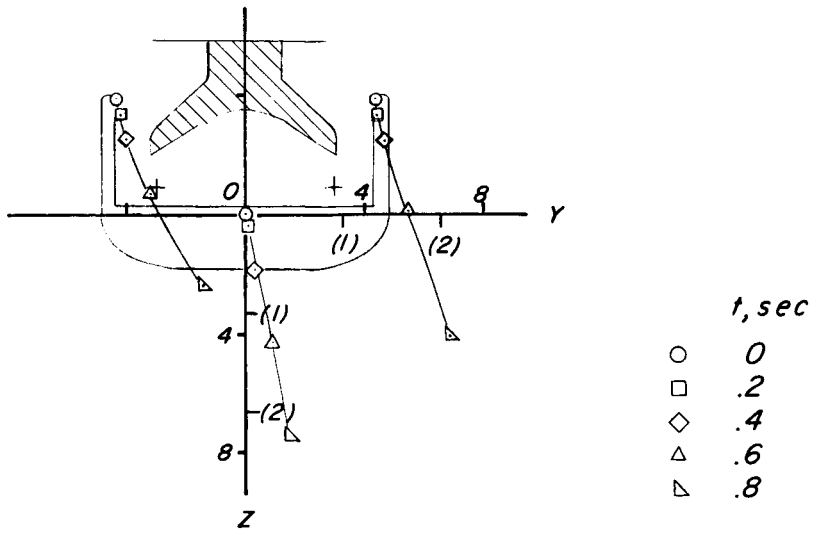

Damper off

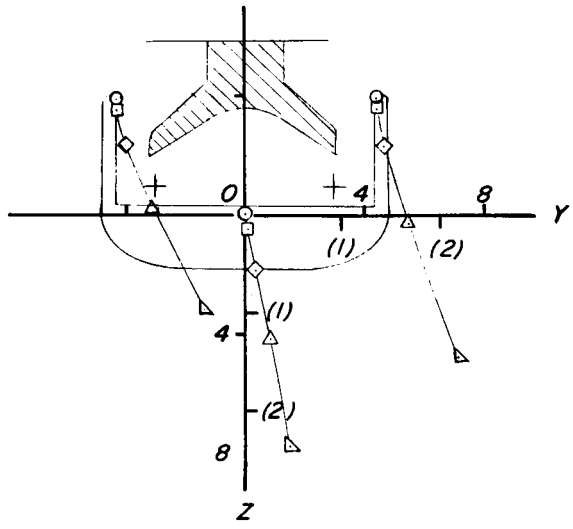

Damper on

(a) Fin-tip and center-of-gravity paths. (Values along the coordinate scales are given in feet and parenthetically in meters.)

Figure 25.- Effect of dampers. $M = 0.60$; $\alpha_{B-52} = 6^0$; $\Delta\alpha = -5^0$; $W_{M2-F2} = 5576$ pounds (24 803 N); $W_{B-52} = 250\,000$ pounds (1 112 055 N).

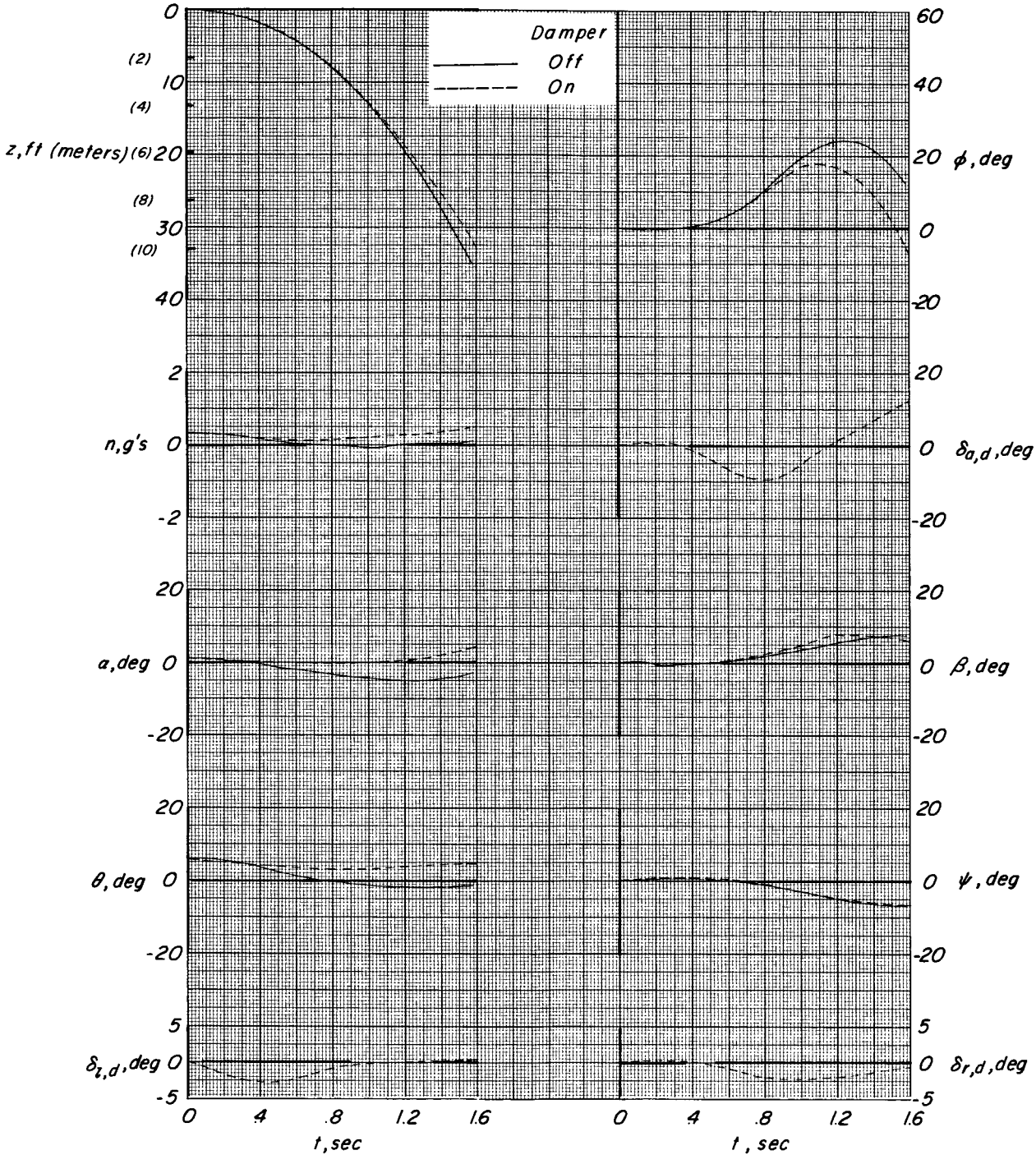

(b) Vehicle motions after launch.

Figure 25.- Concluded.

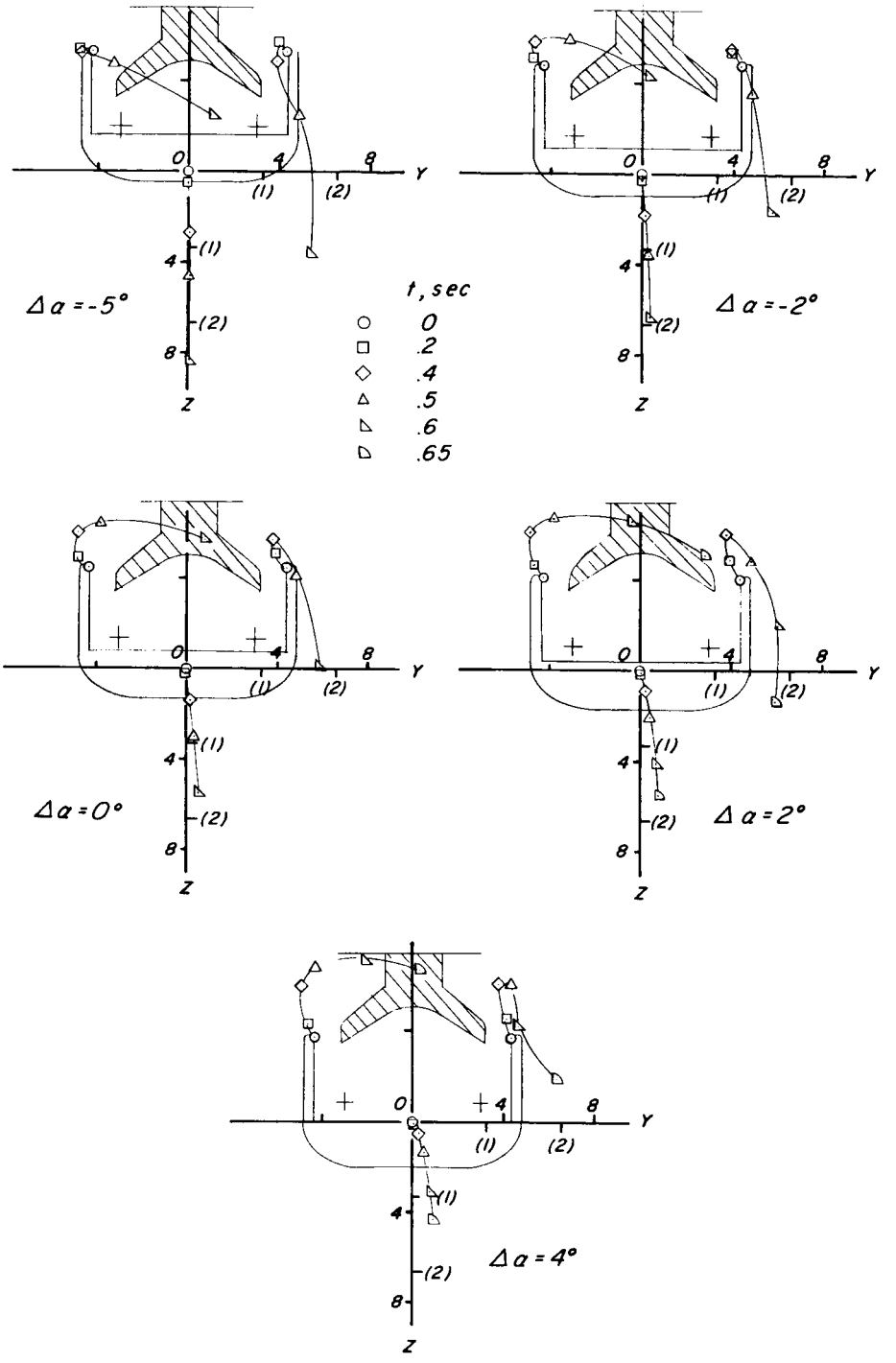

(a) Fin-tip and center-of-gravity paths. (Values along the coordinate scales are given in feet and parenthetically in meters.)

Figure 26.- Effect of $\Delta\alpha$. Dampers off; $M = 0.60$; $\alpha_{B-52} = -2^{0}$; $W_{M2-F2} = 5576$ pounds (24 803 N); $W_{B-52} = 250\,000$ pounds (1 112 055 N).

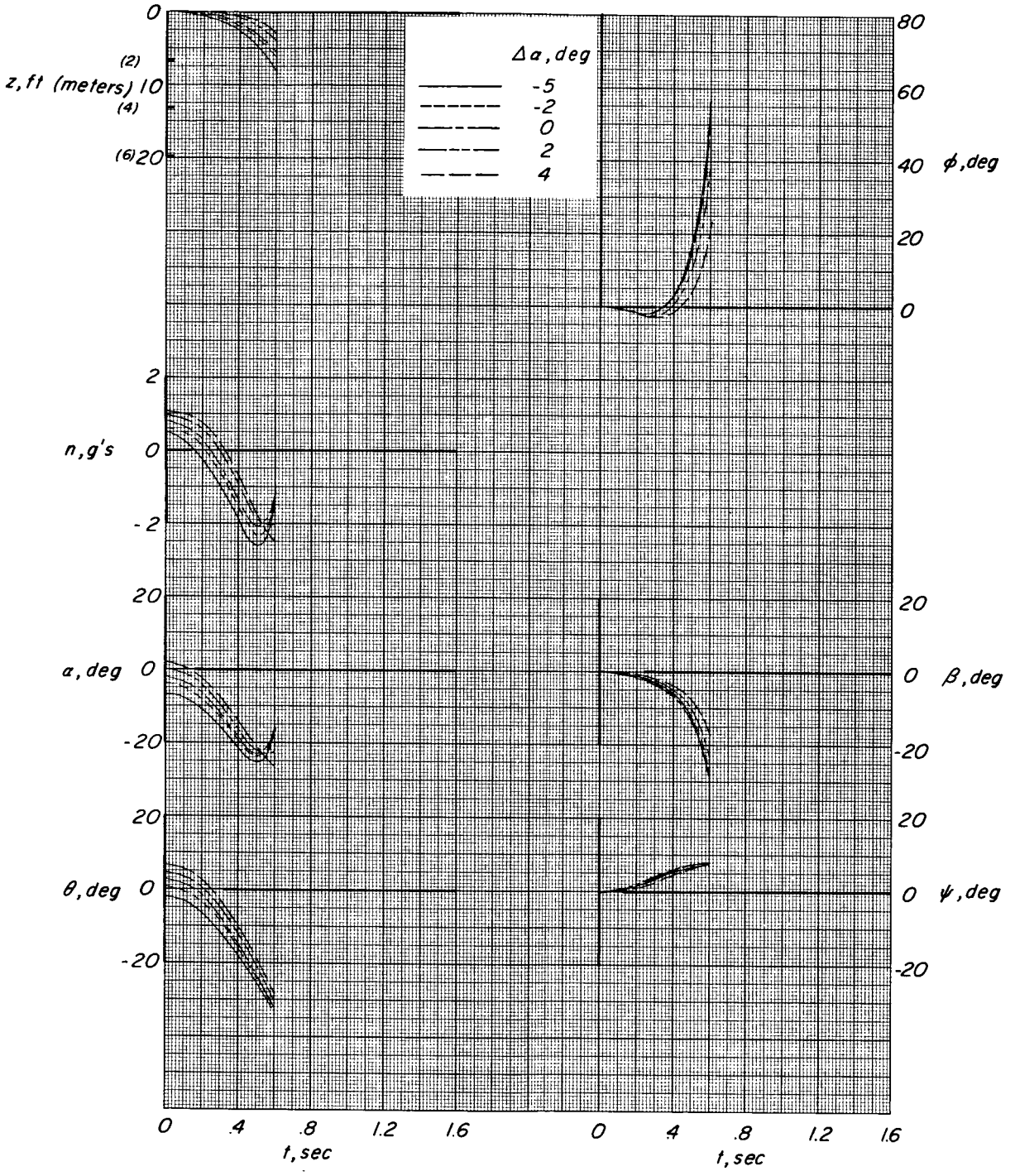

(b) Vehicle motions after launch.

Figure 26.- Concluded.

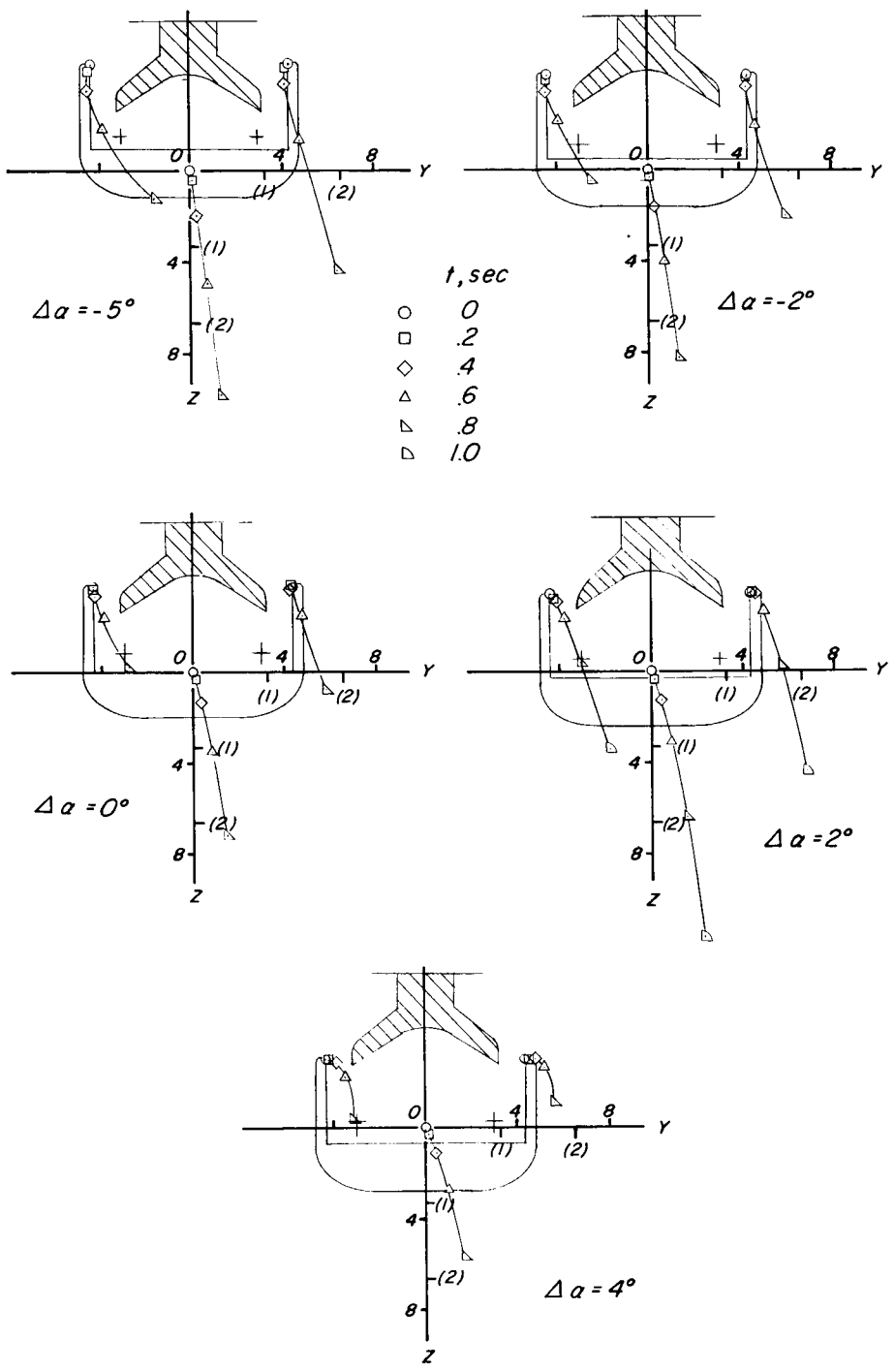

(a) Fin-tip and center-of-gravity paths. (Values along the coordinate scales are given in feet and parenthetically in meters.)

Figure 27.- Effect of $\Delta\alpha$. Dampers off; M = 0.60; $\alpha_{B-52} = 2^{o}$; W_{M2-F2} = 5576 pounds (24 803 N); W_{B-52} = 250 000 pounds (1 112 055 N).

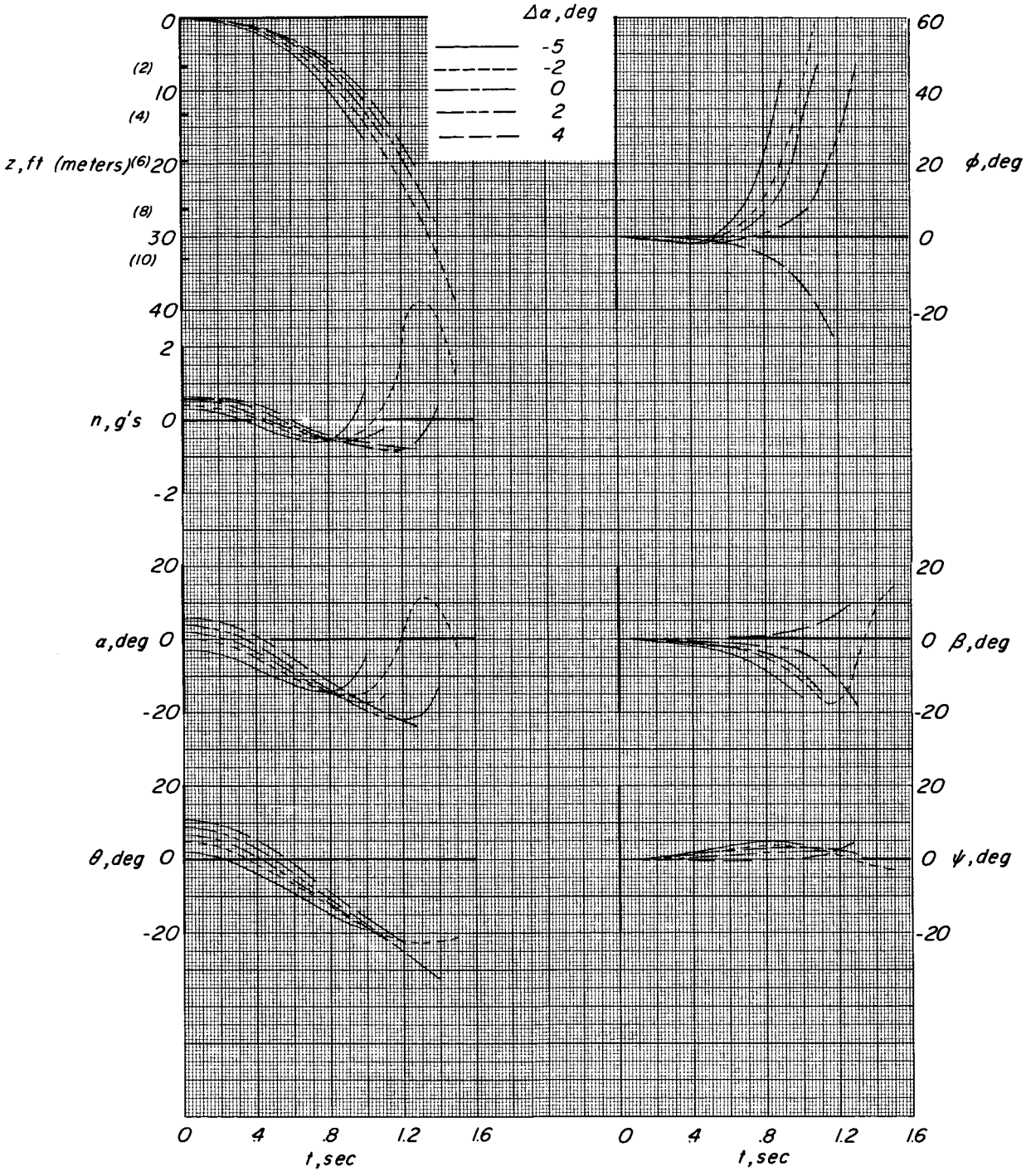

(b) Vehicle motions after launch.

Figure 27.- Concluded.

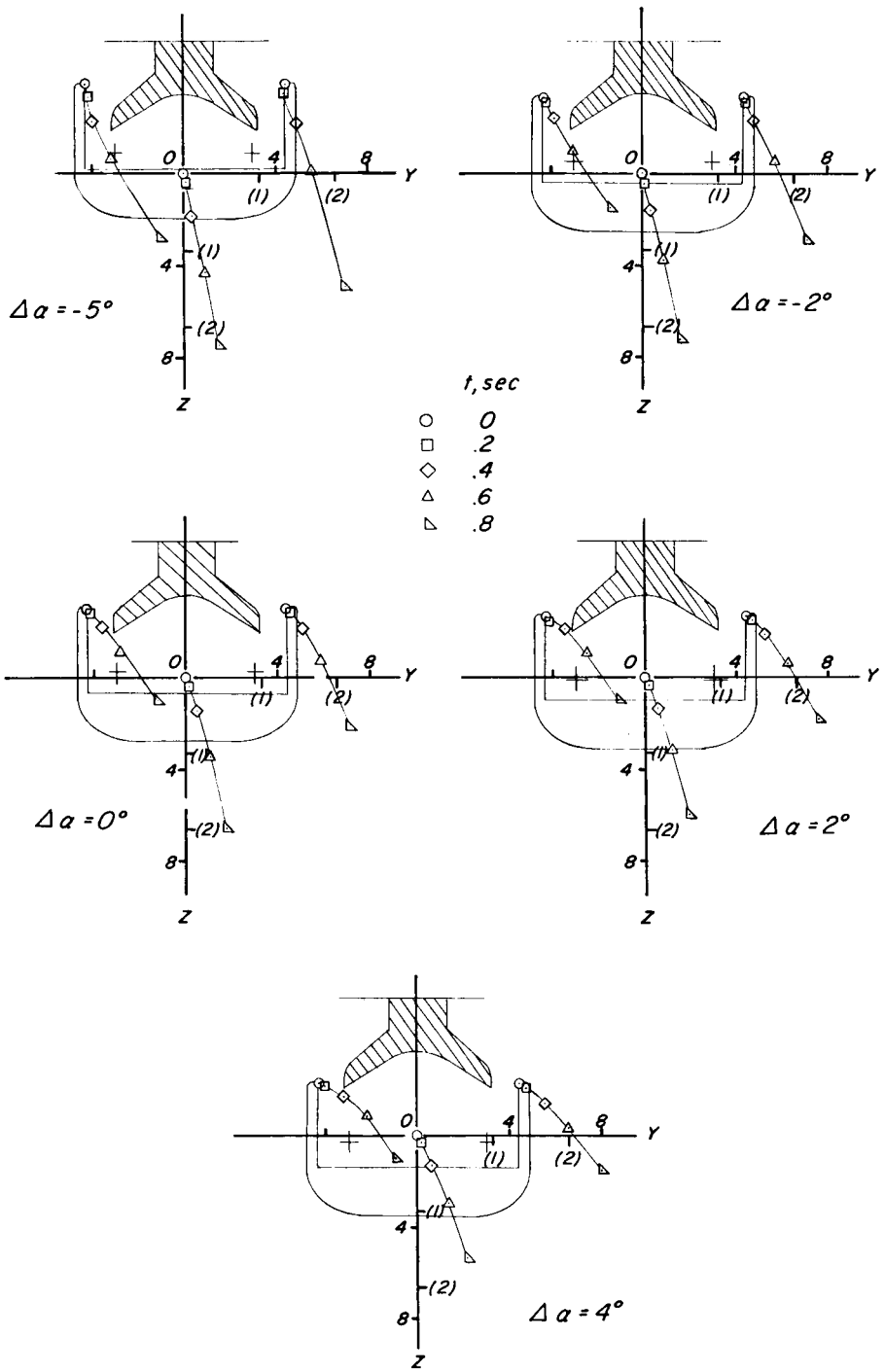

(a) Fin-tip and center-of-gravity paths. (Values along the coordinate scales are given in feet and parenthetically in meters.)

Figure 28.- Effect of $\Delta\alpha$. Dampers off; M = 0.60; $\alpha_{B-52} = 6^0$; W_{M2-F2} = 5576 pounds (24 803 N); W_{B-52} = 250 000 pounds (1 112 055 N).

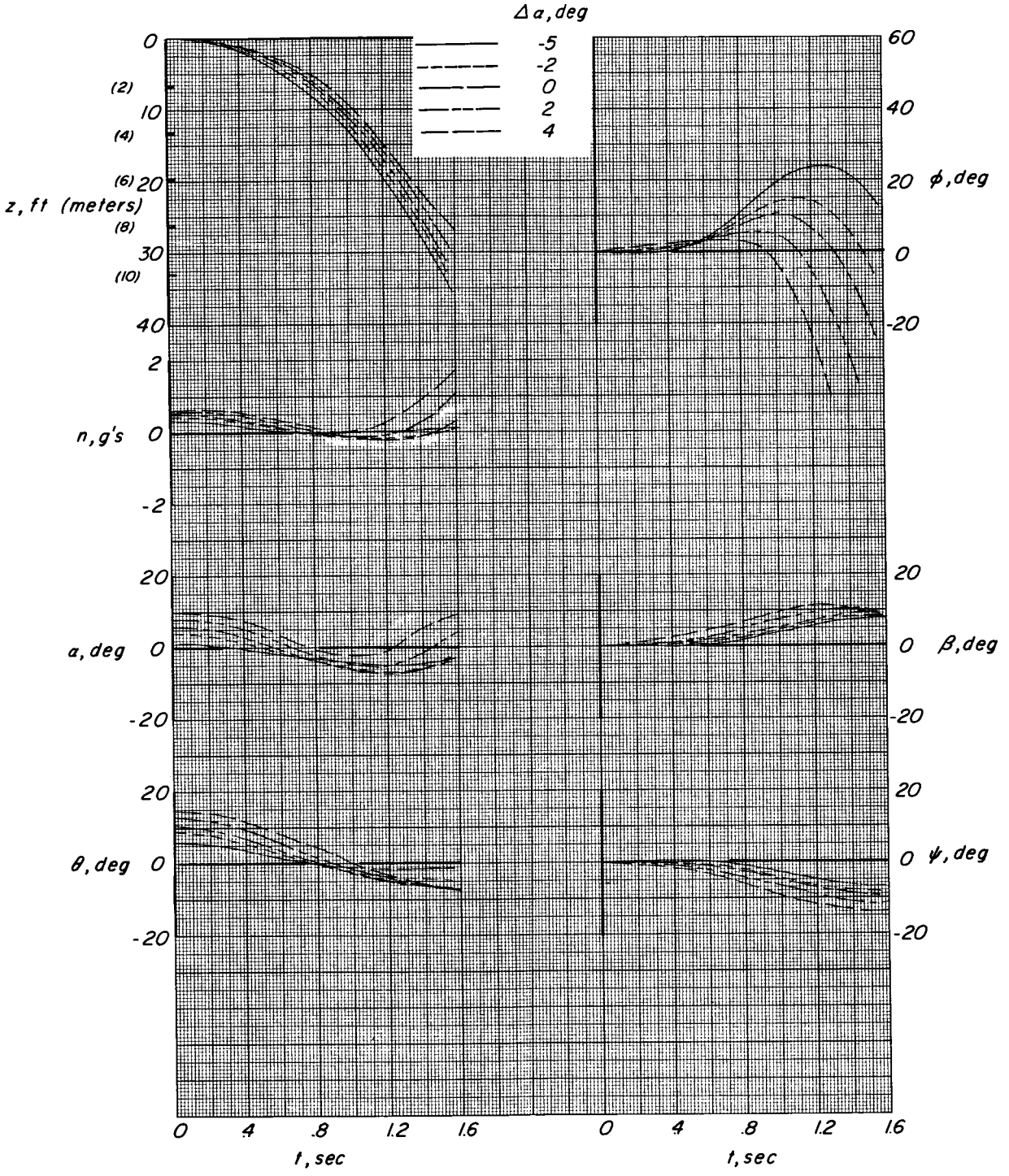

(b) Vehicle motions after launch.

Figure 28.- Concluded.

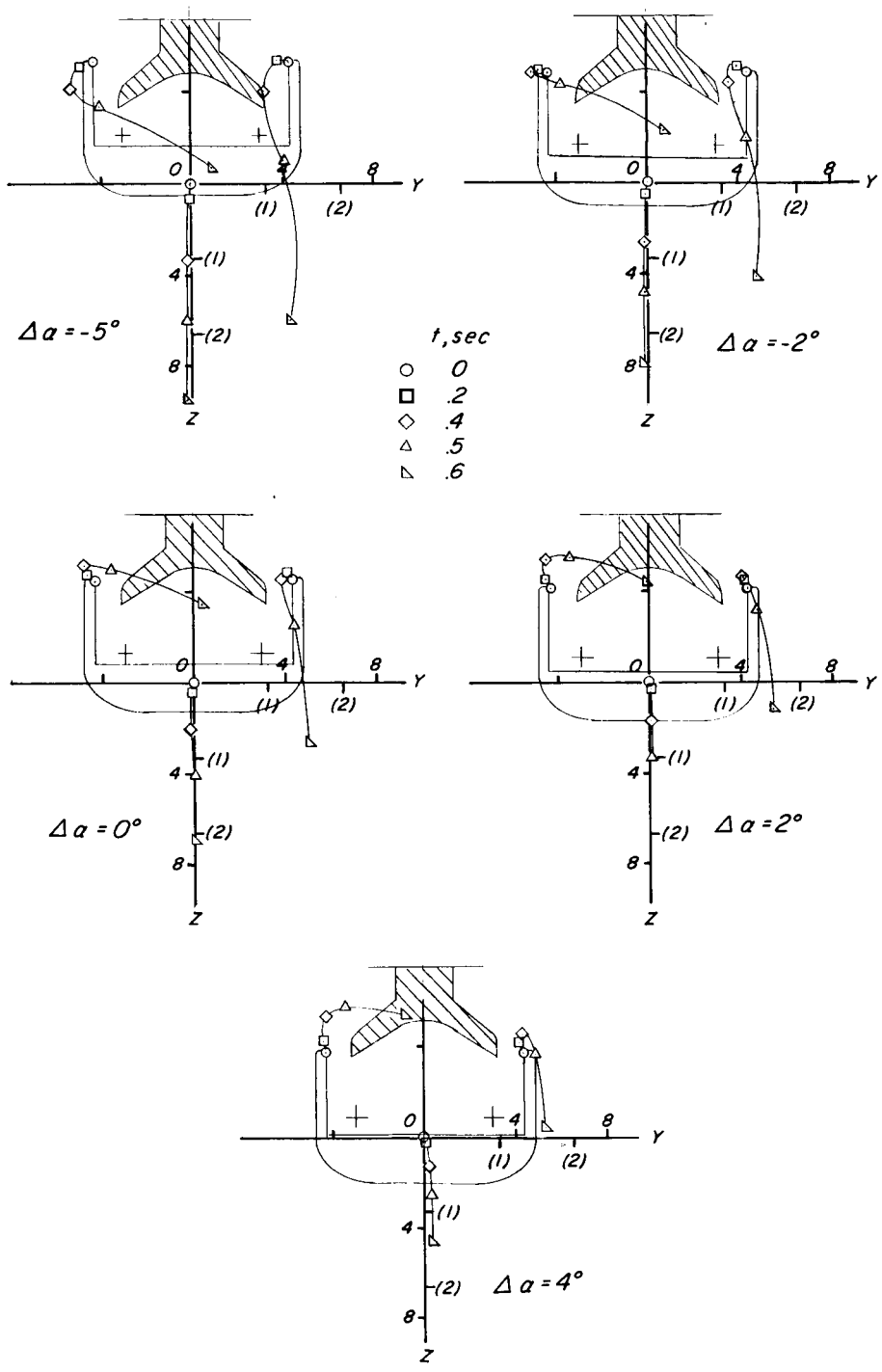

(a) Fin-tip and center-of-gravity paths. (Values along the coordinate scales are given in feet and parenthetically in meters.)

Figure 29.- Effect of $\Delta\alpha$. Dampers off; M = 0.80; $\alpha_{B-52} = -2^{0}$; W_{M2-F2} = 5576 pounds (24 803 N); W_{B-52} = 250 000 pounds (1 112 055 N).

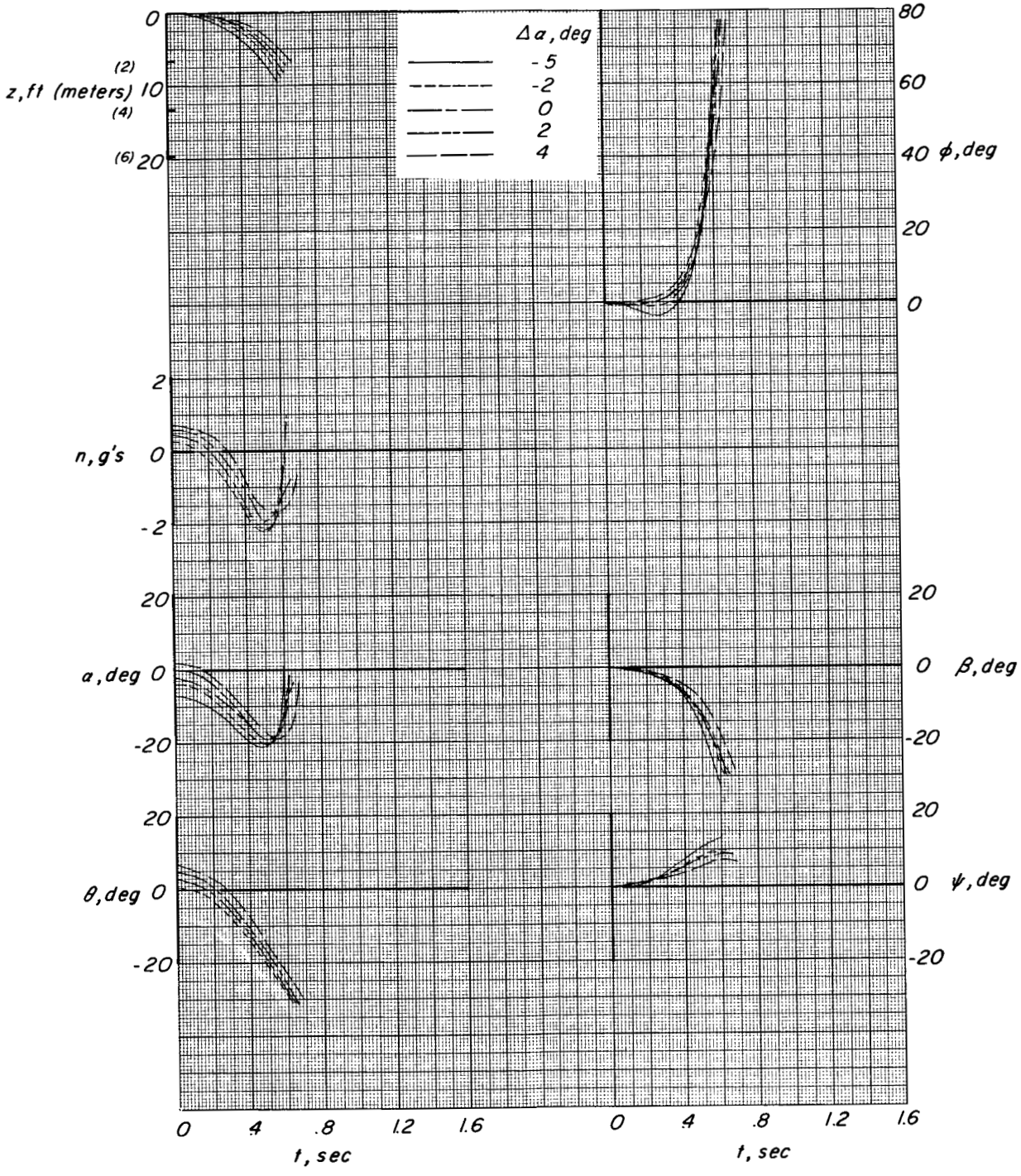

(b) Vehicle motions after launch.

Figure 29.- Concluded.

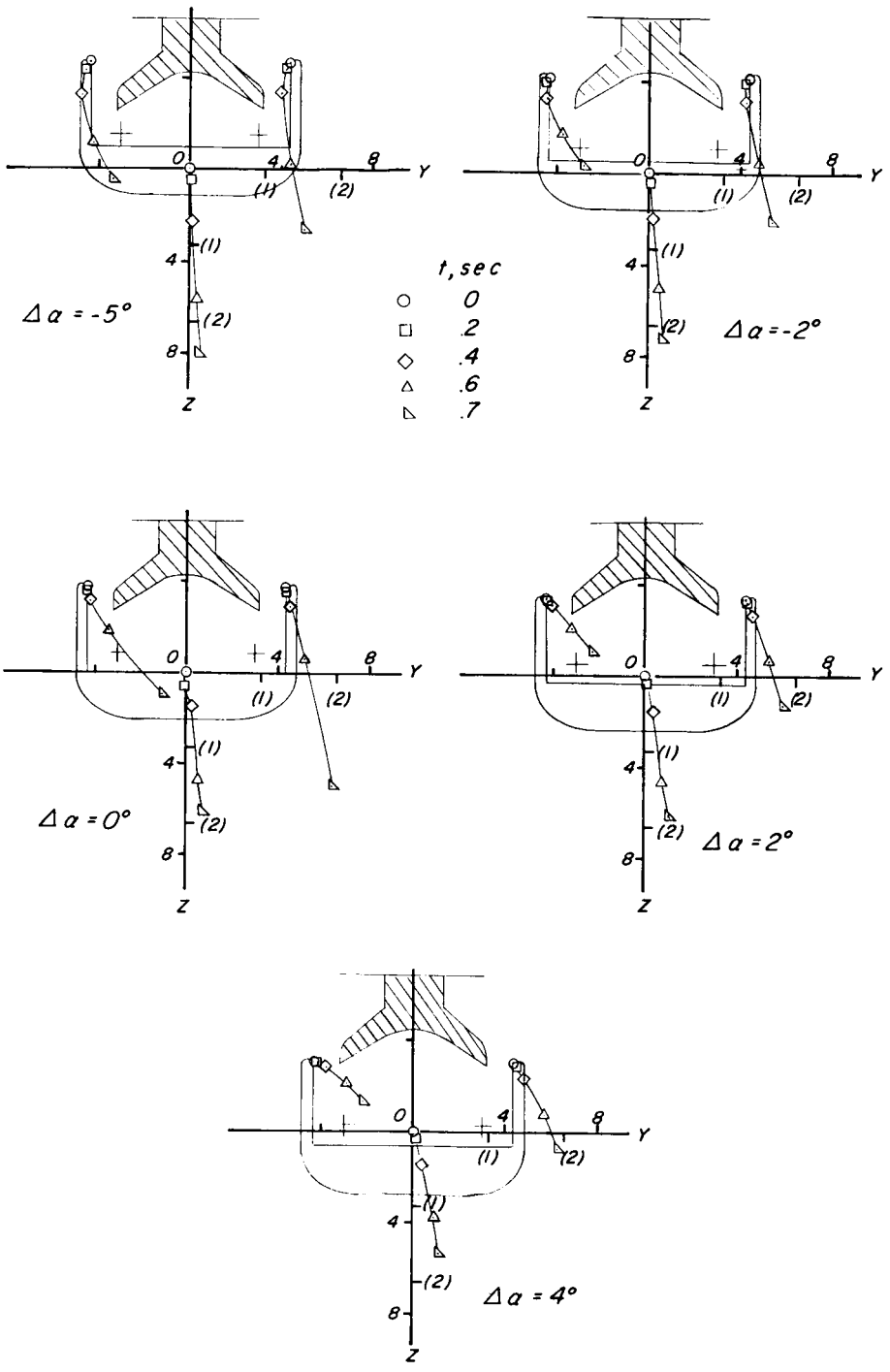

(a) Fin-tip and center-of-gravity paths. (Values along the coordinate scales are given in feet and parenthetically in meters.)

Figure 30.- Effect of $\Delta\alpha$. Dampers off; M = 0.80; $\alpha_{B-52} = 2^{0}$; W_{M2-F2} = 5576 pounds (24 803 N); W_{B-52} = 250 000 pounds (1 112 055 N).

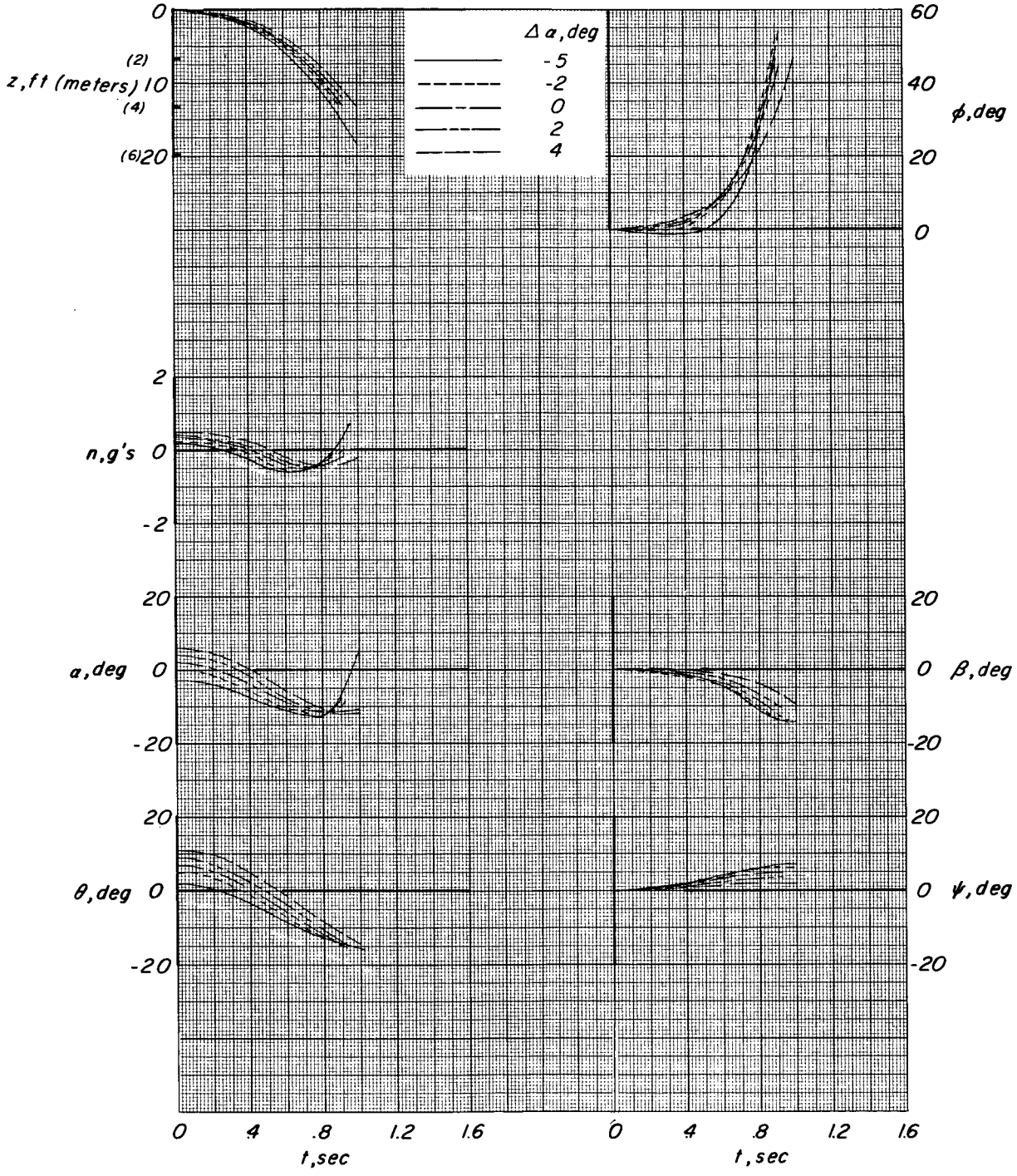

(b) Vehicle motions after launch.

Figure 30.- Concluded.

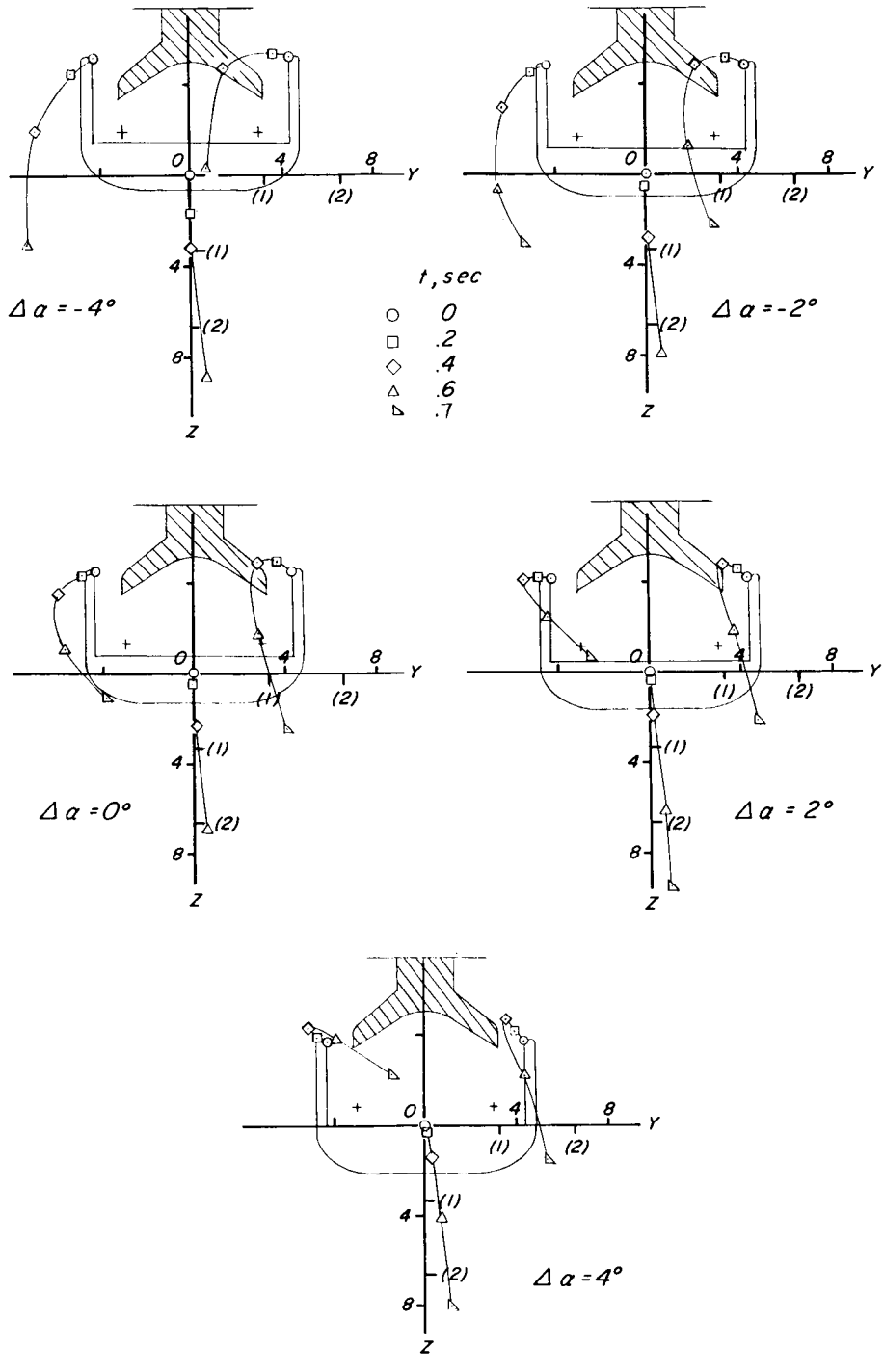

(a) Fin-tip and center-of-gravity paths. (Values along the coordinate scales are given in feet and parenthetically in meters.)

Figure 31.- Effect of $\Delta\alpha$. Dampers off; $M = 0.85$; $\alpha_{B-52} = -2^{0}$; $W_{M2-F2} = 5576$ pounds (24 803 N); $W_{B-52} = 250\,000$ pounds (1 112 055 N).

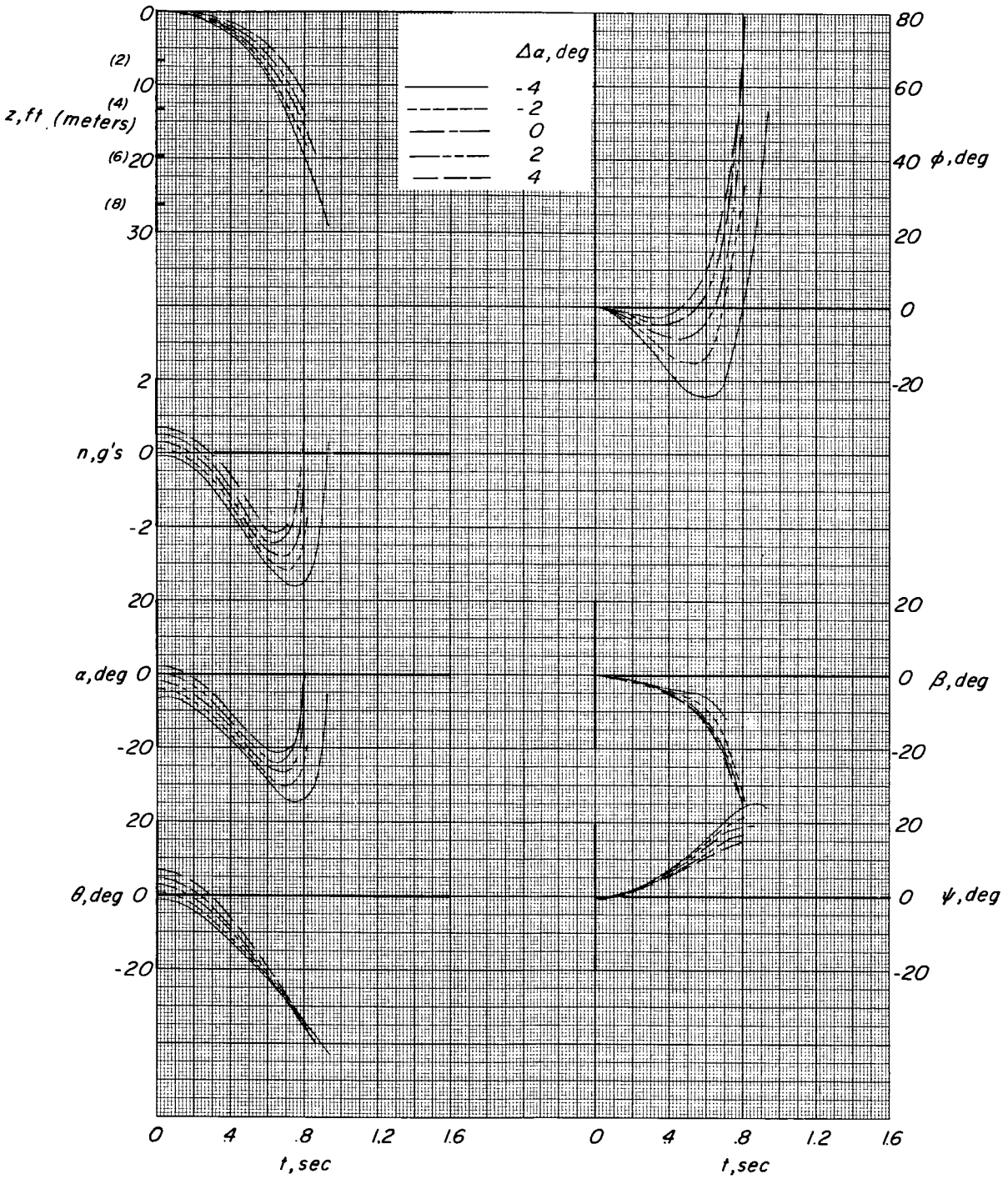

(b) Vehicle motions after launch.

Figure 31.- Concluded.

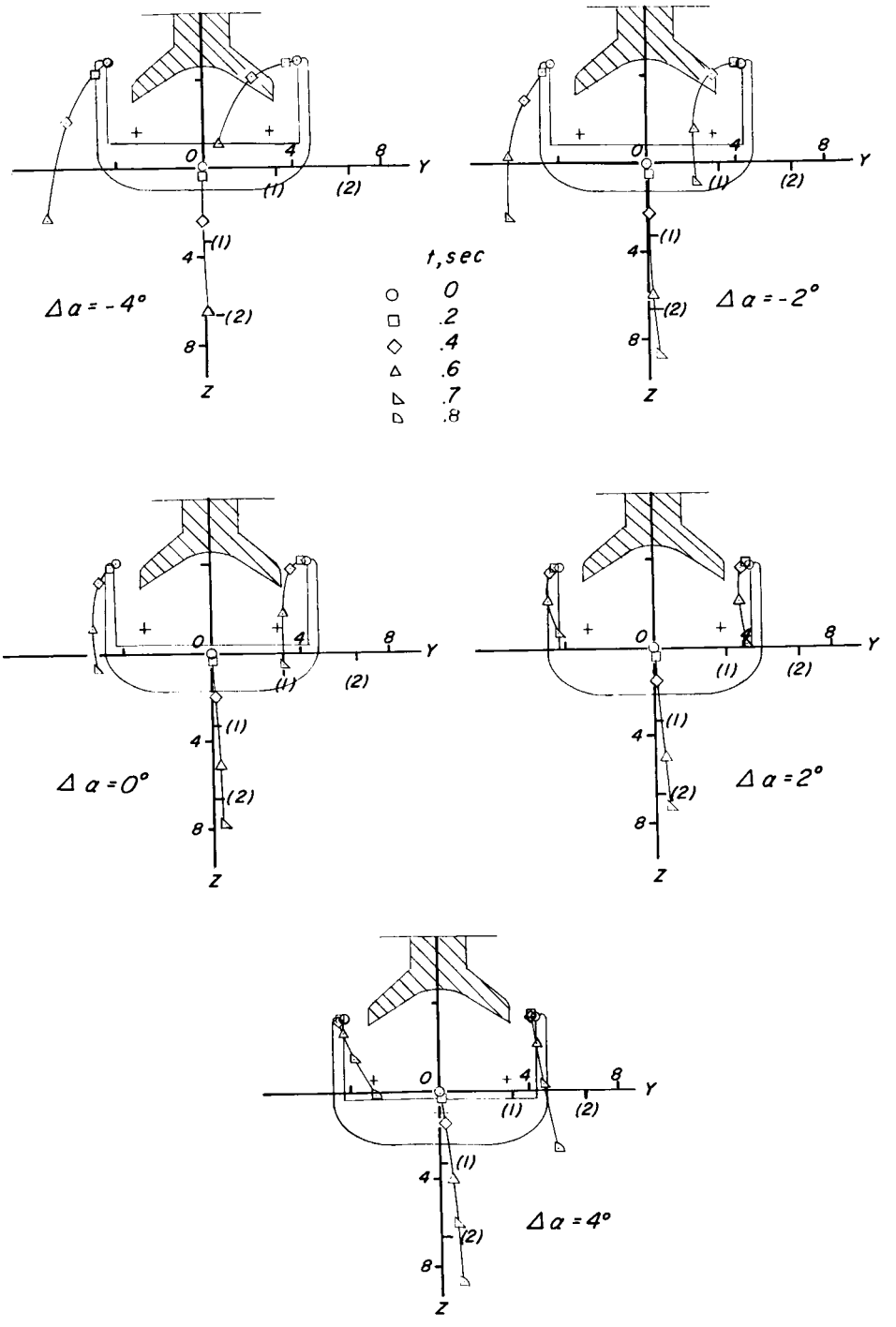

(a) Fin-tip and center-of-gravity paths. (Values along the coordinate scales are given in feet and parenthetically in meters.)

Figure 32.- Effect of $\Delta\alpha$. Dampers off; $M = 0.85$; $\alpha_{B-52} = 0^{0}$; $W_{M2-F2} = 5576$ pounds (24 803 N); $W_{B-52} = 250\,000$ pounds (1 112 055 N).

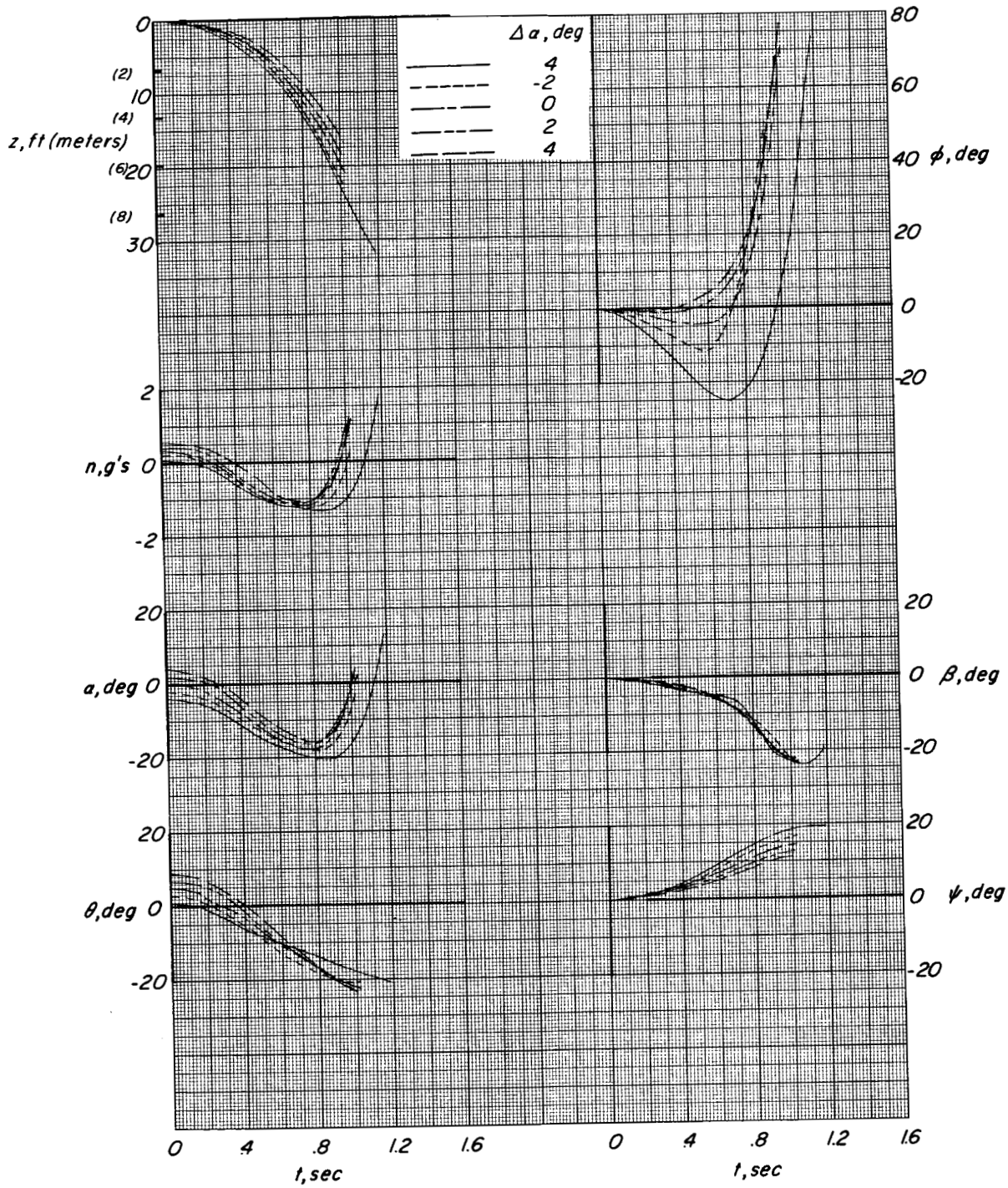

(b) Vehicle motions after launch.

Figure 32.- Concluded.

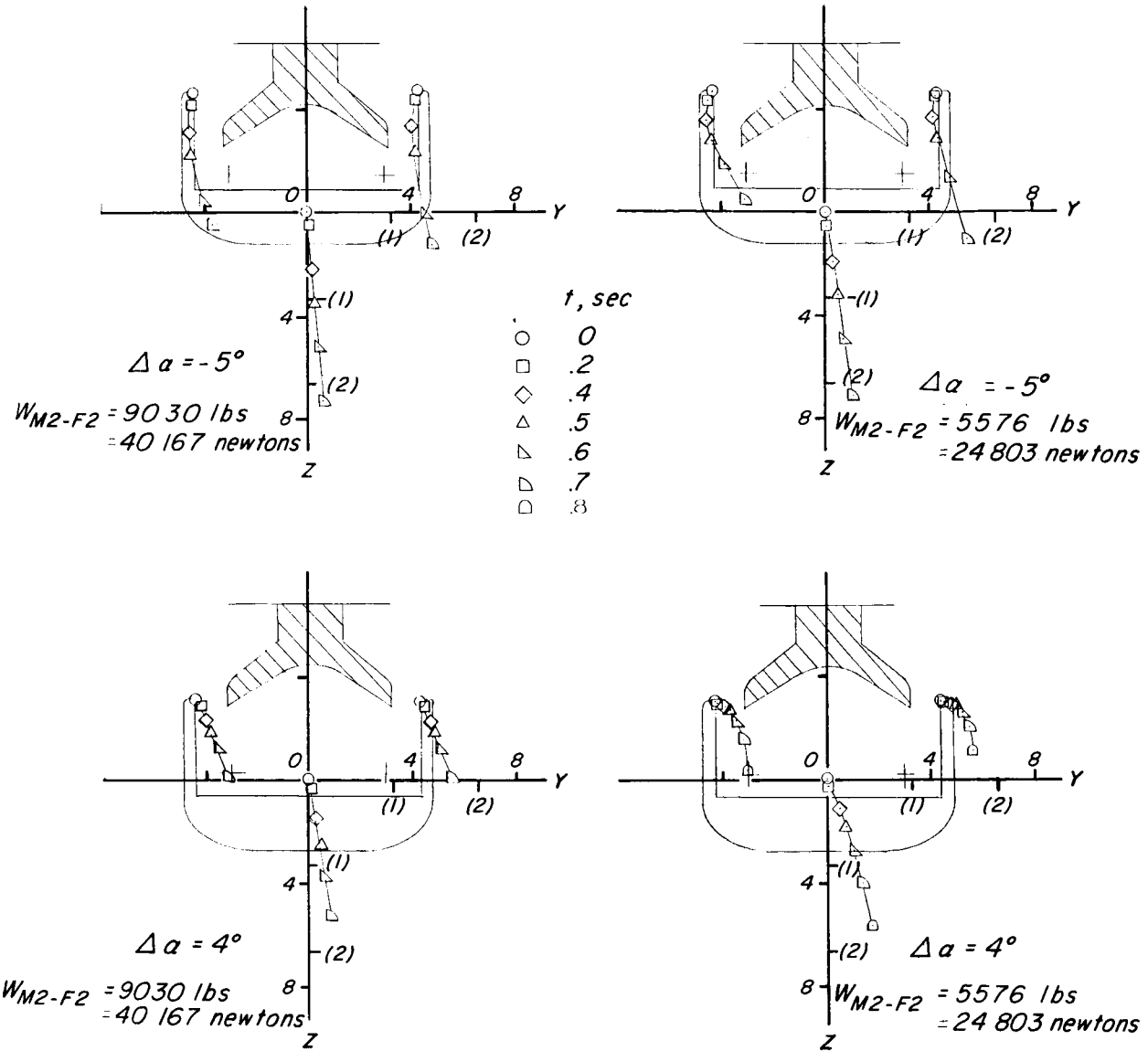

(a) Fin-tip and center-of-gravity paths. (Values along the coordinate scales are given in feet and parenthetically in meters.)

Figure 33.- Effect of M2-F2 launch weight. Dampers off; $M = 0.60$; $\alpha_{B-52} = 2^{0}$; $W_{B-52} = 250\,000$ pounds (1 112 055 N).

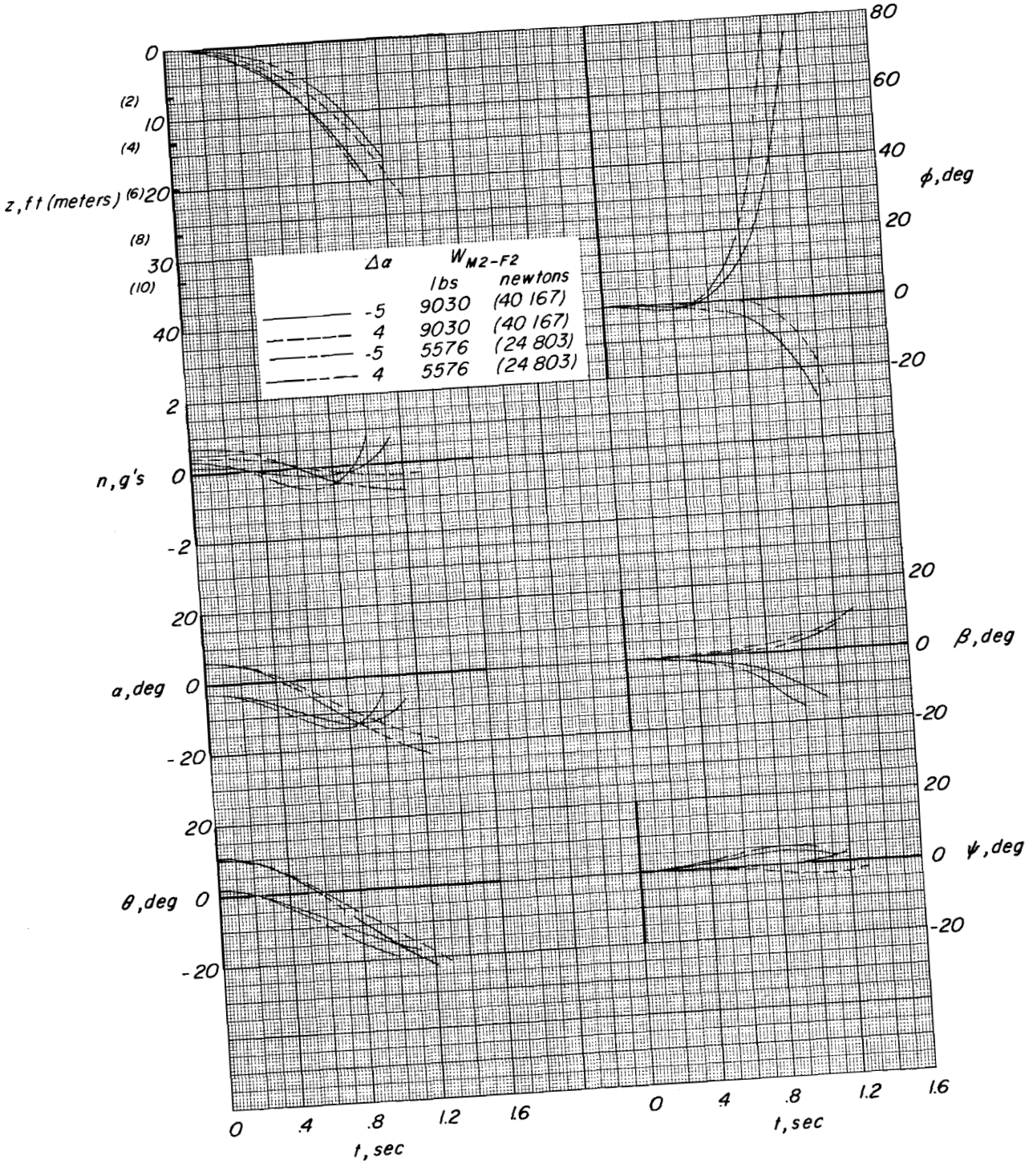

(b) Vehicle motions after launch.

Figure 33.- Concluded.

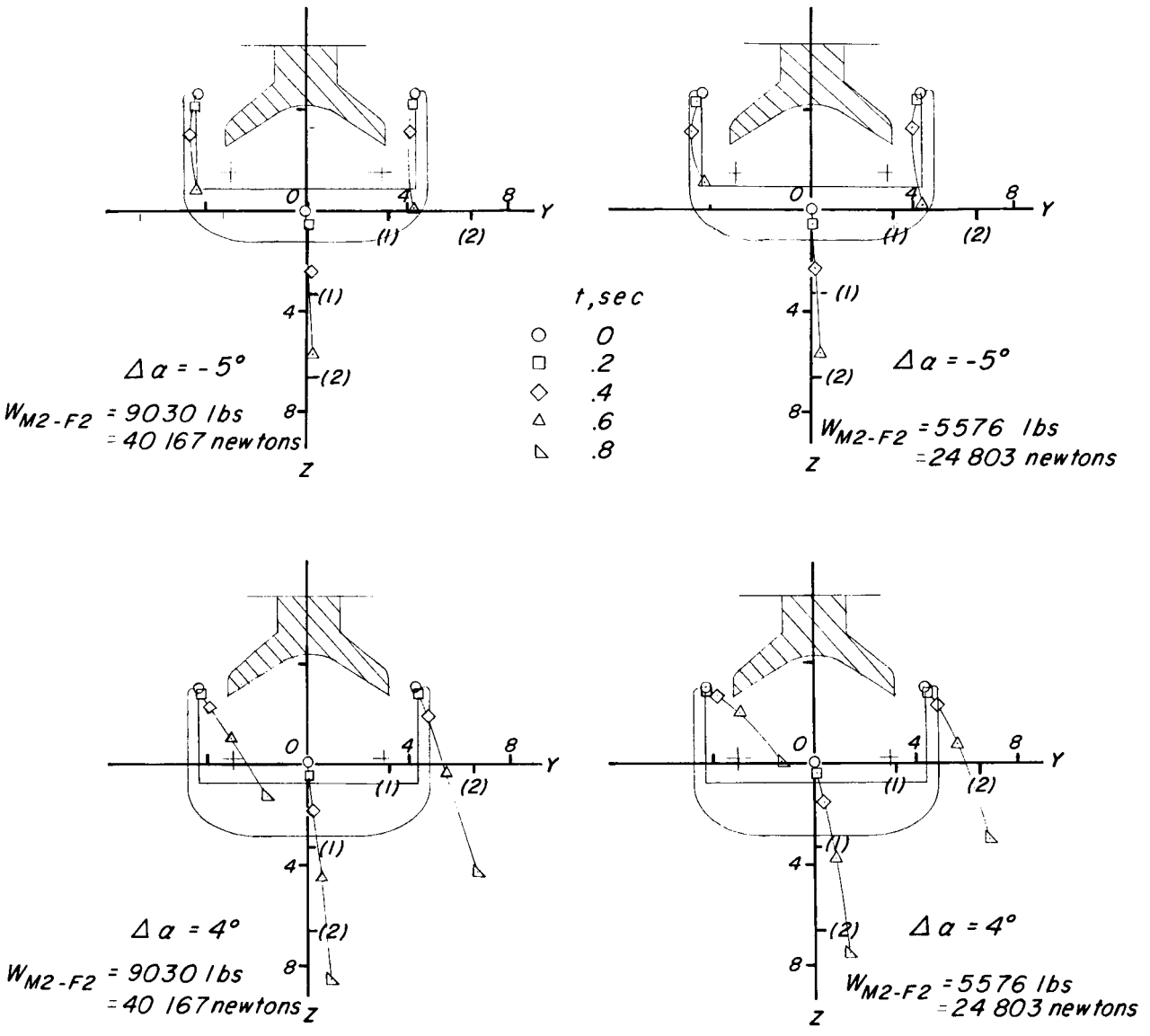

(a) Fin-tip and center-of-gravity paths. (Values along the coordinate scales are given in feet and parenthetically in meters.)

Figure 34.- Effect of M2-F2 launch weight. Dampers off; M = 0.80; $\alpha_{B-52} = 2^{0}$; W_{B-52} = 250 000 pounds (1 112 055 N).

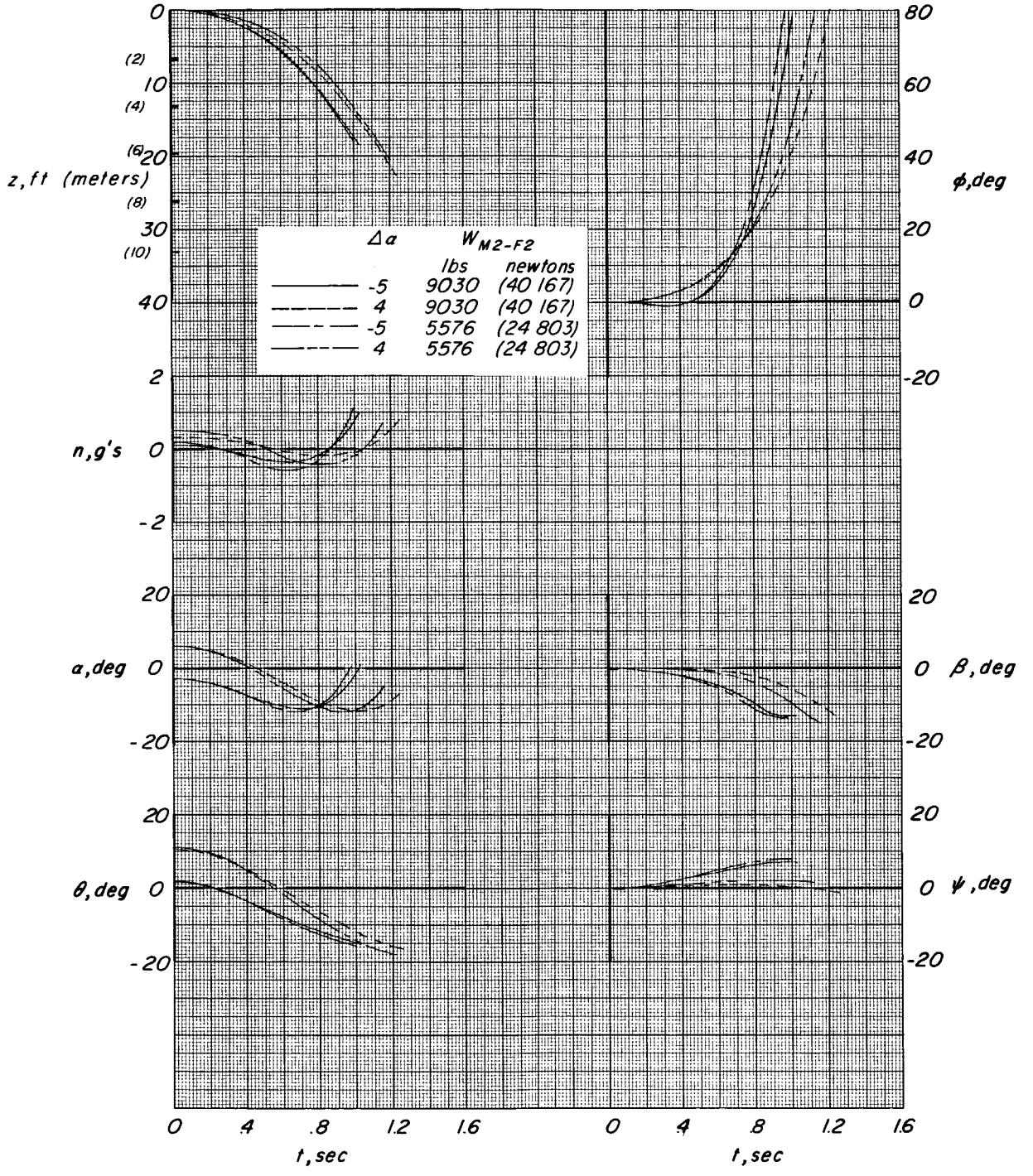

(b) Vehicle motions after launch.

Figure 34.- Concluded.

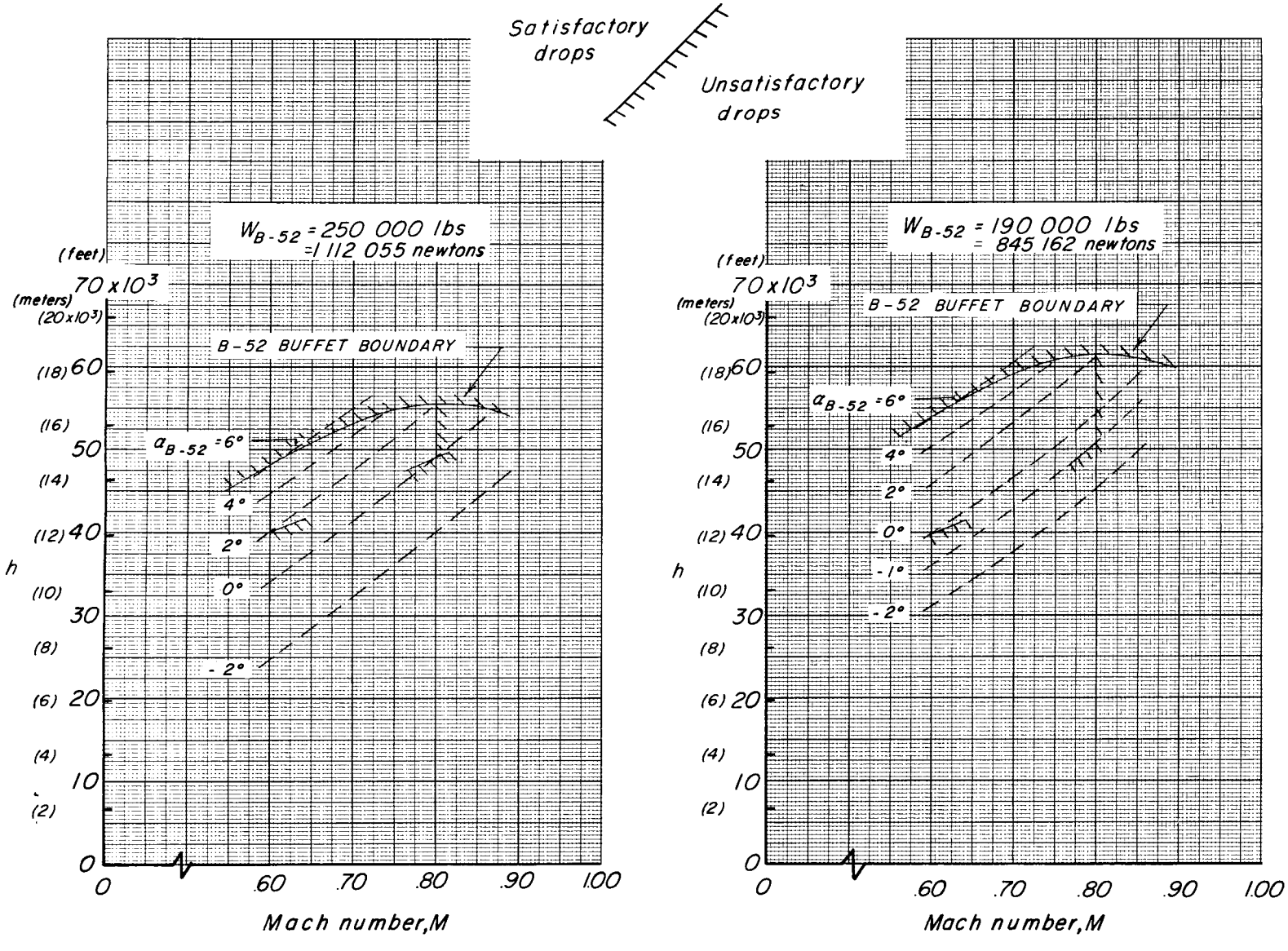

Figure 35.- Launch envelope. Dampers off; $\Delta\alpha = -5^0$; W_{M2-F2} = 5576 pounds (24 803 N).